

# Oncology and Translational Medicine

Volume 5 • Number 2 • April 2019

**Comparison of intra-pleural injection efficacy between Endostar and Bevacizumab combined with pemetrexed/cisplatin for the treatment of malignant pleural effusion in patients with epidermal growth factor receptor-/anaplastic lymphoma kinase-lung adenocarcinoma**

Yi Cheng, Nan Huang, Kai Qin, Jing Zhao, Huihua Xiong, Shiyong Yu, Tingting Huang, Qiuyun Guo 53

**MyD88 exacerbates immunological pathology in experimental viral fulminant hepatitis**

Jianzhao Deng, Qin Ning, Weiming Yan, Xuan Yang, Lizhen Zhao, Yuzhang Wu, Bei Zhang 58

**Prognostic significance of PD-L1 expression in patients with colorectal cancer: a meta-analysis**

Siwen Liu, Rong Ma, Haixia Cao, Dan Chen, Changwen Jing, Zhuo Wang, Junying Zhang, Yang Wu, Jifeng Feng, Jianzhong Wu 68

**Clinical significance of *BRAF*<sup>V600E</sup> and *TERT* promoter mutation in papillary thyroid microcarcinoma**

Jincai Xue, Qinjiang Liu, Youxin Tian, Xiaofeng Hou 75

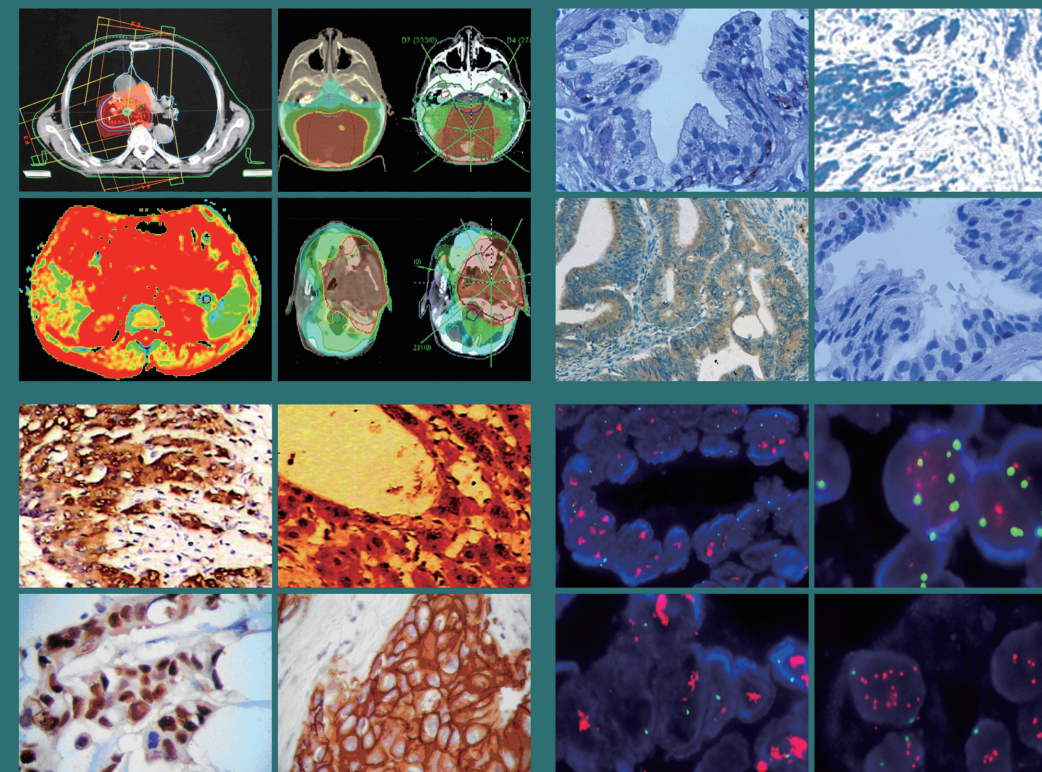
Oncology and Translational Medicine

Volume 5 • Number 2 • April 2019

pp 53-101

# Oncology and Translational Medicine

ISSN 2095-9621  
CN 42-1865/R



**Online First**  
Immediately Online

[otm.tjh.com.cn](http://otm.tjh.com.cn)

Faster  
publication!

邮发代号: 38-121

ISSN 2095-9621



9 772095 962198



GENERAL INFORMATION  
>> [otm.tjh.com.cn](http://otm.tjh.com.cn)

Volume 5  
Number 2  
April 2019





## Honorary Editors-in-Chief

W.-W. Höpker (Germany)  
Mengchao Wu (China)  
Yan Sun (China)

## Editors-in-Chief

Anmin Chen (China)  
Shiying Yu (China)

## Associate Editors

Yilong Wu (China)  
Shukui Qin (China)  
Xiaoping Chen (China)  
Ding Ma (China)  
Hanxiang An (China)  
Yuan Chen (China)

## Editorial Board

A. R. Hanauske (Germany)  
Adolf Grünert (Germany)  
Andrei Iagaru (USA)  
Arnulf H. Hölscher (Germany)  
Baoming Yu (China)  
Bing Wang (USA)  
Binghe Xu (China)  
Bruce A. Chabner (USA)  
Caicun Zhou (China)  
Ch. Herfarth (Germany)  
Changshu Ke (China)  
Charles S. Cleeland (USA)  
Chi-Kong Li (China)  
Chris Albanese (USA)  
Christof von Kalle (Germany)  
D Kerr (United Kingdom)  
Daoyu Hu (China)  
Dean Tian (China)  
Di Chen (USA)  
Dian Wang (USA)  
Dieter Hoelzer (Germany)  
Dolores J. Schendel (Germany)  
Dongfeng Tan (USA)  
Dongmin Wang (China)  
Ednin Hamzah (Malaysia)  
Ewerbeck Volker (Germany)  
Feng Li (China)  
Frank Elsner (Germany)  
Gang Wu (China)  
Gary A. Levy (Canada)  
Gen Sheng Wu (USA)  
Gerhard Ehninger (Germany)  
Guang Peng (USA)  
Guangying Zhu (China)  
Gunther Bastert (Germany)  
Guoan Chen (USA)

Guojun Li (USA)  
Guoliang Jiang (China)  
Guoping Wang (China)  
H. J. Biersack (Germany)  
Helmut K. Seitz (Germany)  
Hongbing Ma (China)  
Hongtao Yu (USA)  
Hongyang Wang (China)  
Hua Lu (USA)  
Huaqing Wang (China)  
Hubert E. Blum (Germany)  
J. R. Siewert (Germany)  
Ji Wang (USA)  
Jiafu Ji (China)  
Jianfeng Zhou (China)  
Jianjie Ma (USA)  
Jianping Gong (China)  
Jihong Wang (USA)  
Jilin Yi (China)  
Jin Li (China)  
Jingyi Zhang (Canada)  
Jingzhi Ma (China)  
Jinyi Lang (China)  
Joachim W. Dudenhausen (Germany)  
Joe Y. Chang (USA)  
Jörg-Walter Bartsch (Germany)  
Jörg F. Debatin (Germany)  
JP Armand (France)  
Jun Ma (China)  
Karl-Walter Jauch (Germany)  
Katherine A. Siminovitch (Canada)  
Kongming Wu (China)  
Lei Li (USA)  
Lei Zheng (USA)  
Li Zhang (China)  
Lichun Lu (USA)  
Lili Tang (China)  
Lin Shen (China)  
Lin Zhang (China)  
Lingying Wu (China)  
Luhua Wang (China)  
Marco Antonio Velasco-Velázquez (Mexico)  
Markus W. Büchler (Germany)  
Martin J. Murphy, Jr (USA)  
Mathew Casimiro (USA)  
Matthias W. Beckmann (Germany)  
Meilin Liao (China)  
Michael Buchfelder (Germany)  
Norbert Arnold (Germany)  
Peter Neumeister (Austria)  
Qing Zhong (USA)  
Qinghua Zhou (China)

Qingyi Wei (USA)  
Qun Hu (China)  
Reg Gorczynski (Canada)  
Renyi Qin (China)  
Richard Fielding (China)  
Rongcheng Luo (China)  
Shenjiang Li (China)  
Shenqiu Li (China)  
Shimosaka (Japan)  
Shixuan Wang (China)  
Shun Lu (China)  
Sridhar Mani (USA)  
Ting Lei (China)  
Ulrich Sure (Germany)  
Ulrich T. Hopt (Germany)  
Ursula E. Seidler (Germany)  
Uwe Kraeuter (Germany)  
W. Hohenberger (Germany)  
Wei Hu (USA)  
Wei Liu (China)  
Wei Wang (China)  
Weijian Feng (China)  
Weiping Zou (USA)  
Wenzhen Zhu (China)  
Xianglin Yuan (China)  
Xiaodong Xie (China)  
Xiaohua Zhu (China)  
Xiaohui Niu (China)  
Xiaolong Fu (China)  
Xiaoyuan Zhang (USA)  
Xiaoyuan (Shawn) Chen (USA)  
Xichun Hu (China)  
Ximing Xu (China)  
Xin Shelley Wang (USA)  
Xishan Hao (China)  
Xiuyi Zhi (China)  
Ying Cheng (China)  
Ying Yuan (China)  
Yixin Zeng (China)  
Yongjian Xu (China)  
You Lu (China)  
Youbin Deng (China)  
Yuankai Shi (China)  
Yuguang He (USA)  
Yuke Tian (China)  
Yunfeng Zhou (China)  
Yunyi Liu (China)  
Yuquan Wei (China)  
Zaide Wu (China)  
Zefei Jiang (China)  
Zhangqun Ye (China)  
Zhishui Chen (China)  
Zhongxing Liao (USA)

# Oncology and Translational Medicine

April 2019 Volume 5 Number 2

## Contents

Comparison of intra-pleural injection efficacy between Endostar and Bevacizumab combined with pemetrexed/cisplatin for the treatment of malignant pleural effusion in patients with epidermal growth factor receptor-/anaplastic lymphoma kinase-lung adenocarcinoma

*Yi Cheng, Nan Huang, Kai Qin, Jing Zhao, Huihua Xiong, Shiyong Yu, Tingting Huang, Qiuyun Guo* 53

*MyD88* exacerbates immunological pathology in experimental viral fulminant hepatitis

*Jianzhao Deng, Qin Ning, Weiming Yan, Xuan Yang, Lizhen Zhao, Yuzhang Wu, Bei Zhang* 58

Prognostic significance of PD-L1 expression in patients with colorectal cancer: a meta-analysis

*Siwen Liu, Rong Ma, Haixia Cao, Dan Chen, Changwen Jing, Zhuo Wang, Junying Zhang, Yang Wu, Jifeng Feng, Jianzhong Wu* 68

Clinical significance of *BRAF*<sup>V600E</sup> and *TERT* promoter mutation in papillary thyroid microcarcinoma

*Jincai Xue, Qinjiang Liu, Youxin Tian, Xiaofeng Hou* 75

Safety and efficacy of EGFR and VEGF signaling pathway inhibition therapy in patients with colorectal cancer: a meta-analysis

*Siwen Liu, Rong Ma, Haixia Cao, Shaorong Yu, Dan Chen, Changwen Jing, Zhuo Wang, Junying Zhang, Jifeng Feng, Jianzhong Wu* 80

Investigation of therapeutic modalities of G719X, an uncommon mutation in the EGFR gene in non-small cell lung cancer

*Hua Zheng (Co-first author), Yuan Gao (Co-first author), Zan Liu (Co-first author), Zhe Qian, Tongmei Zhang, Jie Li, Hongmei Zhang, Qunhui Wang, Fanbin Hu, Baolan Li* 91

Brown tumor of the femur and ulna in a woman with hyperparathyroidism

*Lu Jiang, Yi Huang, Yazhou Han* 98

Contribution Invitation of Oncology and Translational Medicine /

# Oncology and Translational Medicine

## Aims & Scope

**Oncology and Translational Medicine** is an international professional academic periodical. The Journal is designed to report progress in research and the latest findings in domestic and international oncology and translational medicine, to facilitate international academic exchanges, and to promote research in oncology and translational medicine as well as levels of service in clinical practice. The entire journal is published in English for a domestic and international readership.

## Copyright

Submission of a manuscript implies: that the work described has not been published before (except in form of an abstract or as part of a published lecture, review or thesis); that it is not under consideration for publication elsewhere; that its publication has been approved by all co-authors, if any, as well as – tacitly or explicitly – by the responsible authorities at the institution where the work was carried out.

The author warrants that his/her contribution is original and that he/she has full power to make this grant. The author signs for and accepts responsibility for releasing this material on behalf of any and all co-authors. Transfer of copyright to Huazhong University of Science and Technology becomes effective if and when the article is accepted for publication. After submission of the Copyright Transfer Statement signed by the corresponding author, changes of authorship or in the order of the authors listed will not be accepted by Huazhong University of Science and Technology. The copyright covers

the exclusive right and license (for U.S. government employees: to the extent transferable) to reproduce, publish, distribute and archive the article in all forms and media of expression now known or developed in the future, including reprints, translations, photographic reproductions, microform, electronic form (offline, online) or any other reproductions of similar nature.

## Supervised by

Ministry of Education of the People's Republic of China.

## Administered by

Tongji Medical College, Huazhong University of Science and Technology.

## Submission information

Manuscripts should be submitted to:  
<http://otm.tjh.com.cn>  
[dmedizin@sina.com](mailto:dmedizin@sina.com)

## Subscription information

ISSN edition: 2095-9621  
CN: 42-1865/R

### ■ Subscription rates

Subscription may begin at any time. Remittances made by check, draft or express money order should be made payable to this journal. The price for 2017 is as follows: US \$ 30 per issue; RMB ¥ 28.00 per issue.

## Database

**Oncology and Translational Medicine** is abstracted and indexed in EM-BASE, Index Copernicus, Chinese Science and Technology Paper Citation Database (CSTPCD), Chinese Core Journals Database, Chinese Journal Full-text Database (CJFD), Wanfang

Data; Weipu Data; Chinese Academic Journal Comprehensive Evaluation Database.

## Business correspondence

All matters relating to orders, subscriptions, back issues, offprints, advertisement booking and general enquiries should be addressed to the editorial office.

## Mailing address

Editorial office of  
*Oncology and Translational Medicine*  
Tongji Hospital  
Tongji Medical College  
Huazhong University of Science and Technology  
Jie Fang Da Dao 1095  
430030 Wuhan, China  
Tel.: +86-27-69378388  
Email: [dmedizin@sina.com](mailto:dmedizin@sina.com)

## Printer

Changjiang Spatial Information Technology Engineering Co., Ltd. (Wuhan)  
Hangce Information Cartography Printing Filial, Wuhan, China  
Printed in People's Republic of China

## Managing director

Jun Xia

## Executive editors

Jing Chen  
Yening Wang  
Jun Xia  
Qiang Wu

# Comparison of intra-pleural injection efficacy between Endostar and Bevacizumab combined with pemetrexed/cisplatin for the treatment of malignant pleural effusion in patients with epidermal growth factor receptor-/anaplastic lymphoma kinase-lung adenocarcinoma\*

Yi Cheng<sup>1</sup>, Nan Huang<sup>2</sup>, Kai Qin<sup>1</sup>, Jing Zhao<sup>1</sup>, Huihua Xiong<sup>1</sup>, Shiyong Yu<sup>1</sup>, Tingting Huang<sup>1</sup>, Qiuyun Guo<sup>1</sup> (✉)

<sup>1</sup> Department of Oncology, Tongji Hospital, Tongji Medical College, Huazhong University of Science and Technology, Wuhan 430030, China

<sup>2</sup> Allergy Department, Tongji Hospital, Tongji Medical College, Huazhong University of Science and Technology, Wuhan 430030, China

## Abstract

**Objective** To compare intra-pleural injection efficacy and safety between Endostar and bevacizumab combined with pemetrexed/cisplatin for the treatment of malignant pleural effusion in patients with epidermal growth factor receptor (EGFR)-/anaplastic lymphoma kinase (ALK)-lung adenocarcinoma.

**Methods** Sixty-four patients with EGFR-/ALK- lung adenocarcinoma with malignant pleural effusion (MPE) were admitted to the authors' hospital between January 2016 and June 2017. Patients were randomly divided into two groups: Endostar combined with pemetrexed/cisplatin (Endostar group); and bevacizumab plus pemetrexed/cisplatin (Bevacizumab group). They underwent thoracic puncture and catheterization, and MPE was drained as much as possible. Both groups were treated with pemetrexed 500 mg/m<sup>2</sup>, intravenous drip (d1), cisplatin 37.5 mg/m<sup>2</sup> per time, intra-pleural injection (d1, d3). Patients in the Endostar group were treated with Endostar 30 mg per time, intra-pleural injection (d1, 3), and patients in the Bevacizumab group were treated with bevacizumab 5 mg/kg per time, intra-pleural injection (d1). Only one cycle of treatment was applied. MPE was extracted before treatment and on day 7 after treatment. The levels of vascular endothelial growth factor (VEGF) were determined using ELISA. Efficacy and side effects were evaluated according to the Response Evaluation Criteria in Solid Tumors (RECIST) version 1.1, and National Cancer Institute Common Terminology Criteria for Adverse Events (CTCAE) version 3.0 criteria.

**Results** The objective response rates in the Endostar and Bevacizumab groups were 50.0% and 56.3%, respectively; there was no statistical difference between the groups ( $P > 0.05$ ). After one cycle of treatment, the mean VEGF levels in MPE in both groups decreased significantly, and there was no significant difference in the degree of decline between the two groups ( $P > 0.05$ ). In both groups, pre-treatment VEGF levels for patients achieving complete response were significantly higher than those for patients achieving stable disease + progressive disease ( $P < 0.05$ ). No specific side effects were recorded.

**Conclusion** Endostar and Bevacizumab demonstrated similar efficacy in controlling MPE in patients with EGFR-/ALK- lung adenocarcinoma through an anti-angiogenesis pathway, with tolerable side effects. The levels of VEGF in MPE could predict the efficacy of intra-pleural injection of anti-angiogenesis drugs.

**Key words:** Endostar; bevacizumab; malignant pleural effusion; EGFR-/ALK-lung adenocarcinoma; cisplatin; pemetrexed; intra-pleural injection

Received: 29 March 2019

Revised: 17 April 2019

Accepted: 25 April 2019

✉ Correspondence to: Qiuyun Guo. Email: happyyun.1985@163.com

\* Supported by a grant from the Nature Science Foundation of Hubei Province, China (No. 2017CFB472).

© 2019 Huazhong University of Science and Technology

Malignant pleural effusion (MPE) is a common complication of lung cancer. Fifteen percent of newly diagnosed lung cancer patients experience MPE, which seriously affects quality of life, and suggests that the median survival time of patients is approximately 3.3 months, with a poor prognosis depending on the tumor subtype tumor and its clinical stage. For advanced non-small cell lung cancer (NSCLC), the incidence is as high as 50%, which can cause respiratory and circulatory failure, seriously affecting safety<sup>[1]</sup>. Presently, local therapeutic treatment approaches for MPE in patients with NSCLC mainly include thoracic puncture and drainage, and intra-pleural injection of drugs. Chemotherapeutic drugs are widely used, although with limited efficacy.

Vascular endothelial growth factor (VEGF) has been found to be a critical pathological factor in the occurrence and development of MPE. It can promote capillary permeability and angiogenesis. The levels of VEGF are significantly increased in MPE caused by lung cancer, mesothelioma, and breast cancer. Both endostatin and bevacizumab can inhibit VEGF. Clinical trials have shown that intra-pleural injection of either drug combined with cisplatin can effectively control MPE; however, the preferred agent remains unclear<sup>[2]</sup>. The purpose of this study was to compare intra-pleural injection efficacy and safety between Endostar and bevacizumab combined with pemetrexed/cisplatin in the treatment of MPE in patients with epidermal growth factor receptor (EGFR)-/anaplastic lymphoma kinase (ALK)- lung adenocarcinoma lung adenocarcinoma, and to preliminarily evaluate the utility of both drugs in the treatment of MPE.

## Materials and methods

### Baseline

Sixty-four patients with EGFR-/ALK- lung adenocarcinoma with MPE were admitted to the authors' hospital between January 2016 and June 2017. All patients were diagnosed with pathologically confirmed adenocarcinoma, and EGFR-/ALK- using gene detection methods. After providing informed consent, the patients were randomly divided into two groups: Endostar combined with pemetrexed/cisplatin group (Endostar group); and bevacizumab plus pemetrexed/cisplatin group (Bevacizumab group). General information for the two groups is summarized in Table 1.

**Table 1** Characteristic of patients

Group	n	Male/Female	Age (years)	ECOG		
				0	1	2
Endostar	32	18/14	58.2 (44–67)	1	25	6
Bevacizumab	32	17/17	57.8 (43–68)	0	27	5

## Inclusion and exclusion criteria

### Inclusion criteria

All patients with EGFR-/ALK-lung adenocarcinoma were confirmed by histopathology; pleural effusion was moderate to large detected by computed tomography or ultrasound; malignant tumor cells were found in the effusion fluid; and routine blood, cardiac function, liver and kidney function, and electrolyte levels were normal.

### Exclusion criteria

Patients with organ dysfunction, such as liver and kidney, those with a history of neurological or psychiatric disorders, and pregnant or lactating women, were excluded from this study.

## Protocol

All patients underwent thoracic puncture and catheterization monitored by ultrasound. MPE was drained as much as possible within 2 to 3 days. Both groups were treated with pemetrexed 500 mg/m<sup>2</sup>, intravenous drip (d1), cisplatin 37.5 mg/m<sup>2</sup> per time, intra-pleural injection (d1, d3). Patients in the Endostar group were treated with Endostar 30 mg per time, intra-pleural injection (d1, 3), and patients in the Bevacizumab group were treated with bevacizumab 5 mg/kg per time, intra-pleural injection (d1). All patients were turned over every 20 min within a 2 h period after intra-pleural injection. Ultrasound was used to re-examine the MPE volume on day 21.

Three milliliters of MPE was extracted before treatment and on day 7 after treatment. The supernatant was centrifuged at 4000 rpm for 10 min at 4 °C. VEGF levels were determined using ELISA. The Human VEGF-A ELISA kit was purchased from R&D Systems (Minneapolis, MN, USA), and the microplate reader from Bio Rad Laboratories (Hercules, CA, USA).

## Endpoints

### Objective efficacy

Objective efficacy was evaluated according to the Response Evaluation Criteria in Solid Tumors (RECIST) version 1.1 criteria: Complete remission (CR), pleural effusion completely disappeared, lasting > 4 weeks; partial remission (PR), the amount of pleural effusion decreased > 30% compared with pre-treatment (based on the maximum depth of pleural effusion detected by ultrasound), lasting > 4 weeks; stable disease (SD), the amount of pleural effusion decreased by < 30% or increased by < 20% compared with pre-treatment; Progressive disease (PD), the amount of pleural effusion increased by > 20% compared with pre-treatment. The objective response rate (ORR) was calculated as: CR + PR. Side effects were evaluated according to National Cancer Institute Common Terminology Criteria for Adverse Events (CTCAE) version 3.0 criteria.

### Statistical analysis

SPSS version 16.0 (IBM Corporation, Chicago, IL, USA) was used to analyze the data. Numerical data are expressed as mean ( $\pm$  standard deviation), and the *t*-test was used for comparisons. Categorical data are expressed as percentage, and the  $\chi^2$  test was used for comparisons; *P* < 0.05 was considered to be statistically significant.

## Results

### Comparison of clinical efficacy between the two groups

After the treatment period, 2 of 32 patients in the Endostar group achieved CR, 14 achieved PR, and the ORR was 50.0%. In the Bevacizumab group, 3 patients achieved CR, 15 achieved PR, and the ORR was 56.3%. There was no statistical difference between the two groups (*P* > 0.05) (Table 2).

### Relationship between VEGF levels in MPE and efficacy in the two groups

Before treatment, the mean VEGF level in MPE was 405.33  $\pm$  127.78 pg/mL in the Endostar group and 402.87  $\pm$  129.28 pg/mL in the Bevacizumab group; there was no statistically significant difference between the two groups (i.e., *P* > 0.05). After one cycle of treatment, the mean value of VEGF levels in MPE in both groups decreased significantly, with no significant difference in the degree of decline between the two groups (*P* > 0.05) (Table 3). Further analysis revealed that in both groups, pre-treatment VEGF levels in patients achieving CR were significantly higher than those in patients achieving SD + PD (*P* < 0.05) (Table 4).

### Side effects

In the Endostar group, changes in T wave and ST-T segment of electrocardiogram, and diarrhea or rash did not occur. In the Bevacizumab group, no mucosal hemorrhage or hemorrhage occurred at the orifice of the thoracic drainage catheter, and no proteinuria occurred. In the bevacizumab group, there were 3 patients with hypertension grade I and 3 patients with hypertension grade 2. Blood pressure was evenly controlled during treatment. There were no significant differences in digestive tract reactions, such as bone marrow suppression, liver and kidney dysfunction, or nausea and vomiting, between the two groups.

**Table 2** Comparison of clinical efficacy between two groups (*n*, %)

Group	<i>n</i>	CR	PR	SD + PD	ORR
Endostar	32	2	14	16	50.0%
Bevacizumab	32	3	15	14	56.3%*

\**P* > 0.05

**Table 3** The change in VEGF levels pre- and post-treatment (pg/mL,  $\bar{x} \pm s$ )

Group	<i>n</i>	pre-treatment	post-treatment
Endostar	32	405.33 $\pm$ 127.78	200.56 $\pm$ 64.10
Bevacizumab	32	402.87 $\pm$ 129.28	198.73 $\pm$ 63.85*

\**P* > 0.05 compared with Endostar group

**Table 4** The relationship between pre-treatment VEGF levels in MPE and efficacy (pg/mL,  $\bar{x} \pm s$ )

Group	<i>n</i>	CR	PR	SD + PD
Endostar	32	452.19 $\pm$ 18.27	407.64 $\pm$ 72.07	300.23 $\pm$ 25.16*
Bevacizumab	32	450.27 $\pm$ 16.68	409.43 $\pm$ 63.85	280.89 $\pm$ 12.86*

\**P* < 0.05 compared with patients achieving CR

## Discussion

MPE, a type of malignant serous cavity effusion, refers to the abnormal increase of pleural fluid caused by malignant tumors involving the pleura or primary pleural tumors. MPE accounts for 25% of pleural effusion, 75% of which is caused by lung cancer, breast cancer, or lymphoma. Factors such as VEGF and matrix metalloproteinases (MMPs), which can induce vascular permeability, play a key role in the pathophysiological mechanism of MPE formation. Tumor cells can secrete autocrine VEGF and MMPs, both of which increase the permeability of the capillary network and, on the other hand, and promote neovascularization of tumors, and then increase the total infiltration area of the capillary intima [2]. In animal models, the levels of VEGF in MPE increased significantly. The increase in peritoneal microvascular permeability was observed in tumor-bearing mice, which were injected with exogenous VEGF, while ascites formation was inhibited when the mice were transfected with antisense oligonucleotides of VEGF [3]. It was also found that there was a significant increase of VEGF in MPE samples from patients with NSCLC who were at higher risk for distant metastasis [4]. Elevated messenger RNA expression levels of VEGF and endostatin in pleural effusion were more frequently detected in MPE than in pleural effusions caused by non-malignant diseases [5]. These studies provide new avenues for the treatment of malignant serous cavity effusion, especially MPE, in patients with NSCLC and high levels of VEGF.

Presently, the clinical treatment of MPE includes diuresis, restriction of sodium chloride intake, and systemic treatment, among others. Local treatment includes thoracic puncture and catheterization, intra-pleural administration of drugs, intra-pleural hyperthermic perfusion and surgical treatment. Many types of drug could be chosen for intra-pleural injection, with each having its own advantages and disadvantages.

Chemotherapeutic drugs often cause bone marrow suppression and digestive tract reactions; biological agents can cause fever; and pleural adhesion induced by talcum powder and other pleurodesis agents can cause pain and fever [2]. In contrast, with an improved understanding of the pathogenesis of MPE, anti-angiogenesis drugs targeting VEGF have attracted increasing attention due to their unique advantages of strong efficacy and fewer side effects. Of all these novel drugs, recombinant human endostatin (Endostar) and the monoclonal VEGF antibody bevacizumab have demonstrated promising therapeutic benefits for patients with NSCLC and MPE.

Endostar, a modification of endostatin, has many targets, including VEGF and fibroblast growth factor-beta, which can specifically act on vascular endothelial cells of newly formed blood vessels, inhibit endothelial cell migration, induce endothelial cell apoptosis and, thus, inhibit the growth of tumor vessels. Qin *et al* [6] performed a prospective, randomized controlled, national multi-center phase III clinic trial on intra-pleural injection of Endostar and/or cisplatin for the treatment of MPE and malignant ascites. The results showed that for MPE, the ORR of the combined group was 42%, which was significantly higher than that of the Endostar (32%) and cisplatin (22%) groups. The result is consistent with a series of small sample studies [7-10]. However, there remains a lack of consensus on what the dose, interval, and course should be for the administration of the drug. There has been no report on the evaluation of efficacy of intra-pleural administration of Endostar combined with cisplatin in systemic chemotherapy. Feng *et al* found that Endostar combined with cisplatin for the treatment of MPE in patients with NSCLC could reduce the levels of VEGF and HIF-1 $\alpha$  in MPE [8], which was consistent with the findings of Zou *et al* [9].

Bevacizumab, a recombinant, humanized monoclonal anti-VEGFA antibody, was approved for use as first-line treatment for advanced non-squamous NSCLC by the United States Food and Drug Administration in 2006. Ma *et al* found that intra-pleural administration of bevacizumab alone was superior to cisplatin alone for the treatment of MPE and malignant ascites [11]. Han *et al* found that intra-pleural administration of bevacizumab combined with cisplatin was superior to cisplatin alone in the treatment of MPE when pemetrexed was intravenously administered. After one cycle of chemotherapy, the ORR in the bevacizumab group was 55.0%, which was higher than chemotherapy group (31.8%) [12]. Lower dose (5 mg/kg) of intra-pleural administration can also achieve better results, which was different from the 15 mg/kg dosage of intravenous chemotherapy [12-13]. Different studies have suggested that bevacizumab combined with cisplatin could effectively reduce the levels of VEGF in MPE [12-14]. Zhang *et al* found that inflammatory factors (interleukin

[IL]-4 and IL-10) also decreased, suggesting that bevacizumab controls MPE through various pathways [14].

This was the first phase II study of intra-pleural injection of Endostar or bevacizumab combined with pemetrexed/cisplatin for the treatment of MPE in patients with EGFR-/ALK- lung adenocarcinoma. Only one cycle of therapy was applied. Pemetrexed/cisplatin is the standard first-line treatment for advanced EGFR-/ALK- lung adenocarcinoma, and anti-angiogenesis drugs can further improve its effect. Our results demonstrated no significant difference in the control of MPE between the two groups. The levels of VEGF in the pleural effusion fluid of both groups decreased significantly after treatment, but there was no significant difference in the degree of decline between the two groups. It was confirmed again that Endostar and bevacizumab had similar efficacy in controlling MPE through an anti-angiogenesis pathway. Previous studies have confirmed that the levels of VEGF in pleural effusion may be a predictor of efficacy for both drugs in controlling MPE [8-9, 12-14]. This study also confirmed that patients with higher levels of VEGF in pleural effusion before chemotherapy in both groups were more likely to benefit from anti-angiogenesis drugs to a similar extent. There was no difference in side effects between the two groups, and there were no specific side effects, suggesting that the use of anti-angiogenesis drugs in intra-pleural administration is safe and may be superior to intravenous methods.

There were several limitations to this study, the first of which was its small sample size. Patients underwent only one cycle of treatment, and whether both drugs have the same efficacy in controlling MPE under multi-course medication requires further study. Although currently used dosages of bevacizumab have been established, further adjustments may be necessary; however, the dose, interval, and course of Endostar remain unclear. Whether the two drugs can alleviate MPE to a greater extent after adjusting the regimen remains to be clarified. Some studies have suggested that hyperthermic perfusion chemotherapy may be a more advantageous method and, as such, adjusting the method of administration may be an option [15]. The patients were tested for the EGFR and ALK genes, but not for immunotherapy. Therefore, it is not clear whether they are more suitable for molecular-therapy targeting other genes and immunotherapy than for chemotherapy. Future studies investigating the efficacy of intra-pleural injection of anti-angiogenesis drugs when molecular-targeted therapy or immunotherapy is applied are warranted.

### Conflicts of interest

The authors declare no conflict of interest.

## References

1. Sugiura S, Ando Y, Minami H, *et al.* Prognostic value of pleural effusion in patients with non-small cell lung cancer. *Clin Cancer Res*, 1997, 3: 47–50.
2. Chen Y, Mathy NW, Lu H. The role of VEGF in the diagnosis and treatment of malignant pleural effusion in patients with nonsmall cell lung cancer (Review). *Mol Med Rep*, 2018, 17: 8019–8030.
3. Byrne AT, Ross L, Holash J, *et al.* Vascular endothelial growth factor-trap decreases tumor burden, inhibits ascites, and causes dramatic vascular remodeling in an ovarian cancer model. *Clin Cancer Res*, 2003, 9: 5721–5728.
4. Hsu LH, Hsu PC, Liao TL, *et al.* Pleural fluid osteopontin, vascular endothelial growth factor, and urokinase-type plasminogen activator levels as predictors of pleurodesis outcome and prognosticators in patients with malignant pleural effusion: a prospective cohort study. *BMC Cancer*, 2016, 16: 463.
5. Fafiora E1, Hatzoglou C1,2,3, Gourgoulialis KI, *et al.* Systematic review and meta-analysis of vascular endothelial growth factor as a biomarker for malignant pleural effusions. *Physiol Rep*, 2016, 4: e12978.
6. Qin SK, Yang LQ, Liang J, *et al.* Intra-pleural injection of recombinant human endostatin and/or cisplatin in treatment of malignant hydrothorax and ascites: A multicenter randomized controlled trial. *Chin Clin Oncol (Chinese)*, 2017, 22: 193–202.
7. Zhao QH, Ouyang XH, Li KS, *et al.* Observe the curative effect in the treatment of malignant pleural effusion intrapleural injection of Endostar. *J Clin Med*, 2017, 1: 14–15.
8. Feng ZY. Effect of Endostar combined with cisplatin on platelet parameters and levels of VEGF, HIF-1  $\alpha$  in the treatment of malignant pleural effusion in patients with non-small cell lung cancer. *Henan Med Res (Chinese)*, 2017, 24: 4454–4455.
9. Zou JT, Hu ZZ, Chen YL. Clinical efficacy and adverse reactions of cisplatin combined with Endostar thoracic perfusion in the treatment of malignant pleural effusion of lung cancer. *Chin Mod Med (Chinese)* 2016, 24: 22–24.
10. Wu Q, Cai XF, Fang XH. Clinical observation of recombinant humanized endostatin in the treatment of malignant pleural effusion. *J Basic Clin Oncol (Chinese)*, 2017, 1: 61–62.
11. Ma J. Intrapleural and intraperitoneal combination therapy with bevacizumab and cisplatin for malignant pleural effusion and ascites. Dalian: Dalian Medical University, 2014: 1–37.
12. Han N, Zhang MX, Yu SY, *et al.* Efficacy of bevacizumab in combination with cisplatin and pemetrexed in treatment of malignant pleural effusion in patients with non-squamous non-small cell lung cancer. *Acta Med Univ Sci Technol Huazhong (Chinese)*, 2013, 5: 588–591.
13. Bai M. Efficacy of bevacizumab combined with cisplatin in the treatment of malignant pleural effusion in non-small cell lung cancer. *Henan Med Res (Chinese)*, 2017, 4: 672–673.
14. Zhang ZJ, Xu C, Hu YZ, *et al.* Application of bevacizumab combined with chemotherapy for malignant pleural effusion in non-small cell lung cancer patients. *Pract J Cancer (Chinese)*, 2018, 7: 1155–1157.
15. Zang MQ, Ren JL, Chen WT, *et al.* Hyperthermic perfusion chemotherapy combined with bevacizumab for treatment of malignant ascites or pleural effusion: a meta-analysis of efficacy. *Cancer Res Clin (Chinese)*, 2018, 7: 481–486.

DOI 10.1007/s10330-019-0347-7

Cite this article as: Cheng Y, Huang N, Qin K, *et al.* Comparison of intra-pleural injection efficacy between Endostar and Bevacizumab combined with pemetrexed/cisplatin for the treatment of malignant pleural effusion in patients with epidermal growth factor receptor-/anaplastic lymphoma kinase-lung adenocarcinoma. *Oncol Transl Med*, 2019, 5: 53–57.

# *MyD88* exacerbates immunological pathology in experimental viral fulminant hepatitis\*

Jianzhao Deng<sup>1</sup>, Qin Ning<sup>2</sup>, Weiming Yan<sup>2</sup>, Xuan Yang<sup>1</sup>, Lizhen Zhao<sup>1</sup>, Yuzhang Wu<sup>3</sup> (✉), Bei Zhang<sup>1</sup> (✉)

<sup>1</sup> Department of Immunology, Medical College of Qingdao University, 308 NingXia Road, Qingdao 266071, China

<sup>2</sup> Institute of Infectious Disease, Tongji Hospital of Tongji Medical College, Huazhong University of Science and Technology, Wuhan 430030, China

<sup>3</sup> Institute of Immunology, Army Medical University, Chongqing 400038, China

## Abstract

**Objective** To explore the role of *MyD88* signaling in MHV-3 virus-mediated fulminant hepatitis.

**Methods** We evaluated liver lesion status, the expression of multiple pro-inflammatory cytokines and HMGB1, the recruitment of inflammatory ILC3, and mortality in *MyD88*<sup>-/-</sup> and WT mice.

**Results** The expression of multiple pro-inflammatory cytokines that recruit inflammatory ILC3 to the liver was severely impaired in *MyD88*<sup>-/-</sup> mice resulting in reduced liver pathology, viral replication, and mortality post-infection. Additionally, MHV-3 markedly increased the expression of high-mobility group box 1 (HMGB1) in infected hepatocytes/macrophages and induced HMGB1 protein migration from the nucleus to the extracellular milieu, where it activates *MyD88*-dependent inflammation.

**Conclusion** Our findings indicate that *MyD88* exacerbates immunological pathology in experimental viral fulminant hepatitis.

**Key words:** *MyD88*; MHV-3; HMGB1; ILC3

Received: 9 January 2019  
Revised: 10 March 2019  
Accepted: 27 March 2019

Severe viral hepatitis is a disease with a large annual mortality rate. Its main clinical symptoms are massive necrosis of hepatocytes and hepatic encephalopathy. The development of clinically effective interventions has been hindered by insufficient understanding of the immune mechanism of severe viral hepatitis (FH). It was recently found that when BALB/cJ and C57BL/6 mice were infected with mouse hepatitis virus strain-3 (MHV-3), mononuclear/macrophage-specific coagulant and fibrinogen-like protein-2 (FGL2) were up-regulated and the coagulation cascade was activated *in vivo*, resulting in hepatic sinus thrombosis and hepatocyte necrosis. This phenomenon, called virus-induced “procoagulant activity”, is very similar to the clinical manifestations of FH patients [1–3]. Therefore, we used FH animal models infected with MHV-3 to explore the pathogenesis of severe viral hepatitis.

Pattern recognition receptors (PRRs) are key to the early detection of invading pathogens. PRRs are activated

by specific pathogen-associated molecular patterns (PAMPs) that are present in pathogenic microbes or the nucleic acids of viruses or bacteria [4]. Toll-like-receptors (TLRs), the most well-studied group of PRRs, are displayed on the cell surface or within endosomal compartments where they act as molecular sentinels to detect invading microbes [5]. Myeloid differentiation primary response gene 88 (*MyD88*) is a crucial adaptor protein in most *TLR*-dependent inflammatory signaling pathways and activation of *MyD88* leads to the induction of chemokines, inflammatory cytokines, and type I interferons (IFN) through stimulation of NF- $\kappa$ B, JNK, and p38 MAPK pathway [6]. *MyD88* signaling plays a critical role in immune responses against a wide variety of pathogens including viruses. For example, *MyD88* signaling is not required for clearance of reovirus infection after oral inoculation of mice [7], but *MyD88*-mediated inflammation induces specific antibody production and protects against influenza virus-caused

✉ Correspondence to: Yuzhang Wu. Email: wuyuzhang@tmmu.edu.cn. Bei Zhang. Email: zhangbei124@aliyun.com

\* Supported by grants from the National Natural Sciences Foundation of China (No. 81361120400 and 81222023).

© 2019 Huazhong University of Science and Technology

mortality [8-9]. Conversely, *MyD88*<sup>-/-</sup> mice infected with lymphocytic choriomeningitis virus (LCMV), vesicular stomatitis virus (VSV), respiratory syncytial virus (RSV), and a recombinant mouse-adapted SARS-CoV virus (rMA15) have more severe pathology than that of the WT [10-13]. Nevertheless, the role of *MyD88* signaling in MHV-3 virus-mediated pathogenesis has not yet been investigated.

Damage-associated molecular patterns (DAMPs), which have the capacity to activate TLRs, are substances produced by damaged or dead cells that initiate inflammatory responses in a paracrine manner [14]. High-mobility group box 1 (HMGB1), a non-histone chromatin-associated nuclear protein, is a classic DAMP, which is highly expressed in most eukaryotic cells. Within the nucleus, HMGB1 acts as an architectural protein that binds to DNA and promotes the assembly of nucleoprotein complexes, thereby facilitating maintenance of genome stability [15-16]. Conversely, exogenous stimulation, including pathogen infection, can lead to cytoplasmic translocation of HMGB1 and its subsequent release into the extracellular milieu [17]. Cytoplasmic translocation and release of HMGB1 by virus-infected cells has been reported following infection with Dengue virus, HIV, West Nile virus (WNV), herpes simplex virus type 2 (HSV-2), hepatitis C virus (HCV), and porcine reproductive and respiratory syndrome virus (PRRSV) [18]. HMGB1 concentrations were significantly higher in patients infected with WNV and HCV [19-20]. Additionally, HMGB1 also supports influenza virus growth by enhancing the activity of viral polymerases [21]. However, whether HMGB1 participates in the pathogenesis of MHV-3 as a host-derived molecular factor remains to be determined.

In a mouse model of FH caused by MHV-3 infection, we found that MHV-3 markedly increased the expression of HMGB1 in infected cells and induced the migration of HMGB1 protein from the nucleus to the extracellular milieu, where it activated *MyD88*-dependent inflammation. Therefore, mice deficient in *MyD88* (*MyD88*<sup>-/-</sup>) are resistant to MHV-3-mediated FH because of reduced expression of multiple pro-inflammatory cytokines and limited recruitment of pro-inflammatory NKp46<sup>+</sup>Lin<sup>-</sup>Thy1.2<sup>+</sup>Royt<sup>+</sup> ILC3 to the liver compared to WT littermates. This work suggests that *MyD88* may play an essential role in the pathogenesis of viral FH.

## Materials and methods

### Mice

C57BL/6 background *MyD88*-deficient (*MyD88*<sup>-/-</sup>, #009088), *IL-1RI*<sup>-/-</sup> (#003245), *TNF-α*<sup>-/-</sup> (#005540), *Rag-1*<sup>-/-</sup> (#002216) and wild type (WT) mice were imported from the Jackson Laboratory (Bar Harbor, Maine, USA).

*Trif*<sup>-/-</sup> C57BL/6 background mice were purchased from *Oriental BioService* (OBS) in Kyoto, Japan [22]. *Fgl2*<sup>-/-</sup> mice were kindly provided by Prof. Gary Levy (Multi Organ Transplant Program, University Health Network, University of Toronto, Toronto, Canada). Mice were maintained in the animal facility, fed with standard laboratory chow diet and water, and housed in the animal colony at the animal center of Army Medical University. Mice of approximately 12 weeks of age were used for these experiments.

### Cells

Raw264.7 cells were provided by the Cell Institute of the Chinese Academy of Sciences (Shanghai, China). GM-CSF-induced BMDMs and peritoneal exudative macrophages (PEMs) were prepared. Cells were cultured in 6-well plates and propagated in DMEM supplemented with 10% FBS, 100 μg/mL streptomycin, and 100 U/mL penicillin.

### Virus and infection

MHV-3 viruses were amplified in murine 17CL1 cells to a concentration of 1×10<sup>7</sup> plaque forming unit (PFU)/mL. Supernatants containing the virus were stored at -80 °C until use. Raw264.7 cells were infected with MHV-3 (multiplicity of infection, MOI = 1) in vitro and mice were injected intraperitoneally (i.p.) with 100 PFU of MHV-3. The virus titers in liver were determined by plaque assay.

### Tissue morphology detection and immunohistochemistry

Paraffin-embedded liver tissue blocks were cut into 4 μm slices. Endogenous peroxidase activity was blocked with 2.0% H<sub>2</sub>O<sub>2</sub> for 20 min. The slides were then immersed in citrate buffer (pH 6.0) for 10 min at 120 °C. Sections were then incubated overnight at 4 °C with anti-mouse FGL2 (Santa Cruz, USA, 1:100, mouse), anti-Fibrinogen (Abcam, Cambridge, England, 1:1000, Rabbit), anti-HMGB1 (Santa Cruz, USA, 1:50, mouse), anti-TNF-α (Cell Signaling Technology (CST), 1:100, rabbit), anti-IL-6 (Santa Cruz, 1:200, mouse), anti-IFN-γ (Santa Cruz, 1:200, rat), and anti-pro-IL-1β (CST, 1:100, mouse). After washing, the sections were incubated with the corresponding secondary antibodies for 2 h at room temperature. A Vectastain ABC kit (Vector Laboratories, San Diego, USA) was used to create avidin-biotin complexes, which were then visualized with a DAB kit (K3465, DAKO), where brown coloration of tissues represented positive expression. Histopathological analysis of liver was performed by hematoxylin and eosin (H&E). Cellular apoptosis was detected by TUNEL staining (Roche, Berlin, Germany) according to the manufacturer's instructions.

### Immunofluorescence staining

Paraffin-embedded tissue blocks were cut into 5 mm slices, which were mounted on polylysine-charged glass slides. Endogenous peroxidase activity was blocked with 2.0% H<sub>2</sub>O<sub>2</sub> for 25 min. The glass slides were then placed in citrate buffer (pH 6.0) for 10 min at 120 °C. Sections were then incubated overnight at 4 °C with anti-HMGB1 (eBioscience). After washing, sections were further incubated with the corresponding fluorescent secondary antibodies for an additional 1 h. Finally, the sections were incubated with 1 µg/mL DAPI (Sigma, St. Louis, MO, USA) for 10 min to stain the nuclei. Sections incubated with isotype control antibodies were used as negative controls. The results were visualized using fluorescence microscopy (Nikon, Tokyo, Japan).

### Real-time quantitative RT-PCR

TRIzol reagent (Invitrogen, NY, USA) was used to extract total RNA from cultured cells or liver tissues according to the manufacturer's instructions. Reverse transcription was used to synthesize cDNA using a PrimeScript RT-PCR Kit (Takara, Dalian, China). The expression of mRNA encoding for proinflammatory cytokines (including *TNF-α*, *IL-6*, *IFN-γ*, *fgl2*, *proIL-1β*, *HMGB1*) was quantified by real-time quantitative PCR with the SYBR Premix ExTaq kit (Takara, Kyoto, Japan) and normalized to β-actin expression. The primer sequences are shown in Table 1. Relative mRNA expression was calculated and compared by the 2<sup>-ΔΔC<sub>t</sub></sup> method.

### ELISA and western-blotting

Serum FGL2, IL-17, TNF-α, IL-1β, and HMGB1 levels were measured by ELISA. The expression of HMGB1, FGL2, TNF-α, and IL-6 in MHV-3 infected livers was detected by western-blotting.

### Flow cytometry

Liver infiltration by GR-1<sup>high</sup>CD45<sup>+</sup> neutrophils, CD11b<sup>+</sup>/F4/80<sup>+</sup> monocytes/macrophages, and NKp46<sup>+</sup> Lin<sup>-</sup>Thy1.2<sup>+</sup>Royt<sup>+</sup> ILC3, and the secretion of TNF-α, IL-6, and proIL-1β from PEMs isolated from virus-infected mice at 24 h were detected by flow cytometry (FACSARIA

cytometer, BD, Franklin Lakes, NJ, USA). Dead cells were excluded by staining with a LIVE/DEATH® Fixable Near-IR Dead Cell Stain Kit (Life technologies, Eugene, Oregon, USA). In total, 10,000 live cells were analyzed. All the FACS data were analyzed using CellQuest Pro software. These antibodies were purchased from eBioscience.

### Statistical analysis

Statistical analysis of the data was performed using GraphPad Prism 6.0. An unpaired Student's *t*-test (two-tailed) was used to compare two groups when the data met the assumptions of the *t*-test. Survival curves were generated using the log-rank test. *P* < 0.05 was considered statistically significant.

## Results

### Reduced liver tissue lesions and mortality in *MyD88*<sup>-/-</sup> mice post MHV-3 infection

To assess the contributions of innate and adaptive immune responses in MHV-3-induced FH, age matched C57BL/6 (WT, *n* = 10), congenic *Rag-1*<sup>-/-</sup> (*n* = 6), *MyD88*<sup>-/-</sup> (*n* = 11) and *Trif*<sup>-/-</sup> (*n* = 5) mice were infected with MHV-3 (100 PFU) via *i.p.* injection and monitored for virus-induced mortality. Surprisingly, we found that all the WT, *Rag-1*<sup>-/-</sup> and *Trif*<sup>-/-</sup> mice died within 8 days of infection, whereas over 72.7% (8/11) of the *MyD88*<sup>-/-</sup> group were still alive after 20 days (*P* = <0.0001, Fig. 1a). Hematoxylin and eosin (H&E) staining showed severe necrosis with sparse polymorphonuclear leucocyte infiltration in the livers of WT mice at both 48 h and 72 h post MHV-3 infection. In contrast, the morphology of *MyD88*<sup>-/-</sup> livers was mostly normal after 48 h, and the area of necrosis was also dramatically smaller at 72 h (Fig. 1b). Additionally, fewer cells were found to be apoptotic in MHV-3 infected *MyD88*<sup>-/-</sup> livers 72 h postinfection (Fig. 1c). The expression of biliary glycoprotein-1 (Bgp1), the receptor for MHV-3 [23], appeared to be significantly lower in viral infected *MyD88*<sup>-/-</sup> livers than in the WT controls (Fig. 1d), supporting the plaque assay showing limited virus entry and amplification in *MyD88*<sup>-/-</sup> livers 72 h postinfection (Fig. 1e). These findings indicate that the absence of *MyD88* but not *Trif* significantly protects

**Table 1** Primer sequences for RT-qPCR

Drug	Forward-primers	Reverse-primers
TNF-α	CACGCTCTTCTGTCTACTGAAC	ATCTGAGTGTGAGGGTCTGG
IL-6	TAGTCCTTCCCTACCCCAATTTCC	TTGGTCCTTAGCCACTCCTTC
FGL2	TGGACAACAAAGTGGCAAATCT	TGGAACACTTGCCATCCAAA
IFN-γ	TCAAGTGGCATAGATGTGGAAG	CGCTTATGTTGTTGCTGATGG
pro-IL-1β	GACAGTGATGAGAATGACCTGTTC	CCTGACCACTGTTGTTTCCC
HMGB1	GATTATCGTTCTCTTAAAGTGCCAG	TATCATCCAGGACTCATGTTCCAGTA
β-actin	ATATCGCTGCGCTGGTCGTC	AGGATGGCGTGAGGGAGAGC

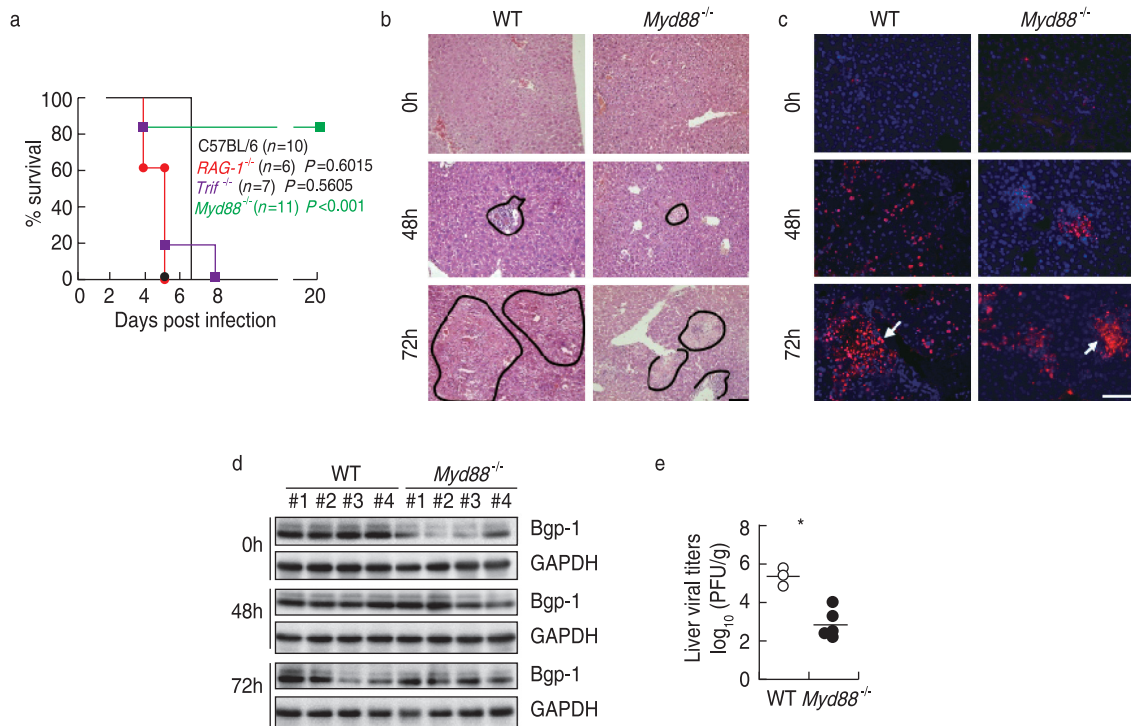


**Fig. 1** *MyD88* deficiency attenuates MHV-3-induced hepatitis. Age matched C57BL/6 (WT) and congenic *MyD88*<sup>-/-</sup> mice were infected with MHV-3 (100 PFU), (a) the survival rate was monitored for a total of 20 days. One representative of three experiments with similar results is shown. \**P* < 0.05. Liver tissues were isolated from virus infected WT and congenic *MyD88*<sup>-/-</sup> mice at different time points; (b) The morphology was analyzed by H&E staining; (c) Cells undergoing apoptosis was analyzed by TUNEL staining. Scale bar = 20 μm; (d) The expression of Bgp1 in livers at 24 h and 72 h post-infection was analyzed by western-blotting. Four representative samples *per* group are shown; (e) The virus titers in livers at 72h post-infection were analyzed by plaque assay, and results were compared by statistical analysis. \**P* < 0.05

against MHV-3-induced morbidity and mortality, while adaptive immunity (*Rag-1* deficiency) does not play a major role in the pathogenesis.

**MHV-3 fails to induce the production of FGL2 and other pro-inflammatory cytokines in *MyD88*<sup>-/-</sup> mice**

FGL2 plays an essential role in inducing hepatocellular necrosis following MHV-3 infection [2], we therefore examined *fgl2* expression in liver tissues isolated from MHV-3 infected *MyD88*<sup>-/-</sup> mice. Quantitative RT-PCR (qRT-PCR) showed that *fgl2* mRNA transcription in the liver was induced by MHV-3, and that its expression was dramatically reduced in *MyD88*<sup>-/-</sup> livers (Fig. 2a). The reduction in FGL2 protein levels in virus-infected *MyD88*<sup>-/-</sup> livers was also confirmed by western-blot (Fig. 2b), and the FGL2 serum concentration in *MyD88*<sup>-/-</sup> mice was substantially lower 72 h postinfection (Fig. 2c). Therefore, *MyD88*<sup>-/-</sup> mice responded with limited fibrinogen formation, leading to reduced liver coagulation and necrosis (Fig. 2d). Moreover, the *Fgl2*<sup>-/-</sup> mice were completely resistant to MHV-3-mediated mortality (Fig. 2e). These results suggest that the attenuation of viral FH

by *MyD88* deficiency could be the result of suppressed FGL2 production.

Pathologic proinflammatory cytokines, including TNF-α, IL-1β, and C5a, can promote FGL2 expression and worsen the pathogenesis of MHV-3-mediated FH [24-26]. To clarify the molecular mechanism that is responsible for *MyD88* signaling-mediated FGL2 upregulation, liver tissues were isolated from MHV-3-infected *MyD88*<sup>-/-</sup> mice and their control littermates 72 h post MHV-3 infection. The expression of some proinflammatory cytokines including *Ifn-γ*, *Tnf-α*, *proIL-1β*, and *IL-6* was measured by qRT-PCR. Interestingly, the concentrations of these cytokines were significantly reduced in *MyD88*<sup>-/-</sup> mice compared to their viral-infected WT littermates (Fig. 3a). These results were also confirmed at the protein level by western-blot (Fig. 3b) and immunohistochemistry (Fig 3c). Finally, we showed that both *Tnf-α*<sup>-/-</sup> and *IL-1R*<sup>-/-</sup> mice are phenocopied *MyD88*<sup>-/-</sup> mice and are resistant to MHV-3-mediated mortality (Fig. 3d). These results indicate that *MyD88* is required for the induction of *fgl2* and other proinflammatory cytokines in response to MHV-3 infection.

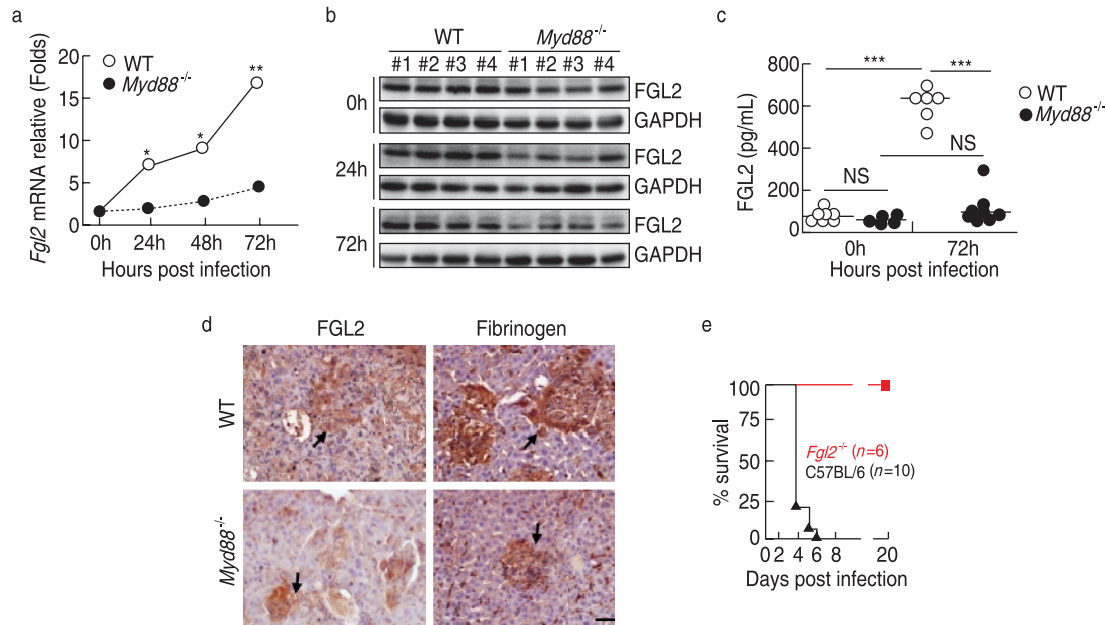


**Fig. 2** Reducing FGL2 expression and FB deposition in *MyD88*<sup>-/-</sup> livers post MHV-3 infection. *MyD88*<sup>-/-</sup> mice and their C57BL/6 WT littermates were infected with MHV-3 (100 PFU). (a) Liver *fgl2* mRNA transcription was detected by quantitative RT-PCR at different time points; (b) Liver FGL2 protein expression at 24 h and 72 h post infection was detected by Western-blot,  $n = 4$  per group; (c) Serum accumulation of FGL2 at 72h of infection was measured by ELISA; (d) Liver fibrinogen deposition was detected by immunohistochemistry; (e) Age matched C57BL/6 (WT) and congenic *Fgl2*<sup>-/-</sup> mice were infected with MHV-3 (100 PFU), the survival rate was monitored for a total of 20 days. One representative of three experiments with similar results is shown. \* $P < 0.05$ ,  $n = 5$  per group

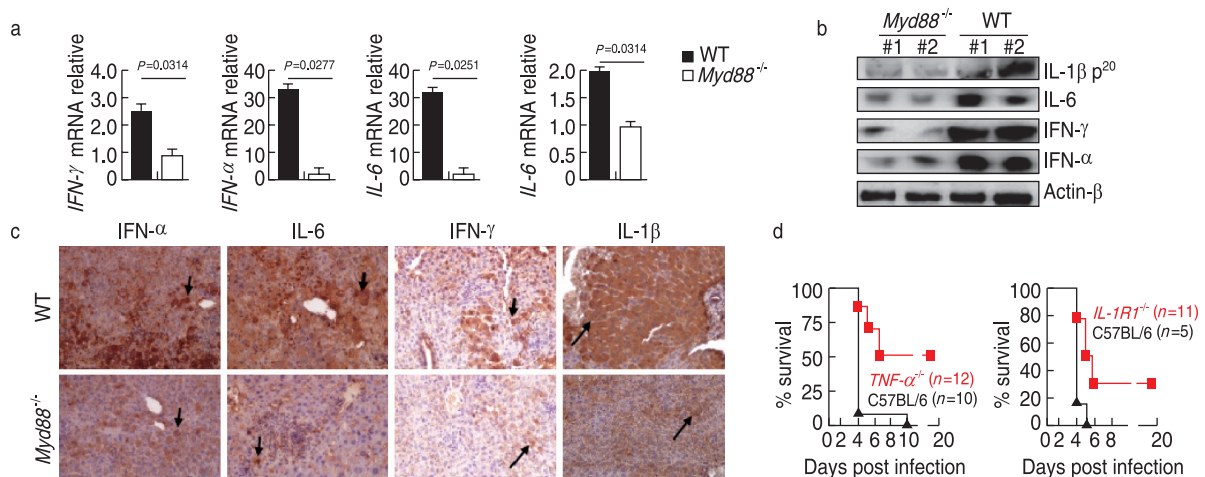


**Fig. 3** Reducing proinflammatory cytokine secretion in *MyD88*<sup>-/-</sup> livers post MHV-3 infection. *MyD88*<sup>-/-</sup> mice and their C57BL/6 WT littermates were infected with MHV-3 (100 PFU). (a) The transcription of pathologic proinflammatory cytokines, including *TNF- $\alpha$* , *proIL-1 $\beta$* , and *IL-6* in MHV-3-infected liver tissues at 72 h was detected by quantitative RT-PCR; (b) The expression of pathologic proinflammatory cytokines in MHV-3-infected liver tissues at 72 h was analyzed by western-blot; (c) The expression of pathologic proinflammatory cytokines in MHV-3-infected liver tissues at 72 h was analyzed by immunohistochemistry; (d) Age matched C57BL/6 (WT) and congenic *IL-1R1*<sup>-/-</sup>, *TNF- $\alpha$* <sup>-/-</sup> mice were infected with MHV-3 (100 PFU), the survival rate was monitored for a total of 20 days. One representative of three experiments with similar results is shown. \* $P < 0.05$ ,  $n = 5$  per group

### The recruitment of pro-inflammatory NKp46<sup>+</sup> Lin<sup>+</sup>Thy1.2<sup>+</sup>Royt<sup>+</sup> group 3 innate lymphoid cells was severely impaired in *MyD88*<sup>-/-</sup> livers post

### MHV-3 infection

Monocytes/macrophages and neutrophils are known to be crucial during viral FH due to these cells capacity

to produce pro-inflammatory cytokines, including FGL2 [26]. We determined whether liver infiltration of these cells was affected by *MyD88* signaling during viral FH. Liver infiltration by both CD11b<sup>+</sup>/F4/80<sup>+</sup> monocytes/macrophages and Gr-1<sup>high</sup>CD45<sup>+</sup> neutrophils was detected by flow cytometry in mice infected with MHV-3 (Fig. 4a). However, the difference between these two groups was not statistically significant (Fig. 4b), suggesting that liver infiltration by monocytes/macrophages and neutrophils was not affected by *MyD88* signaling.

Innate lymphoid cells (ILCs) have recently been discovered to play an important role in protective immunity against microbes like intracellular parasites, bacteria, fungi, and parasitic worms [27–28]. Flow cytometry showed that in liver-tissue samples 24 h and 48 h postinfection, infiltration by ILCs (Lin<sup>−</sup>Thy1.2<sup>+</sup>) was significantly higher in the WT than in their *MyD88*<sup>−/−</sup> littermates (Fig. 4c and 4d). Additionally, statistical analysis showed that NKp46<sup>+</sup>Lin<sup>−</sup>Thy1.2<sup>+</sup>Royt<sup>+</sup> ILC3s were severely impaired in MHV-3-infected *MyD88*<sup>−/−</sup> liver

tissues (Fig. 4d). Furthermore, these ILC3 have the ability to produce proinflammatory mediators, like TNF- $\alpha$ , proIL-1 $\beta$ , and IL-17 (Fig. 4e). These results suggest that attenuation of viral FH by *MyD88* deficiency could be at least partly due to limited proinflammatory NKp46<sup>+</sup>Lin<sup>−</sup>Thy1.2<sup>+</sup>Royt<sup>+</sup> ILC3 infiltration into the liver.

### Reduced secretion of HMGB1 in *MyD88*<sup>−/−</sup> mice post MHV-3 infection

HMGB1 is one of the canonical DAMPs that can be either passively released from necrotic/damaged cells, or can be secreted by activated innate immune cells. In addition to its nuclear role, extracellular HMGB1 triggers proinflammatory responses through *MyD88* signaling [29–30]. Thus, we decided to investigate the role of HMGB1 in Raw264.7 macrophage cells infected with MHV-3 (MOI = 1) by immunofluorescent confocal microscopy showed that HMGB1 localized to the nucleus of mock-infected Raw264.7 cells but was distributed in both the nucleus

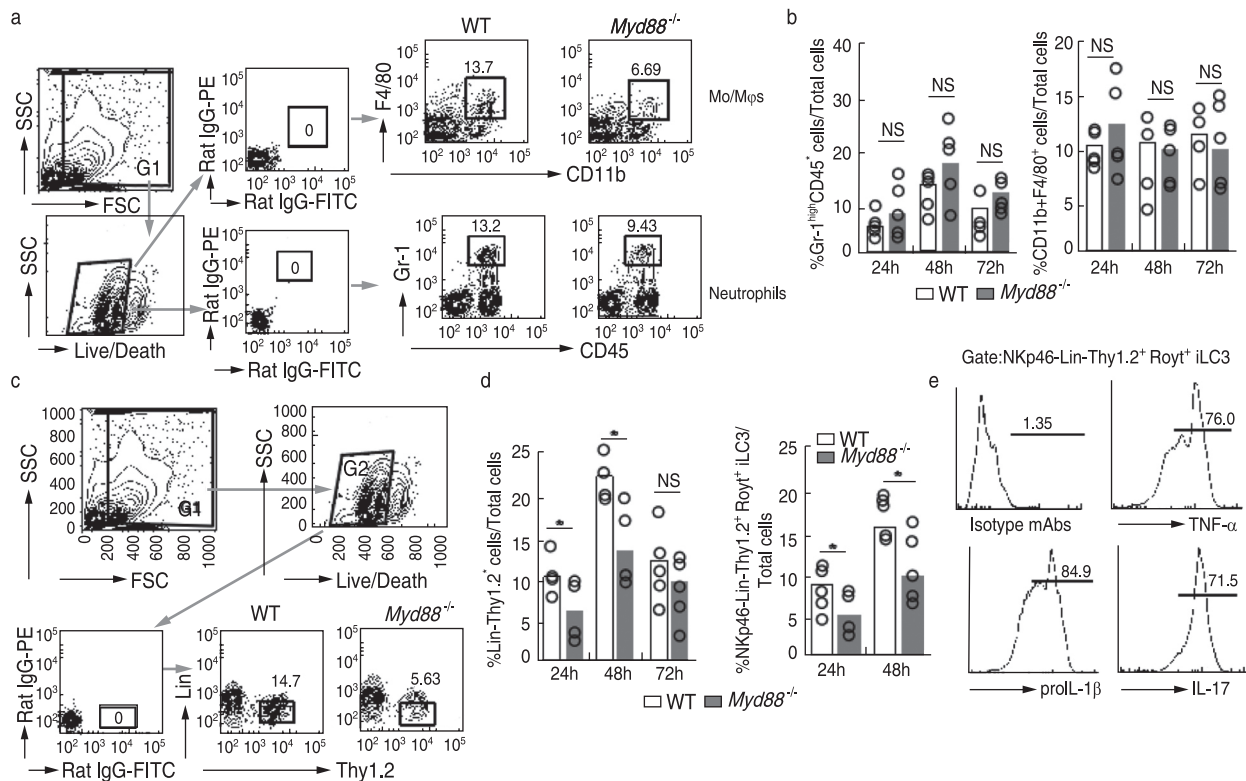


**Fig. 4** *MyD88* deficiency prevents the recruitment of proinflammatory NKp46<sup>+</sup>Lin<sup>−</sup>Thy1.2<sup>+</sup> Royt<sup>+</sup> ILC3 into livers. Age matched C57BL/6 (WT) and *MyD88*<sup>−/−</sup> mice were infected with MHV-3 (100 PFU), cells were isolated from virus infected livers. (a) Liver recruitment of CD11b<sup>+</sup>/F4/80<sup>+</sup> monocytes/macrophages, Gr-1<sup>high</sup>CD45<sup>+</sup> neutrophils of infection was measured by flow cytometry. Number indicates the percentage of positive cells in the gate. One representative sample from five mice *per* group is showed; (b) Statistical analysis of liver infiltration of CD11b<sup>+</sup>/F4/80<sup>+</sup> monocytes /macrophages, Gr-1<sup>high</sup>CD45<sup>+</sup> neutrophils at 24 h, 48 h and 72 h; (c) Liver infiltration of Lin<sup>−</sup>Thy1.2<sup>+</sup> ILCs of MHV-3 infection was detected by flow cytometry; (d) Statistical analysis of liver infiltration of Lin<sup>−</sup>Thy1.2<sup>+</sup> ILCs and NKp46<sup>+</sup>Lin<sup>−</sup>Thy1.2<sup>+</sup> Royt<sup>+</sup> ILC3 of MHV-3 infection; (e) The secretion of IL-17, TNF- $\alpha$  and IL-1 $\beta$  from NKp46<sup>+</sup>Lin<sup>−</sup>Thy1.2<sup>+</sup> Royt<sup>+</sup> ILC3 was analyzed by flow cytometry. One representative of three experiments with similar results is shown. \**P* < 0.05, *n* = 5 *per* group

and cytoplasm of their MHV-3-infected counterparts (Fig. 5a). Furthermore, a time-dependent increase in HMGB1 supernatant concentration was seen over 72 h of infection (Fig. 5b). Immunohistochemistry showed that HMGB1 protein was localized in nucleus of hepatocytes/macrophages of normal liver tissues, whereas it was mostly found within the cytoplasm of MHV-3-infected hepatocytes, especially in necrotic liver tissue (Fig. 5c). HMGB1 is secreted by damaged/necrotic hepatocytes and *MyD88* deficiency protects the liver from necrosis during MHV-3 infection, suggesting that *MyD88* signaling controls HMGB1 expression. To investigate this possibility, the serum concentration of HMGB1 in MHV-3 infected mice was measured by ELISA, and HMGB1 levels were found to be severely reduced in virus-infected *MyD88*<sup>-/-</sup> mice compared to their WT littermates (Fig. 5d). Moreover, MHV-3 infected *MyD88*<sup>-/-</sup> liver tissues also exhibited reduced HMGB1 protein (Fig. 5e). This combination indicates that the virus triggers HMGB1 expression in the infected cells and induces HMGB1 migration from the nucleus to the cytoplasm. *MyD88*<sup>-/-</sup> mice are protected from MHV-3 infection via reduced HMGB1 concentration in infected liver tissues.

## Discussion

Viral fulminant hepatitis (FH) has become a major public health concern. However, insufficient understanding of the immune mechanisms at play in severe viral hepatitis has largely hampered the development of clinically effective interventions. When BALB/cJ and C57BL/6 mice were infected with MHV-3, their mononuclear/macrophage cells were activated, resulting in a significant increase in proinflammatory mediators, eventually leading to hepatic sinus thrombosis and hepatocyte necrosis [1-3]. These syndromes are very similar to the clinical manifestations in FH patients. Therefore, the mouse FH model can improve our understanding of the pathogenesis of the disease. In this study, we report that mice deficient in *MyD88* are resistant to MHV-3-mediated FH due to limited recruitment of proinflammatory NKp46<sup>+</sup> Lin<sup>-</sup> Thy1.2<sup>+</sup> Royt<sup>+</sup> ILC3 to the liver, as well as reduced expression of multiple proinflammatory cytokines like TNF- $\alpha$ , IFN- $\gamma$ , IL-6 and FGL2, thus limiting liver pathology and prolonging survival post-infection. MHV-3 also triggers the expression of HMGB1 in infected hepatocytes/

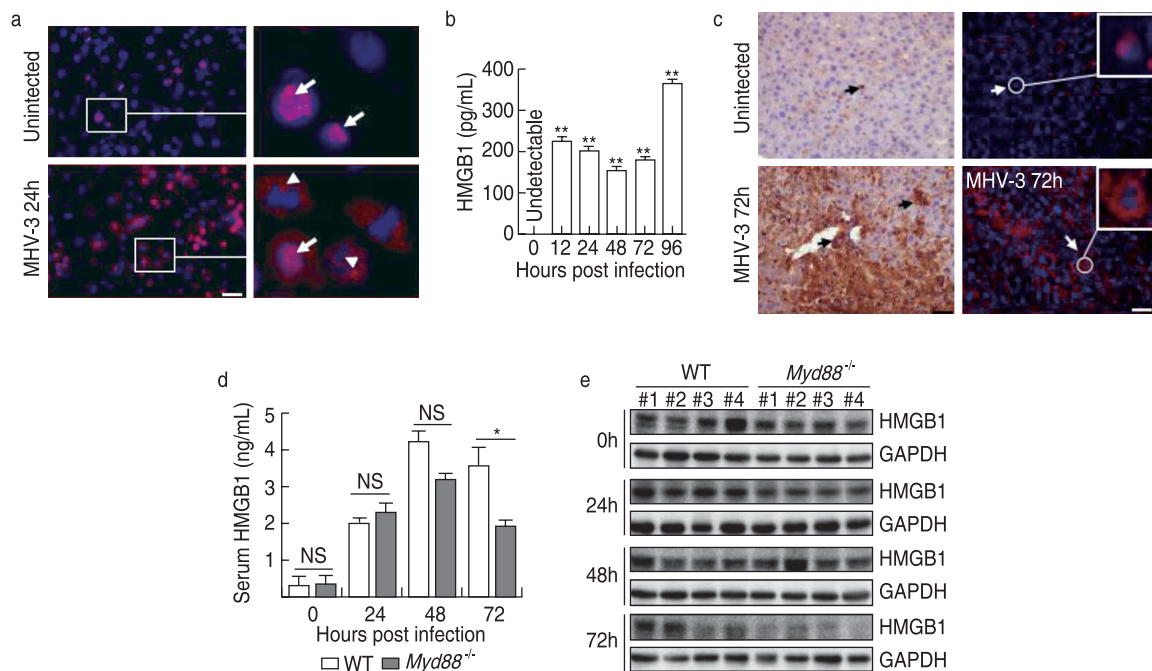


**Fig. 5** *MyD88* deficiency reduced the secretion of HMGB1. The macrophage cell line, Raw264.7 cells, were infected with MHV-3-infected (MOI = 1). (a) HMGB1 localization before and after 24 h of infection was monitored by immunofluorescent confocal microscopy; (b) The accumulation of HMGB1 in the supernatants was detected by ELISA; (c) The expression of HMGB1 protein in normal and MHV-3-infected liver tissues was detected by immunohistochemistry; (d) Serum concentration of HMGB1 in *MyD88*<sup>-/-</sup> and WT mice was detected by ELISA,  $n = 5$  per group, \* $P < 0.05$ ; (e) Liver concentration of HMGB1 in *MyD88*<sup>-/-</sup> and WT mice was detected by western-blot,  $n = 4$  per group, \* $P < 0.05$

macrophages and induces HMGB1 translocation from the nucleus to the cytoplasm and extracellular milieu, where HMGB1 induces *MyD88* dependent proinflammatory cytokine secretion. These results demonstrate that the *MyD88* is part of the essential signaling pathway in controlling inflammation in the viral FH.

FGL2 plays a key role in fulminant hepatitis and host death caused by MHV-3 infection. By blocking the expression of FGL2, sinus fibrin deposition and hepatocyte necrosis can be effectively prevented, thereby reducing the mortality of infected mice [31–32]. Previous studies have shown that pro-inflammatory cytokines, including IL-1 $\beta$ , TNF- $\alpha$ , IFN- $\gamma$  and complement C5a, can aggravate MHV-3-induced FH by promoting FGL2 expression and increasing liver fibrinogen accumulation [24–26]. However, the mechanism by which MHV-3 induces an inflammatory response is unclear. *MyD88* is a key adaptor protein for most TLR-dependent inflammatory signaling pathways as well as the *IL-18R1*, *IL-1R1*, and *IFN- $\gamma$ R1* signaling cascades [6]. Although *MyD88*-mediated proinflammatory signaling has been implicated in the protection from numerous bacterial and parasitic infections, few in vivo studies have found that *MyD88* is protective against viral diseases. Here, we showed that WT C57BL/6 mice are susceptible to lethal MHV-3 infection by a *MyD88*-dependent induction of proinflammatory mediators, and the recruitment of NKp46<sup>+</sup>Lin<sup>-</sup>Thy1.2<sup>+</sup>Royt<sup>+</sup> ILC3 to the liver. Conversely, *MyD88*<sup>-/-</sup> mice are resistant to MHV-3-mediated hepatitis and mortality by preventing proinflammatory cytokine and ILC3 accumulation and thus attenuating FGL2 expression (Fig. 1, Fig. 2 and Fig. 3). Our results differ from previous virological studies, which have shown that *MyD88*<sup>-/-</sup> mice infected with VSV, RSV, LCMV or rMA15 viruses have more severe diseases [33–34]. These results also differ from those seen in MHV-68 viral infections, where *MyD88*-dependent induction of type-I IFN is crucial to control viral replication [35]. These unexpected results imply that *MyD88* has dual effects on the immune system and that the proper balance of its signaling is essential for host protection against various invading viruses as well as prevention of potential collateral damage to the host.

Innate immune cells (ILCs) are lineage negative (Lin<sup>-</sup>) lymphocytes generated by the post fetal liver, which are divided in three major subgroups according to their functional and phenotypic characteristics. These include group 1 (which produces IFN- $\gamma$  and IL-17), group 2 (which produces IL-4 and IL-5) and group 3 (which produces IL-22 and IL-17) ILCs [36–37]. Previous work has shown that ILC3s in lymphoid tissues from SIV-infected macaques can be induced to undergo apoptosis by microbial products through the TLR2 or TLR4 pathway [38]. Moreover, ILCs depletion resulted in the loss of airway epithelial integrity, diminished lung

function and impaired airway remodeling after influenza virus infection [39]. Here, we showed that *MyD88*<sup>-/-</sup> mice are protected from lethal MHV-3 infection by lack of recruitment of NKp46<sup>+</sup>Lin<sup>-</sup>Thy1.2<sup>+</sup>Royt<sup>+</sup> ILC3 to the liver, which may contribute to the pathogenesis of MHV-3-induced FH as these cells have the capacity to produce proinflammatory mediators including TNF- $\alpha$ , IL-17 and FGL2 (Fig. 4c, 4d and 4e). However, we showed that liver recruitment of neither CD11b<sup>+</sup>F4/80<sup>+</sup> monocytes/macrophages, nor Gr-1<sup>high</sup>CD45<sup>+</sup> neutrophils were impaired by *MyD88* signaling (Fig. 4a and 4b), although these cell types have the capacity to promote liver damage by inducing the expression of proinflammatory mediators and boosting viral replication [40–41]. The combination of these results suggests that hepatic infiltration of NKp46<sup>+</sup>Lin<sup>-</sup>Thy1.2<sup>+</sup>Royt<sup>+</sup> ILC3 actively participates in MHV-3-induced hepatitis.

It is critical to identify and characterize “non-PAMP” host-derived molecular patterns that can activate *Myd88*. HMGB1 protein is a highly conserved nuclear protein that participates in DNA organization and the regulation of transcription [15–16] and can be released passively by necrotic and damaged somatic cells into the extracellular milieu [15–16]. HMGB1 activates macrophages/monocytes and endothelial cells to express pro-inflammatory cytokines, chemokines and adhesion molecules by interacting with its receptors, including RAGE, as well as TLR2 and TLR4, in the extracellular space [42]. The contributions of HMGB1 to the pathogenesis of viral infectious diseases have been well described, for examples, both RNA virus (WNV, Dengue virus, and HIV-1) and DNA virus (HSV-2) infections have been shown to result in the secretion of HMGB1 through apoptosis and/or necrosis [43–44], and the elevation of HMGB1 levels in the plasma of HCV patients with chronic hepatitis, liver cirrhosis, and HCC likely is attributable to the cytopathic effects of HCV infection [20]. We found that MHV-3 induces the migration of HMGB1 from the nucleus to the cytoplasm and its accumulation in the supernatants of infected Raw264.7 cells. Moreover, enhanced HMGB1 protein serum concentration was also seen in MHV-3 infected mice (Fig. 5). Therefore, HMGB1 may participate in MHV-3-mediated pathogenesis by acting alone or in combination with other proinflammatory cytokines.

In summary, our study shows that *MyD88*-dependent proinflammatory cytokine production plays a double-edged role in the host immune system. Hepatotropic viral infections, like MHV-3 infections in mice, can induce excessive inflammation of the liver and cause life-threatening viral FH. These results suggest a novel strategy, which would involve modulation of the *MyD88* signaling pathway, in combination with blocking other inflammatory factors to assist in the treatment of viral FH and other severe inflammatory diseases.

## Conflicts of interest

The authors declare no conflict of interest.

## References

- Liu M, Chan CW, McGilvray I, *et al.* Fulminant viral hepatitis: molecular and cellular basis, and clinical implications. *Expert Rev Mol Med*, 2001, 2001: 1–19.
- Marsden PA, Ning Q, Fung LS, *et al.* The Fgl2/fibroleukin prothrombinase contributes to immunologically mediated thrombosis in experimental and human viral hepatitis. *J Clin Invest*, 2003, 112: 58–66.
- Sarin SK, Kumar A, Almeida JA, *et al.* Acute-on-chronic liver failure: consensus recommendations of the Asian Pacific Association for the study of the liver (APASL). *Hepatology*, 2009, 3: 269–282.
- McGuire VA, Arthur JS. Subverting Toll-like receptor signaling by bacterial pathogens. *Front Immunol*, 2015, 6: 607.
- Chow J, Franz KM, Kagan JC. PRRs are watching you: Localization of innate sensing and signaling regulators. *Virology*, 2015, 0: 104–109.
- O'Neill LA, Bowie AG. The family of five: TIR-domain-containing adaptors in Toll-like receptor signalling. *Nat Rev Immunol*, 2007, 7: 353–364.
- Johansson C, Wetzel JD, He JP, *et al.* Type I interferons produced by hematopoietic cells protect mice against lethal infection by mammalian reovirus. *J Exp Med*, 2007, 204: 1349–1358.
- Madera RF, Libraty DH. The role of MyD88 signaling in heterosubtypic influenza A virus infections. *Virus Res*, 2013, 171: 216–221.
- Seo SU, Kwon HJ, Song JH, *et al.* MyD88 signaling is indispensable for primary influenza A virus infection but dispensable for secondary infection. *J Virol*, 2010, 84: 12713–12722.
- Rudd BD, Schaller MA, Smit JJ, *et al.* MyD88-mediated instructive signals in dendritic cells regulate pulmonary immune responses during respiratory virus infection. *J Immunol*, 2007, 178: 5820–5827.
- Phipps S, Lam CE, Mahalingam S, *et al.* Eosinophils contribute to innate antiviral immunity and promote clearance of respiratory syncytial virus. *Blood*, 2007, 110: 1578–1586.
- Zhou SH, Kurt-Jones EA, Mandell L, *et al.* MyD88 is critical for the development of innate and adaptive immunity during acute lymphocytic choriomeningitis virus infection. *Eur J Immunol*, 2010, 35: 822–830.
- Lang KS, Navarini AA, Recher M, *et al.* MyD88 protects from lethal encephalitis during infection with vesicular stomatitis virus. *Eur J Immunol*, 2010, 37: 2434–2440.
- Vénéreau E, Ceriotti C, Bianchi ME. DAMPs from cell death to new life. *Frontiers Immunol*, 2015, 6: 422.
- Andersson U, Tracey KJ. HMGB1 is a therapeutic target for sterile inflammation and infection. *Annu Rev Immunol*, 2011, 29: 139–162.
- Scaffidi P, Misteli T, Bianchi ME. Release of chromatin protein HMGB1 by necrotic cells triggers inflammation. *Nature*, 2002, 418: 191–195.
- Pandolfi F, Altamura S, Frosali S, *et al.* Key role of DAMP in inflammation, cancer, and tissue repair. *Clin Ther*, 2016, 38: 1017–1028.
- Duan E, Wang D, Luo R, *et al.* Porcine reproductive and respiratory syndrome virus infection triggers HMGB1 release to promote inflammatory cytokine production. *Virology*, 2014, 468–470: 1–9.
- Fraisier C, Papa A, Almeras L. High-mobility group box-1, promising serological biomarker for the distinction of human WNV disease severity. *Virus Res*, 2015, 195: 9–12.
- Yu R, Yang DR, Lei SH, *et al.* HMGB1 promotes hepatitis C virus replication by interaction with stem-loop 4 in the viral 5' untranslated region. *J Virol*, 2016, 90: 2332–2344.
- Moisy D, Avilov SV, Jacob Y, *et al.* HMGB1 protein binds to influenza virus nucleoprotein and promotes viral replication. *J Virol*, 2012, 86: 9122–9133.
- Yamamoto M, Sato S, Hemmi H, *et al.* Role of adapter TRIF in the MyD88-independent toll-like receptor signaling pathway. *Science*, 2003, 301: 640–643.
- Godfraind C, Langreth SG, Cardellicchio CB, *et al.* Tissue and cellular distribution of an adhesion molecule in the carcinoembryonic antigen family that serves as a receptor for mouse hepatitis virus. *Lab Invest*, 1995, 73: 615–627.
- Liu JJ, Tan YL, Zhang JY, *et al.* C5aR, TNF- $\alpha$ , and FGL2 contribute to coagulation and complement activation in virus-induced fulminant hepatitis. *J Hepatol*, 2015, 62: 354–362.
- Xu GL, Chen J, Yang F, *et al.* C5a/C5aR pathway is essential for the pathogenesis of murine viral fulminant hepatitis by way of potentiating Fgl2/fibroleukin expression. *Hepatology*, 2014, 60: 114–124.
- Guo S, Yang CY, Diao B, *et al.* The NLRP3 inflammasome and IL-1 $\beta$  accelerate immunologically mediated pathology in experimental viral fulminant hepatitis. *PLoS Pathog*, 2015, 11: e1005216.
- Sonnenberg GF, Artis D. Innate lymphoid cells in the initiation, regulation and resolution of inflammation. *Nat Med*, 2015, 21: 698–708.
- McKenzie ANJ, Spits H, Eberl G. Innate lymphoid cells in inflammation and immunity. *Immunity*, 2014, 41: 366–374.
- Ibrahim, Z.A., *et al.*, RAGE and TLRs: Relatives, friends or neighbours? *Molecular Immunology*, 2013. 56(4): p. 739-744.
- Xie J, Méndez JD, Méndez-Valenzuela V, *et al.* Cellular signalling of the receptor for advanced glycation end products (RAGE). *Cell Signal*, 2013, 25: 2185–2197.
- Shalev I, Wong KM, Foerster K, *et al.* The novel CD4+CD25+ regulatory T cell effector molecule fibrinogen-like protein 2 contributes to the outcome of murine fulminant viral hepatitis. *Hepatology*, 2010, 49: 387–397.
- Parr RL, Fung L, Reneker J, *et al.* Association of mouse fibrinogen-like protein with murine hepatitis virus-induced prothrombinase activity. *J Virol*, 1995, 69: 5033–5038.
- Totura AL, Baric RS. SARS coronavirus pathogenesis: host innate immune responses and viral antagonism of interferon. *Curr Opin Virol*, 2012, 2: 264–275.
- Casanova JL, Abel L, Quintana-Murci L. Human TLRs and IL-1Rs in host defense: natural insights from evolutionary, epidemiological, and clinical genetics. *Ann Rev Immunol*, 2011, 29: 447–491.
- Nash AA, Dutia BM, Stewart JP, *et al.* Natural history of murine  $\gamma$ -herpesvirus infection. *Philos Trans R Soc Lond B Biol Sci*, 2001, 356: 569–579.
- Eberl G, Colonna M, Di Santo JP, *et al.* Innate lymphoid cells. Innate lymphoid cells: a new paradigm in immunology. *Science*, 2015, 348: aaa6566.
- Goldberg R, Prescott N, Lord GM, *et al.* The unusual suspects--innate lymphoid cells as novel therapeutic targets in IBD. *Nat Rev Gastroenterol Hepatol*, 2015, 12: 271–283.
- Xu H, Wang X, Lackner AA, *et al.* Type 3 innate lymphoid cell depletion is mediated by TLRs in lymphoid tissues of simian immunodeficiency virus-infected macaques. *FASEB J*, 2015, 29: 5072–5080.
- Monticelli LA, Sonnenberg GF, Abt MC, *et al.* Innate lymphoid cells promote lung-tissue homeostasis after infection with influenza virus. *Nat Immunol*, 2011, 12: 1045–1054.

40. Yang C, Chen Y, Guo G, *et al.* Expression of B and T lymphocyte attenuator (BTLA) in macrophages contributes to the fulminant hepatitis caused by murine hepatitis virus strain-3. *Gut*, 2013, 62: 1204–1213.
41. Phillipson M, Kubes P. The neutrophil in vascular inflammation. *Nat Med*, 2010, 17: 1381–1390.
42. Bianchi ME. HMGB1 loves company. *J Leukoc Biol*, 2009, 86: 573–576.
43. Borde C, Barnay-Verdier S, Gaillard C, *et al.* Stepwise release of biologically active HMGB1 during HSV-2 infection. *PLoS One*, 2011, 6: e16145.
44. Chen LC, Yeh TM, Wu HN, *et al.* Dengue virus infection induces passive release of high mobility group box 1 protein by epithelial cells. *J Infect*, 2008, 56: 143–150.

**DOI 10.1007/s10330-018-0329-9**

**Cite this article as:** Deng JZ, Ning Q, Yan WM, *et al.* *MyD88* exacerbates immunological pathology in experimental viral fulminant hepatitis. *Oncol Transl Med*, 2019, 5: 58–67.

# Prognostic significance of PD-L1 expression in patients with colorectal cancer: a meta-analysis\*

Siwen Liu<sup>1</sup>, Rong Ma<sup>1</sup>, Haixia Cao<sup>1</sup>, Dan Chen<sup>1</sup>, Changwen Jing<sup>1</sup>, Zhuo Wang<sup>1</sup>, Junying Zhang<sup>1</sup>, Yang Wu<sup>1</sup>, Jifeng Feng<sup>1,2</sup> (✉), Jianzhong Wu<sup>1</sup> (✉)

<sup>1</sup> Research Center for Clinical Oncology, Jiangsu Cancer Hospital & Jiangsu Institute of Cancer Research & The Affiliated Cancer Hospital of Nanjing Medical University, Jiangsu 210009, China

<sup>2</sup> Department of Oncology, Jiangsu Cancer Hospital & Jiangsu Institute of Cancer Research & The Affiliated Cancer Hospital of Nanjing Medical University, Jiangsu 210009, China

## Abstract

**Background** The association between the expression of programmed cell death 1 (PD-1) or its ligand [programmed cell death ligand-1 (PD-L1)] and colorectal cancer (CRC) survival rates remains unclear. Thus, we conducted a meta-analysis to investigate the prognostic value of PD-L1 expression in CRC patients.

**Methods** All eligible studies related to evaluation of PD-L1 expression and survival of CRC patients were searched in PubMed, Medline, Cochrane library, and the EMBASE database. Hazard ratios (HRs) and 95% confidence intervals (CI) of overall survival (OS) were examined to assess the effect of PD-L1 expression on the survival of CRC patients. The outcomes of this meta-analysis were synthesized based on random-effects model. Subgroup analyses were also performed.

**Results** Seven studies, wherein OS data were stratified according to the expression status of PD-L1, were analyzed. CRC patients showing positive PD-L1 expression were associated with significantly poorer prognoses in terms of overall survival, compared with those displaying negative PD-L1 expression (HR = 1.43, 95% CI: 1.07–1.92;  $P = 0.02$ ). In the subgroup analyses, H-scores as well as the percentage of stained cells indicated that PD-L1 expression was significantly associated with poor prognosis (HR = 1.90, 95% CI: 1.38–2.62,  $P < 0.01$ ; HR = 1.81, 95% CI: 1.08–3.03,  $P = 0.02$ ). Immunohistochemical staining, utilizing a rabbit anti-PD-L1 antibody, revealed significantly superior survival in the PD-L1 negative group compared with the PD-L1 positive expression group (HR = 1.92; 95% CI, 1.40–2.63;  $P < 0.01$ ). Moreover, PD-L1 expression was significantly associated with poor prognosis when polyclonal antibodies were used (HR = 1.84; 95% CI, 1.30–2.61;  $P < 0.01$ ).

**Conclusion** Our meta-analysis indicated that PD-L1 expression status is a significant prognostic factor for CRC patients. Positive PD-L1 expression was associated with worse CRC survival. Evaluation via different immunohistochemistry based techniques may partly account for the contradictory results. Therefore, further investigative studies using larger sample sizes are felt to be needed to elucidate the prognostic value of PD-L1 expression in CRC patients.

**Key words:** colorectal cancer (CRC); programmed cell death ligand-1 (PD-L1); prognosis; Meta-analysis

Received: 23 October 2018  
Revised: 10 November 2018  
Accepted: 20 November 2018

Colorectal cancer (CRC) is a common cancer and one of the leading causes of cancer-related morbidity and mortality worldwide [1–2]. Although surgery, chemotherapy, and radiotherapy have significantly improved the clinical outlook for CRC patients, the 5-year survival rate still remains low [3–4]. Thus, alternative strategies, such as immunotherapy, are now being

considered for the management of CRC [5]. Furthermore, many key molecular alterations are used as biomarkers for predicting prognosis. Programmed cell death 1 (PD-1) and PD-1 ligand 1 (PD-L1) expression have been observed in various malignancies and are reported to play an important role in modulating the strength of T cell response [6–7]. Blockade of the PD-1/PD-L1 signaling

✉ Correspondence: Jifeng Feng. Email: fjif@vip.sina.com; Jianzhong Wu. Email: wujzh1528@126.com

\* Supported by the National Natural Science Foundation of China (No. 81372396), Natural Science Foundation of Jiangsu Province (No. BK20141016 and BK20141017).

© 2019 Huazhong University of Science and Technology

pathway can minimize damage to surrounding normal tissues by maintaining T cell activation [8-9]. Previous studies have found that PD-1/PD-L1 expression in tumor cells is correlated with poor prognoses [10-13]. Moreover, some clinical studies have shown that anti-PD-1 or PD-L1 antibodies may prolong the survival of melanoma patients, with particular reference to advanced and refractory patients [14-16].

Despite the development of antibodies against PD-1 and PD-L1, their predictive value of prognosis for CRC patients remains unclear. The association between PD-1/PD-L1 expression in CRC and patient survival also remains controversial. Previous meta-analyses has shown that PD-1/PD-L1 expression status was a significant prognostic factor in malignancies, and that positive PD-1/PD-L1 expression was associated with significantly poorer overall survival (OS), especially in patients with clear cell renal cell carcinoma and pancreatic cancer [17]. However, another meta-analysis contended that there was no statistically significant relationship between PD-L1 expression and the prognosis for non-small-cell lung cancer patients [18]. However, strong PD-L1 expression was observed in patients with CRC and was associated with a significant improvement in the 5-year survival rate [19].

Studies related to the prognostic significance of PD-1/PD-L1 expression in CRC patients have yielded inconsistent results due to a lack of statistical power. Moreover, meta-analyses pertaining to CRC related expression of PD-1 and PD-L1 have not been performed. In order to address these issues, we conducted a meta-analysis to evaluate the association between prognostic value and PD-L1 status in CRC patients.

## Material and methods

### Literature search

All studies evaluating PD-L1 expression and survival of CRC patients were retrieved by searching PubMed, Medline, Cochrane library, and the EMBASE database. Different search term combinations were used, including "colorectal cancer," "PD-L1," "B7-H1," "survival," and "prognosis." A manual search through all references of the relevant articles was also performed.

### Inclusion and exclusion criteria

To be eligible for the current meta-analysis, studies had to meet the following criteria: (1) investigation of the association between PD-L1 expression and the prognosis for CRC patients; (2) the expression level of PD-L1 was scored as either "positive" or "negative" via immunohistochemistry (IHC) staining; (3) The primary outcome of OS according to PD-L1 status was available for estimation. Studies with insufficient data were excluded.

## Data extraction and quality assessment

We extracted the required data from all eligible studies; the name of the first author, the year of publication, IHC evaluation method, cut off value for positive PD-L1 expression, primary antibody, and OS. OS data were extracted in the form of hazard ratios (HRs) with 95% confidence intervals (CI). In order to ensure the quality of our meta-analysis, two authors used the Methodological Index for Nonrandomized Studies (MINORS) to independently evaluate the quality of the eligible studies.

## Statistical analysis

All statistical analyses were performed using RevMan 5.3 (Copenhagen: The Nordic Cochrane Centre, The Cochrane Collaboration, 2014) analysis software and Stata software. HRs for OS with 95% CIs was used to assess the effect of PD-L1 expression on the survival of CRC patients. Subgroup analyses were performed according to patients from different countries, IHC evaluation methods and primary antibodies (source, type, and catalog), respectively. Heterogeneity among studies was assessed using the Q and I<sup>2</sup> statistics [20]. The random effect model was utilized in case of potential heterogeneity. Additionally, publication bias was evaluated using Egger's [21] and Begg-Mazumdar [22] procedures. For all tests, statistical significance was set at  $P < 0.05$  for a two tailed test.

## Results

### Search results

The search results were shown (Fig. 1). The primary literature research retrieved a total of 690 potentially relevant articles. After screening titles and abstracts, 569 references were excluded due to being irrelevant to the

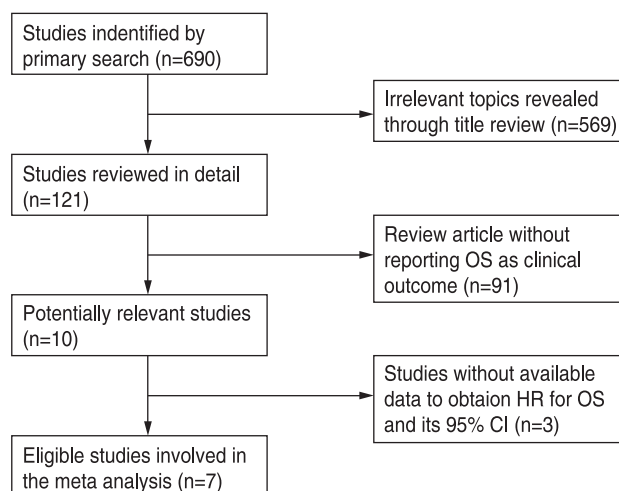


Fig. 1 Process for identification of eligible studies.

subject of the analysis. Additionally, 91 studies, which did not report OS as a clinical outcome, were excluded. Next, three studies with insufficient survival data were excluded after full-texts were read. Ultimately, the seven remaining studies were included for further statistical evaluation [23–29].

### Characteristics of included trials

The characteristics of analyzed studies were summarized (Table 1). In the trials that were included, CRC patients had been used to evaluate PD-L1 expression and its relationship with OS in CRC. PD-L1 expression was evaluated via the IHC method in all included studies.

### Meta-analyses of PD-L1 expression in terms of OS

Seven studies provided 5-year OS for CRC. In CRC patients, positive PD-L1 expression was associated with significantly poorer OS when compared to negative PD-L1 expression (Random-effects model, HR = 1.43, 95% CI: 1.07–1.92;  $P = 0.02$ ; Fig. 2). There was significant heterogeneity among studies ( $I^2 = 51%$ ,  $P = 0.06$ ). However, no evidence of significant publication bias was detected (Egger test,  $t = 2.42$ ,  $P = 0.06$ ; Begg test,  $Z = 0.62$ ,  $P = 0.54$ ).

### Subgroup analysis between PD-L1 expression and OS

PD-L1 expression was not significantly associated with poor prognosis for both Chinese and non-Chinese patients (Fig. 3). With respect to the different methods of IHC evaluation, the H-score system method, as well as the percentage of stained cells method, indicated that positive PD-L1 expression was significantly associated with poor prognosis when compared with negative PD-L1 expression (HR = 1.90, 95% CI: 1.38–2.62,  $P < 0.01$ ; HR = 1.81, 95% CI: 1.08–3.03,  $P = 0.02$ ; Fig. 4). Furthermore, significantly superior survival was shown in the negative PD-L1 expression group compared with the positive PD-L1 expression group when rabbit antibody was used as the primary anti-PD-L1 antibody (HR = 1.92; 95% CI, 1.40–2.63;  $P < 0.01$ ; Fig. 5). Moreover, PD-L1 expression was significantly associated with poor prognosis when the polyclonal antibody (PAB) was used (HR = 1.84; 95% CI, 1.30–2.61;  $P < 0.01$ ; Fig. 6). No statistical relationships between PD-L1 expression and CRC prognosis were detected in the remaining subgroups.

**Table 1** Characteristics of included studies

Study	Year	Country	IHC Evaluation	Cutoff Value for PD-L1/ PD-1 Positive	Antibody (Company)	Antibody			HR for OS	Lower limit of 95% CI	Upper limit of 95% CI
						Source	Type	Catalog			
Shi SJ	2013	China	H-score	> 200	Abcam, UK	Rabbit	PAB	ab58810	China	China	3.576
Song MM	2013	US	DIA	NR	Abcam, UK	NR	NR	NR	US	US	1.979
Liang M	2014	China	H-score	> 20	Santa Cruz Biotechnology, USA	Rabbit	PAB	NR	China	China	2.713
Zhu JJ	2014	China	NR	NR	Boster, China	Mouse	MAB	Clone 2H11	China	China	0.98
Zhu HL	2015	China	Percentage	1%	Abcam, UK	Rabbit	MAB	NR	China	China	4.684
Saigusa	2016	Japan	H-score	NR	LifeSpan BioSciences, USA	Mouse	MAB	Clone 27A2	Japan	Japan	5.016
Wang LS	2016	China	Percentage	1%	Spring Bioscience, USA	NR	MAB	SP142	China	China	2.89

DIA: Digital image analysis; HR: Hazard ratio; MAB: Monoclonal antibody; NR: Not reported; PAB: Polyclonal antibody; H-score: SI (Staining intensity)\*PP (Percentage of positive cells) (SI: 0, negative; 1, weak; 2, moderate; and 3, strong; PP: 0, negative; 1 to 100, 1% to 100% positive cells).

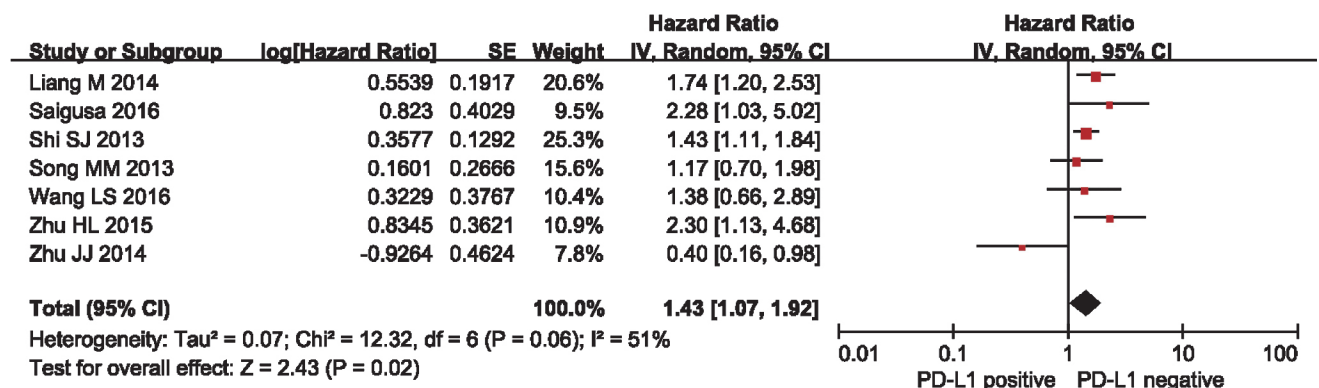


**Fig. 2** Meta-analysis of PD-L1 positive versus PD-L1 negative on CRC tissues.

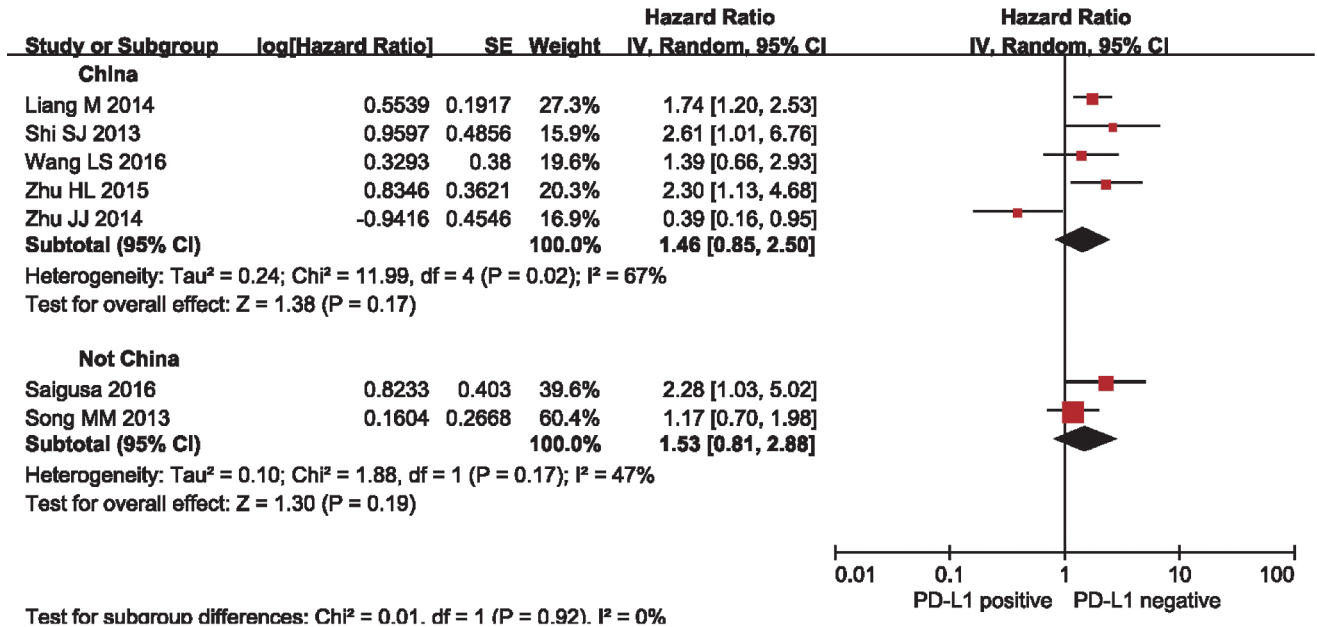


Fig. 3 Subgroup analysis of PD-L1 positive versus PD-L1 negative on CRC tissues of patients from different countries.

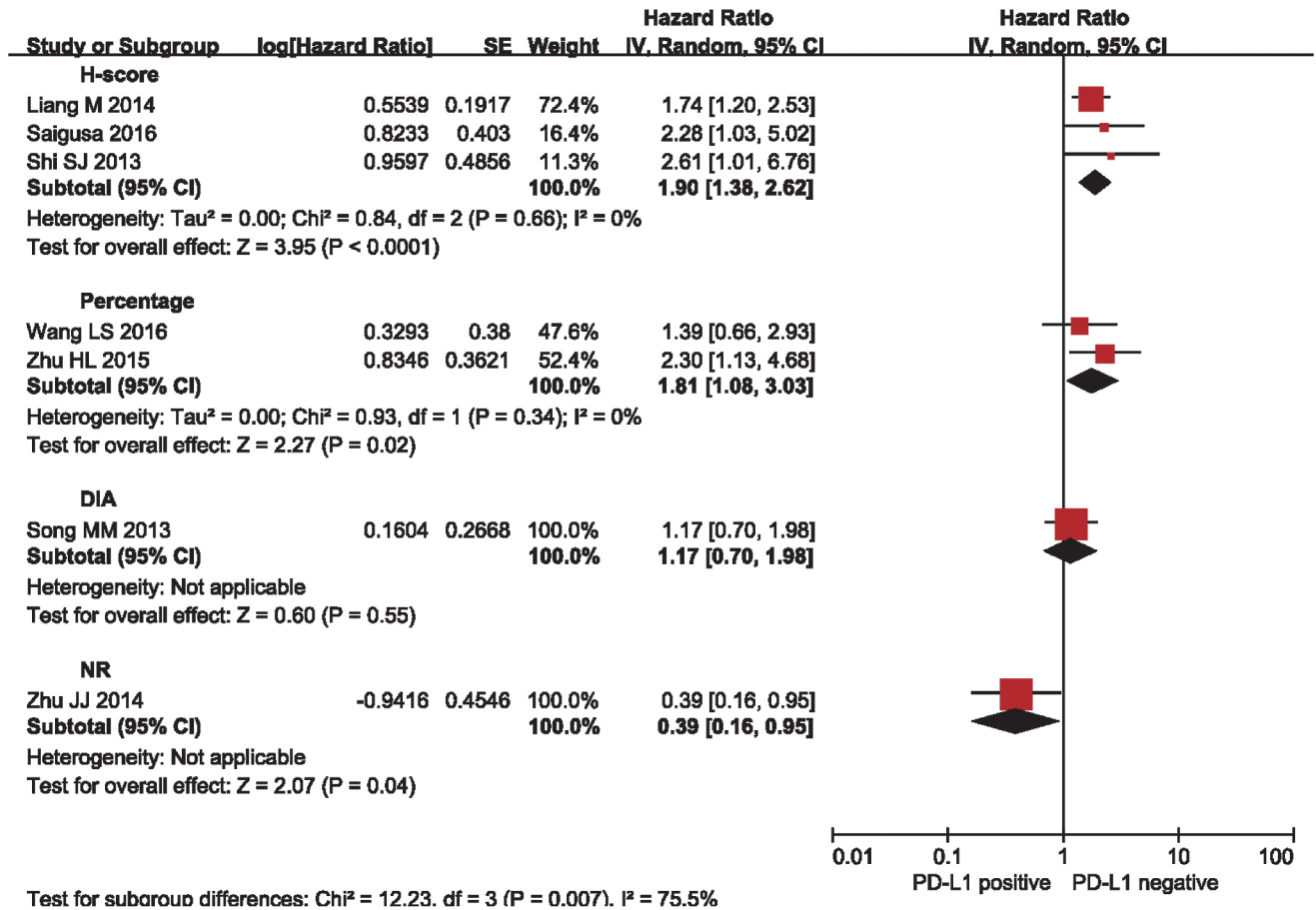


Fig. 4 Subgroup analysis of positive expression of PD-L1 on tumor cells according to IHC evaluation method.

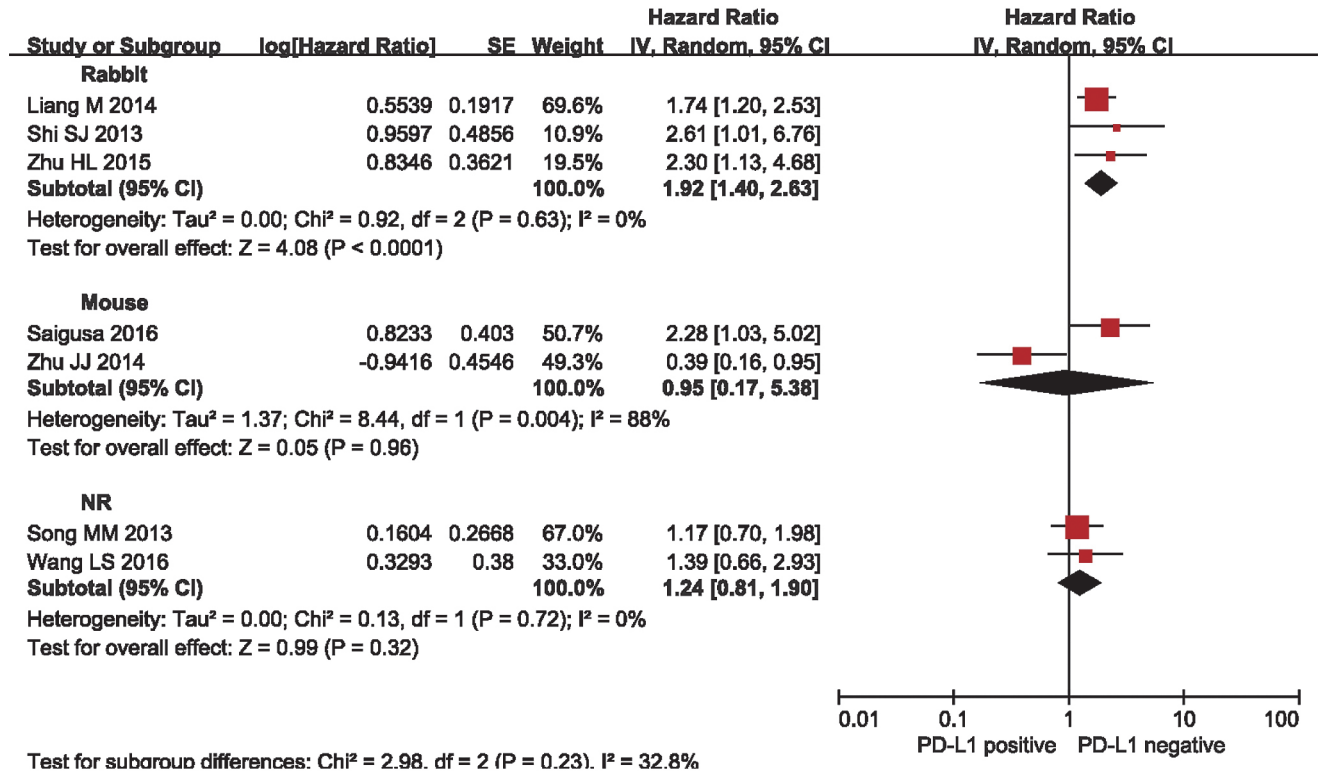


Fig. 5 Subgroup analysis of the association between PD-L1 expression and different source of antibody.

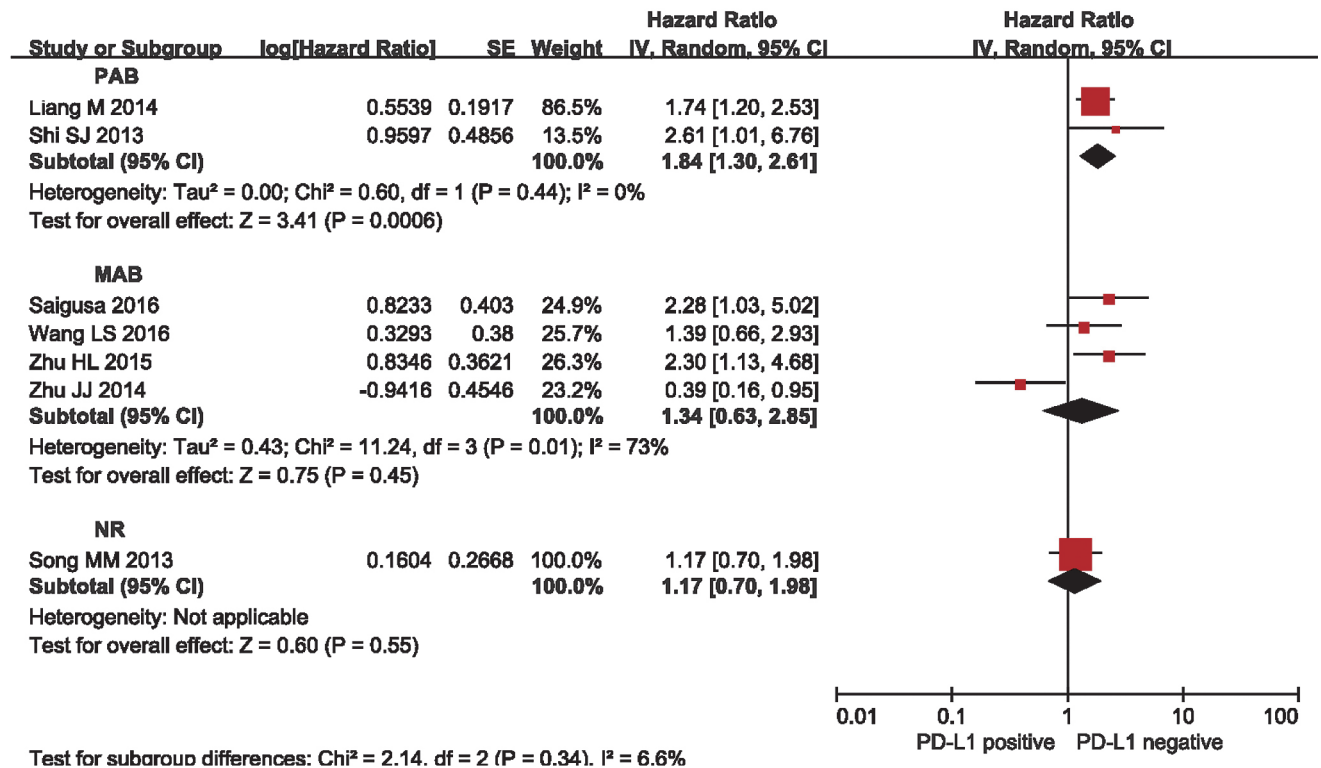


Fig. 6 Subgroup analysis of the association between PD-L1 expression and different type of antibody.

## Discussion

Recent studies have shown that PD-1/PD-L1 is highly expressed in a variety of human cancers<sup>[30-31]</sup>. High PD-1/PD-L1 expression may contribute to tumor immune evasion<sup>[32]</sup>. However, correlation between PD-1/PD-L1 expression levels and cancer progression remains a controversial subject. Previous studies have shown that PD-1/PD-L1 expression levels are indicators of poor prognoses for patients with renal cell carcinoma, gastric carcinoma, and pancreatic cancer<sup>[17]</sup>.

Our meta-analysis explored the association between PD-L1 expression and prognosis for CRC patients. The results indicated that PD-L1 expression was associated with a poor prognosis for CRC. Moreover, subgroup analysis showed that positive PD-L1 expression was associated with poor prognosis for CRC patients when different antibodies or different IHC methods were used. As a whole, these results confirmed that PD-L1 plays a key role in cancer immune escape and that activation of the PD-L1 pathway had a profoundly adverse prognostic impact on CRC patients. Thus, therapies targeting PD-L1, such as blocking PD-L1, may improve antitumor immunity and display clinical responses in CRC patients expressing high PD-L1 levels.

PD-L1 and PD-1 were found to play an important role in cell proliferation, apoptosis, migration, and invasion, leading to the prevention of tumor destruction<sup>[10]</sup>. Results of previous studies have confirmed the role of PD-L1/PD-1 in CRC development<sup>[33]</sup>. Our results indicated that CRC patients with positive PD-L1 expression have a worse 5-year outcome. Previous studies reporting on OS demonstrated that PD-L1 overexpression and PD-1 expression were associated with prognoses for CRC patients<sup>[26-29]</sup>. Potential association between PD-L1/PD-1 expression and prognosis for other tumors has also been assessed by previous meta-analyses<sup>[10, 17]</sup>. PD-1 overexpression in non-small-cell lung cancer (NSCLC) was associated with a poor prognosis for NSCLC<sup>[34-35]</sup>. However, no significant correlation was found between PD-L1 expression and prognosis for NSCLC, suggesting that PD-L1 was not a prognostic predictor for NSCLC patients<sup>[10]</sup>. Differences between methods used in these studies, such as different methods of defining positive vs negative PD-L1/PD-1 expression and the use of different batches of PD-L1/PD-1 antibodies, may partly account for the contradictory results.

Subgroup analyses of IHC methods, definition of positive PD-L1 expression and the sources and types of primary antibodies used showed that both IHC evaluation methods and primary antibodies displayed a consistent prognostic correlation with overall results. Positive PD-L1 expression in tumor-infiltrating immune cells was associated with a worse prognosis compared

with the negative PD-L1 expression group when both rabbit and PAB antibodies were used, as well as when both percentage evaluation method and H-score system were used. A previous study reported that positive PD-1 expression was an independent predictor for colorectal carcinoma prognosis when the H-score system was used as the IHC evaluation method<sup>[17]</sup>. Another study has indicated that PD-L1 expression was a prognostic indicator for CRC patients when digital image analysis was used as the IHC evaluation method<sup>[36]</sup>. These results implied that further studies with larger sample sizes might be needed to confirm the relationship between PD-L1/PD-1 expression and prognosis for CRC patients with different baseline characteristics.

In conclusion, our meta-analysis provided evidence that PD-L1 expression was an independent predictor of prognosis for CRC. Overexpression of PD-L1, as measured via IHC, was associated with a worse prognosis for CRC. These new findings have improved understanding of the association between PD-L1 and the progression of CRC. Moreover, antibody-mediated blockade of PD-L1 may represent a promising treatment target for CRC.

## Conflict of interest

The authors declare that they have no conflict of interest.

## References

1. Vermeer NCA, Snijders HS, Holman FA, *et al.* Colorectal cancer screening: systematic review of screen-related morbidity and mortality. *Cancer treatment reviews*, 2017, 54: 87–98.
2. Chiang JM, Chang CJ, Jiang SF, *et al.* Pre-operative serum albumin level substantially predicts post-operative morbidity and mortality among patients with colorectal cancer who undergo elective colectomy. *Eur J Cancer Care*, 2017, 26: e12403.
3. Breugom AJ, Swets M, Bosset JF, *et al.* Adjuvant chemotherapy after preoperative (chemo) radiotherapy and surgery for patients with rectal cancer: a systematic review and meta-analysis of individual patient data. *Lancet Oncol*, 2015, 16: 200–207.
4. Miller KD, Siegel RL, Lin CC, *et al.* Cancer treatment and survivorship statistics, 2016. *CA: Cancer J Clin*, 2016, 66: 271–289.
5. Xiao Y, Freeman G J. The microsatellite instable subset of colorectal cancer is a particularly good candidate for checkpoint blockade immunotherapy. *Cancer Discov*, 2015, 5: 16–18.
6. Rizvi NA, Hellmann MD, Snyder A, *et al.* Mutational landscape determines sensitivity to PD-1 blockade in non-small cell lung cancer. *Science*, 2015, 348: 124–128.
7. Reck M, Rodríguez-Abreu D, Robinson AG, *et al.* Pembrolizumab versus chemotherapy for PD-L1-positive non-small-cell lung cancer. *New England J Med*, 2016, 375: 1823–1833.
8. Noman M Z, Desantis G, Janji B, *et al.* PD-L1 is a novel direct target of HIF-1 $\alpha$ , and its blockade under hypoxia enhanced MDSC-mediated T cell activation. *J Exp Med*, 2014, 211: 781–790.
9. McAlees JW, Lajoie S, Dienger K, *et al.* Differential control of CD4+ T-cell subsets by the PD-1/PD-L1 axis in a mouse model of allergic asthma. *Eur J Immunol*, 2015, 45: 1019–1029.

10. Wu P, Wu D, Li L, *et al.* PD-L1 and survival in solid tumors: a meta-analysis. *PLoS one*, 2015, 10: e0131403.
11. Chen J, Jiang CC, Jin L, *et al.* Regulation of PD-L1: a novel role of pro-survival signalling in cancer. *Ann Oncol*, 2015, 27: 409–416.
12. Bellmunt J, Mullane SA, Werner L, *et al.* Association of PD-L1 expression on tumor-infiltrating mononuclear cells and overall survival in patients with urothelial carcinoma. *Ann Oncol*, 2015, 26: 812–817.
13. Mony JT, Zhang L, Ma T, *et al.* Anti-PD-L1 prolongs survival and triggers T cell but not humoral anti-tumor immune responses in a human MUC1-expressing preclinical ovarian cancer model. *Cancer Immunol Immunother*, 2015, 64: 1095–1108.
14. Shukuya T, Mori K, Amann JM, *et al.* Relationship between overall survival and response or progression-free survival in advanced non-small cell lung cancer patients treated with anti-PD-1/PD-L1 antibodies. *J Thorac Oncol*, 2016, 11: 1927–1939.
15. Philips G K, Atkins M. Therapeutic uses of anti-PD-1 and anti-PD-L1 antibodies. *Int Immunol*, 2014, 27: 39–46.
16. Herbst RS, Baas P, Kim D W, *et al.* Pembrolizumab versus docetaxel for previously treated, PD-L1-positive, advanced non-small-cell lung cancer (KEYNOTE-010): a randomised controlled trial. *Lancet*, 2016, 387: 1540–1550.
17. Zhang Y, Kang S, Shen J, *et al.* Prognostic significance of programmed cell death 1 (PD-1) or PD-1 ligand 1 (PD-L1) Expression in epithelial-originated cancer: a meta-analysis. *Medicine*, 2015, 94: e515.
18. Zhong A, Xing Y, Pan X, *et al.* Prognostic value of programmed cell death-ligand 1 expression in patients with non-small-cell lung cancer: evidence from an updated meta-analysis. *Onco Targets Ther*, 2015, 8: 3595.
19. Drosier RA, Hirt C, Viehl CT, *et al.* Clinical impact of programmed cell death ligand 1 expression in colorectal cancer. *Eur J Cancer*, 2013, 49: 2233–2242.
20. Higgins JPT, Thompson SG, Deeks JJ, *et al.* Measuring inconsistency in meta-analyses. *BMJ*, 2003, 327: 557.
21. Egger M, Smith GD, Schneider M, *et al.* Bias in meta-analysis detected by a simple, graphical test. *BMJ*, 1997, 315: 629–634.
22. Begg CB, Mazumdar M. Operating characteristics of a rank correlation test for publication bias. *Biometrics*, 1994: 1088–1101.
23. Shi SJ, Wang LJ, Wang GD, *et al.* B7-H1 expression is associated with poor prognosis in colorectal carcinoma and regulates the proliferation and invasion of HCT116 colorectal cancer cells. *PLoS One*, 2013, 8: e76012.
24. Liang M, Li J, Wang D, *et al.* T-cell infiltration and expressions of T lymphocyte co-inhibitory B7-H1 and B7-H4 molecules among colorectal cancer patients in northeast China's Heilongjiang province. *Tumor Biol*, 2014, 35: 55–60.
25. Zhu J, Chen L, Zou L, *et al.* MiR-20b,-21, and-130b inhibit PTEN expression resulting in B7-H1 over-expression in advanced colorectal cancer. *Hum immunol*, 2014, 75: 348–353.
26. Zhu H, Qin H, Huang Z, *et al.* Clinical significance of programmed death ligand-1 (PD-L1) in colorectal serrated adenocarcinoma. *Int J Clin Exp Pathol*, 2015, 8: 9351.
27. Saigusa S, Toiyama Y, Tanaka K, *et al.* Implication of programmed cell death ligand 1 expression in tumor recurrence and prognosis in rectal cancer with neoadjuvant chemoradiotherapy. *Int J Clin Oncol*, 2016, 21: 946–952.
28. Song M, Chen D, Lu B, *et al.* PTEN loss increases PD-L1 protein expression and affects the correlation between PD-L1 expression and clinical parameters in colorectal cancer. *PLoS one*, 2013, 8: e65821.
29. Wang L, Ren F, Wang Q, *et al.* Significance of programmed death ligand 1 (PD-L1) immunohistochemical expression in colorectal cancer. *Mol Diagn Ther*, 2016, 20: 175–181.
30. D'incecco A, Andreozzi M, Ludovini V, *et al.* PD-1 and PD-L1 expression in molecularly selected non-small-cell lung cancer patients. *Bri J Cancer*, 2015, 112: 95.
31. Ohaegbulam KC, Assal A, Lazar-Molnar E, *et al.* Human cancer immunotherapy with antibodies to the PD-1 and PD-L1 pathway. *Trends Mol Med*, 2015, 21: 24–33.
32. Mu CY, Huang JA, Chen Y, *et al.* High expression of PD-L1 in lung cancer may contribute to poor prognosis and tumor cells immune escape through suppressing tumor infiltrating dendritic cells maturation. *Med Oncol*, 2011, 28: 682–688.
33. Rosenbaum MW, Bledsoe JR, Morales-Oyarvide V, *et al.* PD-L1 expression in colorectal cancer is associated with microsatellite instability, BRAF mutation, medullary morphology and cytotoxic tumor-infiltrating lymphocytes. *Mod Pathol*, 2016, 29: 1104.
34. Velcheti V, Schalper KA, Carvajal DE, *et al.* Programmed death ligand-1 expression in non-small cell lung cancer. *Lab investig*, 2014, 94: 107.
35. He J, Hu Y, Hu M, *et al.* Development of PD-1/PD-L1 pathway in tumor immune microenvironment and treatment for non-small cell lung cancer. *Sci Rep*, 2015, 5: 13110.
36. Huang B, Chen L, Bao C, *et al.* The expression status and prognostic significance of programmed cell death 1 ligand 1 in gastrointestinal tract cancer: a systematic review and meta-analysis. *Onco Targets Ther*, 2015, 8: 2617.

DOI 10.1007/s10330-018-0312-2

Cite this article as: Liu SW, Ma R, Cao HX, *et al.* Prognostic significance of PD-L1 expression in patients with colorectal cancer: a meta-analysis. *Oncol Transl Med*, 2019, 5: 68–74.

# Clinical significance of *BRAF*<sup>V600E</sup> and *TERT* promoter mutation in papillary thyroid microcarcinoma\*

Jincai Xue, Qinjiang Liu, Youxin Tian, Xiaofeng Hou (✉)

Department of Head and Neck Surgery, Gansu Province Tumor Hospital, Lanzhou 730050

## Abstract

**Objective** The objective of this study was to analyze the correlation between *BRAF*<sup>V600E</sup> and *TERT* promoter mutations and papillary thyroid microcarcinoma (PTMC) risk factors, and their importance in the risk assessment of papillary thyroid microcarcinoma.

**Methods** This study retrospectively analyzed 107 cases of PTMC, which were diagnosed after the surgery in the department of head and neck surgery in Gansu Province Tumor Hospital from October 2014 to June 2016. The mutations of *BRAF*<sup>V600E</sup> and *TERT* promoter were detected by PCR direct sequencing. We analyzed the data using  $\chi^2$  test and binary Logistic regression analysis.

**Results** Among 107 patients with PTMC, the *BRAF*<sup>V600E</sup> and *TERT* promoter mutation rates were 68.2% and 11.2%, respectively. Single factor analysis showed that there was a significant difference between the presence of membrane invasion, lymph node metastasis, and *BRAF*<sup>V600E</sup> mutations ( $P < 0.01$ ). The age, gender, thyroid capsular invasion, poor pathologic subtype, and lymph node metastasis of patients, was significantly associated with the *TERT* promoter mutation ( $P < 0.05$ ) and the coexistence of the *BRAF*<sup>V600E</sup> and *TERT* promoter mutations; although, there was a difference between the association of these factors with the *TERT* promoter mutation and the association of these factors with the coexistence of the *BRAF*<sup>V600E</sup> and *TERT* promoter mutations. The multifactorial analysis showed that the factors closely related to the *BRAF*<sup>V600E</sup> mutation included capsular invasion ( $P = 0.012$ ) and lymph node metastasis ( $P = 0.000$ ). The following factors were closely associated with the *TERT* promoter mutant: male ( $P = 0.004$ ), aged < 45 years ( $P = 0.026$ ), capsular invasion ( $P = 0.004$ ), pathological subtype ( $P = 0.030$ ), and lymph node metastasis ( $P = 0.043$ ). The following factors were closely related to the simultaneous mutation of *BRAF*<sup>V600E</sup> and *TERT*: male ( $P = 0.022$ ), capsular invasion ( $P = 0.023$ ), poor pathological subtype ( $P = 0.041$ ), and lymph node metastasis ( $P = 0.030$ ).

**Conclusion** The risk of recurrence increases significantly when mutations in *BRAF*<sup>V600E</sup> and *TERT* promoters occur simultaneously in PTMC and may have adverse outcomes. Combined detection of *BRAF*<sup>V600E</sup> and *TERT* promoter mutations is of great value in risk assessment of PTMC.

**Key words:** papillary thyroid microcarcinoma (PTMC); *BRAF*<sup>V600E</sup>; *TERT*; mutation

Received: 27 October 2018  
Revised: 01 December 2018  
Accepted: 01 March 2019

Papillary thyroid microcarcinoma (PTMC) accounts for a large proportion of thyroid cancers with a high annual incidence [1]. PTMC is defined as small papillary thyroid carcinoma that is less than 1.0 cm [2]. Most prognosis of PTMC are considered to be excellent, but some PTMCs have poor prognosis. If the molecular markers of PTMC can be discovered, they can be used to accurately predict prognosis and guide the improvement of clinical diagnosis and treatment. This study will examine *BRAF*<sup>V600E</sup> and telomerase reverse transcriptase (*TERT*) promoter mutation and their relationship with PTMC risk factors; This will hopefully help balance the treatment-associated

benefit and risk of PTMC.

## Material and methods

### Research object and methods

One hundred and seven patients with PTMC without metastasis were included (24 men and 83 women), with a median age of  $44.0 \pm 11.8$  years (ranging from 19 to 76 years). Of these patients, 48 were less than 45 years old and 59 were over 45 years old after the initial diagnosis and treatment in the department of head and neck surgery in Gansu Provincial Tumor Hospital from October 2014

✉ Correspondence to: Qinjiang Liu. E-mail: LIUQJ99@126.com

\* Supported by a grant from the Science and Technology Plan Projects of Lanzhou (No. 2017-4-75).

© 2019 Huazhong University of Science and Technology

to June 2016. There were 38 cases where the size of tumor was less than 5 mm and 69 cases with sizes more than 5 mm, 28 cases with multifocal carcinoma and 79 cases with solitary carcinoma, 41 cases with thyroid capsule invasion and 66 cases with tumor encapsulation. There were 19 cases with poor pathologic types (high cell subtype, columnar cell subtype, eosinophil subtype, etc.) and 88 cases without it, 64 cases had no lymphoid involvement (stage N0) and 43 cases had lymph node involvement (stage N1 N1a + N1b) (Table 1). All subjects had no previous history of tumors, and standardized surgical treatment and pathological diagnosis were performed. This study was approved by the Ethics Committee of Gansu Provincial Tumor Hospital, and the patients were prior informed and consented.

### Sequencing method

The *BRAF*<sup>V600E</sup> and *TERT* promoter mutations were detected by polymerase chain reaction (PCR) and direct sequencing. The *TERT* promoters included the C228T and C250T sites. Tumor tissues were fixed with a 4% formaldehyde solution, embedded in paraffin, and sliced at a thickness of 5 to 10  $\mu\text{m}$ . One slice was taken for routine hematoxylin and eosin (HE) staining, and then identified by the pathologist and evaluated for tumor cell content. Two to four sections were taken to extract genomic DNA, which were then subjected to PCR amplification. After electrophoresis was used to detect the quality of the PCR amplification product, the higher quality PCR amplification products were subjected to

DNA sequencing. These results were compared with the *BRAF*<sup>V600E</sup> and *TERT* gene sequences, to confirm whether or not mutations occurred.

### Statistical analyses

Statistical analysis of relevant data was performed using SPSS v19.0 software. Univariate analysis of each variable was performed using the  $\chi^2$  test and multivariate analysis was performed using binary logistic regression analysis;  $P < 0.05$  was considered statistically significant.

## Results

### *BRAF*<sup>V600E</sup> mutation

The *BRAF*<sup>V600E</sup> mutation rate in patients with PTMC was 68.2% (73/107). There were no significant correlations between gender, age, tumor size, number of primary lesions, adverse pathological subtypes and *BRAF*<sup>V600E</sup> mutations ( $P > 0.05$ ). However, there was a significant correlation between thyroid capsule invasion, lymph node metastasis, and *BRAF*<sup>V600E</sup> mutations ( $P < 0.01$ ). Multivariate logistic analysis revealed significant factors associated with *BRAF*<sup>V600E</sup> mutations, including thyroid capsule invasion ( $P = 0.012$ ) and lymph node metastasis ( $P = 0.000$ ) (Table 1 and 2).

### *TERT* promoter mutation

The mutation rate of *TERT* promoter in PTMC patients was 11.2% (12/107), among which, the *TERT* C228T site mutation rate was 66.7% (8/12) and the *TERT* C250T site

**Table 1** Relationship of *BRAF*<sup>V600E</sup> and *TERT* promoter mutations with Clinicopathological features of PTMC (n, %)

Features	n (%)	BRAF (n = 73)	$\chi^2$	P	TERT (n = 12)	$\chi^2$	P	BRAF + TERT (n = 9)	$\chi^2$	P
Gender										
Male	24 (22.4)	18 (75.0)	0.655	0.418	7 (29.2)	10.014	0.002	5 (20.8)	6.197	0.013
Female	83 (77.6)	55 (66.3)			5 (6.0)			4 (4.8)		
Age (years)										
< 45	48 (44.9)	29 (60.4)	2.448	0.118	1 (2.1)	7.290	0.007	1 (2.1)	4.525	0.033
$\geq$ 45	59 (55.1)	44 (74.6)			11 (18.6)			8 (13.6)		
Tumor size (d/mm)										
$\leq$ 5	38 (35.5)	23 (60.5)	1.611	0.204	3 (7.9)	0.652	0.419	2 (5.3)	0.758	0.384
> 5	69 (64.5)	50 (72.5)			9 (13.0)			7 (10.1)		
Multifocal										
Yes	28 (26.2)	19 (67.9)	0.002	0.961	5 (17.9)	1.680	0.195	3 (10.7)	0.261	0.609
No	79 (73.8)	54 (68.4)			7 (8.9)			6 (7.6)		
Capsular invasion										
Yes	41 (38.3)	34 (82.9)	6.628	0.010	10 (24.4)	11.588	0.001	7 (17.1)	6.474	0.011
No	66 (61.7)	39 (59.1)			2 (3.0)			2 (3.0)		
Pathological subtype										
Low risk	88 (82.2)	58 (65.9)	1.225	0.268	7 (7.9)	5.291	0.021	5 (5.7)	4.792	0.029
High risk	19 (17.8)	15 (78.9)			5 (26.3)			4 (21.1)		
Lymph node Metastasis										
N0	64 (59.8)	34 (54.7)	16.748	0.000	4 (6.3)	3.943	0.047	2 (3.1)	5.777	0.016
N1(N1a + N1b)	43 (40.2)	39 (88.4)			8 (18.6)			7 (16.3)		

**Table 2** Multivariate Logistic regression analysis of  $BRAF^{V600E}$  and  $TERT$  promoter mutations of PTMC

Factors	Partial regression coefficient	Standard deviation	Wald	df <sup>a</sup>	P	Exp <sup>b</sup> (B)	95.0% CI for Exp (B)	
							Lower	Upper
<b>BRAF</b>								
Capsular invasion	-1.213	0.485	6.260	1	0.012	0.297	0.115	0.769
Lymph node Metastasis	2.152	0.582	13.687	1	0.000	8.603	2.751	26.903
<b>TERT</b>								
Gender	-1.860	0.644	8.346	1	0.004	0.156	0.044	0.550
Age	2.377	1.064	4.986	1	0.026	10.771	1.337	86.755
Capsular invasion	-2.334	0.805	8.411	1	0.004	0.097	0.020	0.469
Pathological subtype	1.419	0.653	4.719	1	0.030	4.133	1.149	14.866
Lymph node Metastasis	1.232	0.648	3.816	1	0.043	3.429	0.962	12.215
<b>BRAF + TERT</b>								
Gender	-1.648	0.718	5.272	1	0.022	0.192	0.047	0.786
Age	1.998	1.080	3.423	1	0.064	7.373	0.888	61.194
Capsular invasion	-1.885	0.829	5.167	1	0.023	0.152	0.030	0.771
Pathological subtype	1.488	0.727	4.186	1	0.041	4.427	1.064	18.408
Lymph node Metastasis	1.796	0.829	4.699	1	0.030	6.028	1.188	30.589

<sup>a</sup>df: Degree of freedom, <sup>b</sup>Exp (B): The OR value of the corresponding variable(Advantage ratio), CI: Confidence interval

mutation was 33.3% (4/12). Age, gender, capsule invasion, adverse pathological subtypes, and lymph node metastasis were significantly associated with  $TERT$  promoter mutations ( $P < 0.05$ ). There was no significant correlation between tumor size and the number of primary lesions with  $TERT$  promoter mutations ( $P > 0.05$ ). Multivariate logistic analysis showed that male patients ( $P = 0.004$ ), aged  $< 45$  years ( $P = 0.026$ ), who had thyroid capsule invasion ( $P = 0.004$ ), an adverse pathological subtypes ( $P = 0.030$ ), and lymph node metastasis ( $P = 0.043$ ) were significant associated with the  $TERT$  promoter mutation (Table 1 and 2).

### Coexistence of $BRAF^{V600E}$ and $TERT$ promoter mutations

Twelve PTMC patients had  $TERT$  promoter mutations, and nine of them (75%) had  $BRAF^{V600E}$  mutations as well. Age, gender, capsule invasion, adverse pathological subtypes, and lymph node metastasis were significantly associated with  $BRAF^{V600E}$  and  $TERT$  mutations ( $p < 0.05$ ). There was no significant correlation between tumor size and the number of primary lesions with the  $BRAF^{V600E}$  and  $TERT$  mutations ( $P > 0.05$ ). Multivariate logistic analysis showed significant correlation between male patients ( $P = 0.022$ ), who had thyroid capsule invasion ( $P = 0.023$ ), an adverse pathological subtype ( $P = 0.041$ ), and lymph node metastasis ( $P = 0.030$ ) with  $BRAF^{V600E}$  and  $TERT$  mutations (Table 1 and 2).

### Discussion

PTMC is a common type of papillary thyroid carcinoma, and most prognoses of PTMC are considered to be

excellent with a 15-year survival rate of approximately 90.7% [3]. However, some PTMC have highly invasive clinicopathological features, which may result in cervical lymph node involvement or even multiple metastases with small primary lesions. The treatment of PTMC has been controversial for many years [4-6], including how to screen high-risk patients in PTMC and achieve accurate treatment, which depends on further development of molecular etiology and molecular imaging as well as other related disciplines [7-10].

At present, the key indicators for PTMC risk assessment, such as tumor diameter, multifocal, capsule invasion, adverse pathological subtypes, and lymph node involvement, are mostly based on retrospective studies of postoperative pathological results and have limited value in preoperative evaluations and intraoperative guidance [11]. There is an urgent need to discover more molecular markers for diagnosis, prognostic evaluation, and therapeutic targets. It is extremely important for formulating rational and standardized treatment protocols to screen out valuable molecular biomarkers of PTMC.

The  $BRAF^{V600E}$  gene is a DNA sequence that can be transfected into NIH3T3 cells in human Ewing's sarcoma. The mutation of T1799A in the  $BRAF$  gene can activate the MAPK pathway, which promotes cell proliferation and carcinogenesis, and it is closely related to the occurrence and development of thyroid cancer [12-13].  $BRAF^{V600E}$  is one of the most common mutant genes in thyroid cancer, with high diagnostic specificity and a sensitivity of 85.1% [14]. However, with the increasing sensitivity of molecular biology techniques, the detection rate of the  $BRAF^{V600E}$  gene mutation in thyroid cancer is increasing. Furthermore, the role of the  $BRAF$  gene

mutation, as an independent prognostic indicator, is controversial [15].

Studies have shown that *BRAF* mutations are closely related to the occurrence, development, recurrence, and prognosis of papillary thyroid carcinoma (PTC) and can be used to assess the risk of PTC [16–18]. A meta-analysis found that the *BRAF*<sup>V600E</sup> mutant had a higher recurrence rate (24.9% vs. 12.6%) than the *BRAF* wild type in 2470 PTC patients, and the *BRAF*<sup>V600E</sup> mutation correlated with tumor aggressiveness [19]. Some studies have found PTMC patients with the *BRAF* gene mutation have a higher rate of cervical lymph node metastasis; Hence, it is considered as an independent risk factor for this metastasis. The *BRAF* gene mutation in PTMC patients also has a high rate of lateral lymph node metastasis [20–21].

It was also reported that tumor recurrence was mainly associated with lymph node metastasis and thyroid capsule invasion without the *BRAF*<sup>V600E</sup> mutation. Furthermore, the *BRAF* gene mutation did not increase the invasiveness of PTMC [22–23]. The prognostic value of the *BRAF*<sup>V600E</sup> mutation, in the recurrence of papillary thyroid carcinoma, was evaluated. The results indicated that the *BRAF*<sup>V600E</sup> mutation in the high-risk group (aged < 35 years and ≥ 60 years), had local residual and recurrence rates that were 17.28 to 33.49 times higher than those of the low-risk group, *BRAF*<sup>V600E</sup> [24]. The earliest study on *BRAF* gene mutations in China showed that there was no correlation between the *BRAF* mutation and the prognosis of papillary thyroid carcinoma, except when they were related to the age of the patients [25]. Thus, the prognostic value of *BRAF* gene mutations is a debatable indicator and should be used in combination with other molecules or other clinicopathological factors for tumor prognosis.

This study showed that the *BRAF*<sup>V600E</sup> mutation rate of PTMC was 68.2% (73/107). There was no significant correlation between gender, age, tumor size, number of primary lesions, and adverse pathological subtypes with the *BRAF*<sup>V600E</sup> mutations ( $P > 0.05$ ), when associated with capsule invasion and lymph node metastasis ( $P < 0.01$ ). Multivariate logistic analysis showed that the *BRAF*<sup>V600E</sup> mutation was significantly associated with capsule invasion and lymph node metastasis, which is associated with the prognosis of PTMC [12]. Thus, based on this study, the *BRAF*<sup>V600E</sup> mutation can be considered as a reference index for evaluating the prognosis of PTMC.

The *TERT* promoter mutation in thyroid cancer was first discovered in 2013, and later studies have found that the mutation rate in patients with PTMC is 4.7% and it was related to the degree of tumor differentiation [26–27]. This study found that the mutation rate of the *TERT* promoter in patients with PTMC was 11.2% (12/107). There was a significant correlation between age, gender, capsule invasion, adverse pathological subtypes, and lymph node

involvement with *TERT* promoter mutations ( $P < 0.05$ ). However, there was no significant correlation between tumor size and number of primary lesions with *TERT* promoter mutations ( $P > 0.05$ ). Multivariate logistic analysis showed that male patients, aged < 45 years old, with capsule invasion, adverse pathological subtypes, and lymph node involvement, were significantly associated with the *TERT* promoter mutations. Therefore, this study suggests that *TERT* mutations are closely related to prognosis in patients with PTMC.

Studies have shown that *BRAF*<sup>V600E</sup> is correlated and synergistic with *TERT* promoter mutations [28–29]. This study found that *BRAF*<sup>V600E</sup> mutations in PTMC patients were not significantly associated with gender, age, tumor size, number of primary lesions, and adverse pathological subtypes ( $P > 0.05$ ). However, *BRAF*<sup>V600E</sup> shows significant correlation ( $P < 0.05$ ) when combined with *TERT* mutations. Multivariate logistic analysis showed that males with thyroid capsule invasion, adverse pathological subtype, and lymph node involvement, which are known risk factors for PTMC recurrence, are associated with *BRAF*<sup>V600E</sup> and *TERT* mutations. This study showed that *BRAF*<sup>V600E</sup> and *TERT* promoter mutations have great value for PTMC risk assessment and could be used as primary indicators for predicting prognosis.

While the future of PTMC prognosis is promising, there are controversies surrounding the various treatments and the search for specific molecular markers is ongoing. Many studies about *BRAF*<sup>V600E</sup> mutations have also been reported. However, studies on *BRAF*<sup>V600E</sup> mutations and *TERT* promoter mutations have rarely been reported in patients from other countries. Other studies have mainly concentrated on late-stage tumors or tumors with poor prognosis; only a few have studied PTMC. Our study suggested that simultaneous *BRAF*<sup>V600E</sup> and *TERT* promoter mutations may be associated with poor prognosis of PTMC, but the mechanism is still not clear. *BRAF*<sup>V600E</sup> and *TERT* promoter mutations are potential molecular markers for PTMC prognosis and their combined detected could be a new prognostic approach for this disease.

## Conflicts of interest

The authors indicated no potential conflicts of interest.

## References

1. Morris LG, Sikora AG, Tosteson TD, *et al*. The increasing incidence of thyroid cancer: the influence of access to care. *Thyroid*, 2013, 23: 885–891.
2. Hedinger C, Williams ED, Sobin LH. The WHO histological classification of thyroid tumors: a commentary on the second edition. *Cancer*, 63: 908–911.

3. Yu XM, Wan Y, Sippel RS, *et al.* Should all papillary thyroid microcarcinomas be aggressively treated? An analysis of 18445 cases. *Ann Surg*, 2011, 254: 653–660.
4. Godbert Y, Hwnriques-Figueiredo B, Cazeau AL, *et al.* A papillary thyroid microcarcinoma revealed by a single bone lesion with no poor prognostic factors. *Case Rep Endocrinol*, 2013, 2013: 719304.
5. Ogilvie JB, Patel KN, Heller KS. Impact of the 2009 American Thyroid Association guidelines on the choice of operation for well-differentiated thyroid microcarcinomas. *Surgery*, 2010, 148: 1222–1226.
6. Liu HG. To strengthen the study of papillary thyroid microcarcinoma. *Chinese J Pathol (Chinese)*, 2016, 45: 361–363.
7. Xing MC, Sa A, Kathryn A, *et al.* Association between BRAF V600E mutation and mortality in patients with papillary thyroid cancer. *JAMA*, 2013, 309: 1493–1501.
8. Melck AL, Yip L, Carty SE. The utility of BRAF testing in the management of papillary thyroid cancer. *Oncologist*, 2010, 15: 1285–1293.
9. Nikiforova MN, Wald AI, Roy S, *et al.* Targeted next-generation sequencing panel (ThyroSeq) for detection of mutations in thyroid cancer. *J Clin Endocrinol Metab*, 2013, 98: 1852–1860.
10. Wang YS, Liu QJ, Tian YX. Correlation between sodium-iodide symporter expression and circulating tumor cell positivity in differentiated thyroid carcinoma. *Oncol Transl Med*, 2018, 4: 68–71.
11. PENG C, Wei SF, Zheng XQ, *et al.* Clinicopathological features and risk factors for central compartment nodal metastasis in papillary thyroid microcarcinoma: a study of 1 401 patients. *Chinese J Clin Oncol (Chinese)*, 2016, 43: 95–99.
12. Ikawa S, Fukui M, Ueyama Y, *et al.* B-raf, a new member of the raf family, is activated by DNA rearrangement. *Mol Cell Biol*, 1988, 8: 2651–2654.
13. Wang XM. The future of gene testing and molecular targeted therapy in thyroid cancer. *Med Philos*, 2015, 36: 9–12.
14. Zhang YZ, Xu T, Cui D, *et al.* Value of TIRADS, BSRTC and FNA-BRAFV600E mutation analysis in differentiating high-risk thyroid nodules. *Sci Rep (Chinese)*, 2015, 24: 16927.
15. Xing M. BRAF Mutation and Thyroid Cancer Recurrence. *J Clin Oncol (Chinese)*, 2015, 33: 2482–2483.
16. Xing M, Alzahrani AS, Carson KA, *et al.* Association between BRAFV600E mutation and mortality in patients with papillary thyroid cancer. *J Am Med Assoc*, 2013, 309: 1493–1501.
17. Tufano RP, Teixeira GV, Bishop J, *et al.* BRAF Mutation in papillary thyroid cancer and its value in tailoring initial treatment: a systematic review and meta-analysis. *Medicine (Baltimore)*, 2012, 91: 274–286.
18. RU XT, Liu QJ, Zhou HH, *et al.* BRAF V600E/TERT promoter mutations and NIS/ TSHR expression in differentiated thyroid carcinoma and their clinical significance. *Oncol Transl Medicine*, 2017, 3: 71–76.
19. Gandolfi G, Sancisi V, Piana S, *et al.* Time to re-consider the meaning of BRAF V600E mutation in papillary thyroid carcinoma. *Int J Cancer*, 2015, 137: 1001–1011.
20. Zheng X, Wei S, Han Y, *et al.* Papillary microcarcinoma of the thyroid: clinical characteristics and BRAF(V600E) mutational status of 977 cases. *Ann Surg Oncol*, 2013, 20: 2266–2273.
21. Lin KL, Wang OC, Zhang XH, *et al.* The BRAF mutation is predictive of aggressive clinicopathological characteristics in papillary thyroid microcarcinoma. *Ann Surg Oncol*, 2010, 17: 3294–3300.
22. Czarniecka A, Kowal M, Rusinek D, *et al.* The risk of relapse in papillary thyroid cancer (PTC) in the context of BRAFV600E mutation status and other prognostic factors. *PLoS One*, 2015, 10: e0132821.
23. Walczyk A, Kowalska A, Kowalik A, *et al.* The BRAF(V600E) mutation in papillary thyroid microcarcinoma: does the mutation have an impact on clinical outcome? *Clin Endocrinol (Oxf)*, 2014, 80: 899–904.
24. Takacsova E, Kralik R, Waczulikova I, *et al.* A different prognostic value of BRAFV600E mutation positivity in various age groups of patients with papillary thyroid cancer. *Neoplasma*, 2017, 64: 156–164.
25. Wang YL, Wang JC, WU Y, *et al.* Incidentally simultaneous occurrence of RET/ PTC, H4-PTEN and BRAF mutation in papillary thyroid carcinoma. *Cancer Lett*, 2008, 263: 44–52.
26. Liu X, Bishop J, Shan Y, *et al.* Highly prevalent TERT promoter mutations in aggressive thyroid cancers. *Endocr Relat Cancer*, 2013, 20: 603–610.
27. de Biase D, Gandolfi G, Ragazzi M, *et al.* TERT promoter mutations in papillary thyroid microcarcinomas. *Thyroid*, 2015, 25: 1013–1019.
28. Alzahrani AS, Alsaadi R, Murugan AK, *et al.* TERT promoter mutations in thyroid cancer. *Horm Cancer*, 2016, 7: 165–177.
29. Tang XY, Shi F, Li CL, *et al.* Research progress of TERT promoter mutation in thyroid cancer. *Chinese J Clin Pharmacol Ther (Chinese)*, 2017, 22: 350–354.

DOI 10.1007/s10330-018-0314-4

Cite this article as: Xue JC, Liu QJ, Tian XY, *et al.* Clinical significance of BRAF<sup>V600E</sup> and TERT promoter mutation in papillary thyroid microcarcinoma. *Oncol Transl Med*, 2019, 5: 75–79.

# Safety and efficacy of EGFR and VEGF signaling pathway inhibition therapy in patients with colorectal cancer: a meta-analysis\*

Siwen Liu<sup>1</sup>, Rong Ma<sup>1</sup>, Haixia Cao<sup>1</sup>, Shaorong Yu<sup>2</sup>, Dan Chen<sup>1</sup>, Changwen Jing<sup>1</sup>, Zhuo Wang<sup>1</sup>, Junying Zhang<sup>1</sup>, Jifeng Feng<sup>1,2</sup> (✉), Jianzhong Wu<sup>1</sup> (✉)

<sup>1</sup> Research Center for Clinical Oncology, Jiangsu Cancer Hospital & Jiangsu Institute of Cancer Research & The Affiliated Cancer Hospital of Nanjing Medical University, Nanjing 210009, China

<sup>2</sup> Department of Oncology, Jiangsu Cancer Hospital & Jiangsu Institute of Cancer Research & The Affiliated Cancer Hospital of Nanjing Medical University, Nanjing 210009, China

## Abstract

**Objective** Epidermal growth factor receptor (EGFR) and vascular endothelial growth factor (VEGF) inhibitors are two targeted therapies for metastatic colorectal cancer (mCRC). However, few studies have focused on the safety and efficacy of combined targeted therapy against those of a single inhibition therapy of EGFR or VEGF. This meta-analysis aimed to compare the anti-tumor activity of the combined inhibition therapy and single inhibition therapy in patients with mCRC.

**Methods** We searched PubMed, Medline, the Cochrane library, Embase, and annual meeting proceedings for relevant clinical trials. Objective response rate (ORR), progression-free survival (PFS), overall survival (OS), and adverse events were extracted and calculated.

**Results** Nine trials comprising 3977 patients were selected for the analysis. The combined inhibition therapy showed a 3.7% improvement in ORR compared with single inhibition, and this difference was statistically significant [hazard ratio (HR) = 1.33; 95% confidence interval (CI), 1.01–1.74;  $P = 0.04$ ]. Subgroup analysis showed that the combined EGFR and VEGF inhibitor therapy had an 11.65% improvement in ORR compared with VEGF inhibitor therapy (OR = 2.14; 95% CI, 1.34–3.40;  $P = 0.001$ ). EGFR and VEGF inhibitor therapy and chemotherapy had an 18.08% improvement in ORR compared with chemotherapy (OR = 2.21; 95% CI, 1.05–4.64;  $P = 0.04$ ). Moreover, EGFR and VEGF inhibitor therapy significantly improved PFS compared with VEGF inhibitor therapy (OR = 0.82; 95% CI, 0.69–0.97;  $P = 0.02$ ). VEGF inhibitor therapy and chemotherapy significantly improved PFS compared with EGFR and VEGF inhibitor therapy and chemotherapy (OR = 1.20; 95% CI, 1.11–1.30;  $P = 0.00$ ). In addition, EGFR and VEGF inhibitor therapy showed improved OS compared with VEGF inhibitor therapy (HR = 0.78, 95% CI: 0.65–0.94;  $P = 0.008$ ). Finally, the combined inhibition therapy showed an obviously increased risk of cutaneous and mucosal effects (RR = 6.45; 95% CI: 2.71–15.36;  $P < 0.01$ ), diarrhea/abdominal pain (RR = 1.97; 95% CI: 1.45–2.68;  $P < 0.01$ ), fatigue/asthenia (RR = 1.60; 95% CI: 1.10–2.32;  $P = 0.01$ ), dehydration or electrolyte disturbance (RR = 2.78; 95% CI: 1.48–5.21;  $P < 0.01$ ), nail disorder (RR = 8.23; 95% CI: 1.52–44.57;  $P = 0.01$ ), and dizziness/headache (RR = 3.43; 95% CI: 1.89–6.23;  $P < 0.01$ ) compared with single inhibition therapy.

**Conclusion** Compared with single inhibition therapy, the combined inhibition therapy significantly improved ORR, PFS, and OS in the treatment of mCRC patients. Compared with a single-targeted agent, the combined therapy of anti-EGFR and anti-VEGF drug provided an efficacy advantage, although it led to greater toxicity.

**Key words:** colorectal cancer (CRC); epidermal growth factor receptor (EGFR); vascular endothelial growth factor (VEGF); meta-analysis

Received: 21 November 2018  
Revised: 3 January 2019  
Accepted: 20 February 2019

✉ Correspondence to: Jifeng Feng, Email: fjif@vip.sina.com;  
Jianzhong Wu, Email: wujzh1528@126.com

\* Supported by the grants of the National Natural Science Foundation of China (No. 81372396) and Natural Science Foundation of Jiangsu Province (No. BK20141016 and BK20141017).

© 2019 Huazhong University of Science and Technology

Colorectal cancer (CRC) was a common leading cause of cancer deaths worldwide<sup>[1]</sup>. Though the treatment with surgery was the same as the initial treatment for CRC, the prognosis was poor for patients with the presence of micrometastases at the time of surgery<sup>[2]</sup>. Cytotoxic drugs, the standard first-line treatment for metastatic colorectal cancer (mCRC), including capecitabine, oxaliplatin, 5-fluorouracil (5-FU), and irinotecan were used to improve the survival of patients with mCRC<sup>[3-5]</sup>. However, the toxicity of chemotherapy was unsatisfactory; reducing the side-effects of the therapy was needed<sup>[6]</sup>. With the introduction of the anti-vascular endothelial growth factor (VEGF) antibodies, such as bevacizumab, axitinib, cediranib, and sorafenib, and the antibodies against epidermal growth factor receptor (EGFR), such as cetuximab, gefitinib, and panitumumab, treatment of mCRC has improved, and the survival of patients has improved greatly<sup>[7-8]</sup>.

Tumor cells could promote VEGF production, which might induce the expression of downstream genes and stimulate the signaling pathways<sup>[9]</sup>. VEGF could promote the production of new vasculature by stimulating the endothelial cells<sup>[10]</sup>. The expression of EGFR on the surface of many epithelial tumors was high; this is activated by various ligand-transforming epidermal growth factor and transforming growth factor- $\alpha$ <sup>[11]</sup>. The proliferation, differentiation, and survival of cancer cells could be regulated by key downstream pathways, which are signaled by the receptor activation<sup>[12]</sup>. Compared with chemotherapy alone or chemotherapy plus placebo, the addition of anti-VEGF or/and anti-EGFR antibodies to chemotherapy could prolong the overall survival (OS) of patients with mCRC, especially those with KRAS and NRAS wild-type mCRC<sup>[13]</sup>. Although, improvement in outcomes was achieved by blocking the EGFR and VEGF expression, combining the anti-EGFR and anti-VEGF drugs with chemotherapy resulted in high response rate (RR)<sup>[14]</sup>.

Some trials had evaluated the safety and efficacy of the combination of anti-VEGF or/and anti-EGFR antibodies with or without chemotherapy for mCRC<sup>[15-17]</sup>. In the double blind trial, bevacizumab and panitumumab (40.1%) improved the RR of patients with mCRC compared with folinic acid, 5-FU, and irinotecan (FOLFIRI) (30.1%) when added to FOLFIRI; a series of antibody therapy-associated adverse events (AEs) were observed in the FOLFIRI + bevacizumab and panitumumab group (80.0%) compared with FOLFIRI alone (52.6%)<sup>[18]</sup>. Moreover, the addition of bevacizumab to FU, irinotecan, and leucovorin (IFL) significantly improved OS (20.3 months), progression-free survival (PFS) (10.6 months), and RR (44.8%) in patients with mCRC compared with IFL alone (15.6 months, 6.2 months, 34.8%)<sup>[19]</sup>. Even for patients with mCRC that progresses after all approved

standard therapies, regorafenib offered a potential new line of therapy for late-stage mCRC patients with longer OS (6.4 months) compared with the placebo group (5.0 months)<sup>[20]</sup>.

In recent years, the safety and efficacy of anti-EGFR and anti-VEGF drugs had been studied in patients with mCRC<sup>[15]</sup>. For mCRC, the inhibition of both VEGF receptor (VEGFR) and EGFR signaling pathways showed greater anti-tumor efficacy than chemotherapy or inhibition of either pathways alone<sup>[16]</sup>. However, with regards to the inhibition of both VEGFR and EGFR signaling pathways, the combined therapy might also lead to increased AEs<sup>[16]</sup>. Despite that some previous researches had explored the therapies that inhibit both VEGFR and EGFR as against single EGFR signaling pathways, no systematic review regarding the optimal strategy on combined targeted drugs in patients with mCRC was available. Hence, a meta-analysis of randomized controlled trials (RCTs) was performed to evaluate the safety and efficacy of EGFR and VEGF signaling pathways inhibition therapy in patients with mCRC.

## Materials and methods

### Search strategy and selection criteria

RCTs for comparing EGFR and VEGF signaling pathways inhibition therapy in the treatment of patients with colorectal cancer were selected through a standard search in the PubMed, Medline, the Cochrane library and Embase databases. In addition, reference lists of the selected articles were examined. We performed the search by using the following keywords or expressions: “colorectal cancer (i.e., ‘colorectal’, ‘colon\*’, ‘rectal’, ‘rectum’; ‘cancer’, ‘tumor’, ‘neoplasms’, ‘neoplas\*’, ‘carcinom\*’, ‘malignan\*’), “EGFR”, “VEGFR”, “clinical trial”, and “randomized trial”. All possible combinations of keywords were used as search terms to identify all possible candidates. The final search strategies were as follows: (1) (((colon\*) AND (neoplas\* OR carcinom\* OR malignan\*)) OR (colorectal cancer [MeSH])) AND (EGFR [MeSH] OR VEGFR [MeSH]) AND (randomized controlled trial [pt] OR controlled clinical trial [pt] OR randomized [tiab] OR placebo [tiab] OR clinical trials as topic [mesh: noexp] OR randomly [tiab] OR trial [ti]) NOT (animals [mh] NOT humans [mh])); (2) (((rectal OR rectum) AND (tumor OR neoplasms)) OR (colorectal cancer [MeSH])) AND (EGFR [MeSH] OR VEGFR [MeSH]) AND (randomized controlled trial [pt] OR controlled clinical trial [pt] OR randomized [tiab] OR placebo [tiab] OR clinical trials as topic [mesh: noexp] OR randomly [tiab] OR trial [ti]) NOT (animals [mh] NOT humans [mh])). Article types were restricted to Clinical Trial and RCT.

In addition, the annual meeting proceedings of the

American Society of Clinical Oncology and European Society of Medical Oncology were reviewed. The relevant reviews regarding the role of a therapy that inhibited EGFR and VEGFR signaling pathways for colorectal cancer patients were identified. Moreover, in order not to miss the information of prospective and ongoing trials, we also searched the websites of <http://www.ClinicalTrials.gov> and <http://www.who.int/triasearch>.

### Inclusion criteria

Articles meeting all the following criteria were eligible for inclusion in the review: (1) English language published articles; (2) those exploring clinical outcomes of colorectal cancer patients treated with either anti-EGFR or anti-VEGFR therapy; (3) those reporting one or more of the following indicators to assess the tumor response and prognosis of patients, including objective RR (ORR), PFS, and OS; (4) RCTs in human, or retrospective trials and prospective trials; and (5) those providing sufficient data to calculate the odds ratios (ORs) and the corresponding 95% confidence intervals (CIs).

### Exclusion criteria

Articles meeting all the following exclusion criteria were excluded: (1) case or reviews or meta-analyses or duplicate reports; (2) trials without complete data or full-text online articles or ongoing trials; (3) articles which lacked control groups; and (4) those which lacked critical information.

### Data extraction and quality assessment

The data extraction and quality assessment were conducted independently by two investigators (Siwen Liu and Dan Chen) in accordance with the Preferred Reporting Items for Systematic Reviews and Meta-Analyses guidance. Disagreements were resolved by discussions between the two or by a third reviewer after referring to the original articles (Shaorong Yu). The quantitiveness of articles were assessed using the quantitative 5-point Jadad scale [21].

Using a standardized data recording form, we extracted the following critical information: (1) publication details, including first author's surname, publication year; (2) methodological components; and (3) patient and trial characteristics, such as median age, sex, World Health Organization (WHO) performance status, and number of subjects; and trial phase, treatment protocols, and outcome measures. End points of interest included ORR, PFS, OS, and AEs.

### Statistical analysis

All included articles were separated into two groups (combined and single inhibition therapy groups) in order to analyze their efficacy and safety; all the summary

effect estimates were conducted with Review Manager 5.3 analysis software (Copenhagen: The Nordic Cochrane Centre, The Cochrane Collaboration, 2014).

For time-to-event data, the impact of combined and single inhibition therapy on OS and PFS was measured in terms of the hazard ratios (HRs) [22]. The log HRs and their variances were used directly if provided by the article. If not appropriate for direct analysis, they were computed according to the previous reported method from CIs of the HRs extracted from each trial before data pooling. In addition, the summary HRs and their 95% CIs were estimated in accordance with a general variance-based method. For ORR (including complete response and partial response), the pooled OR of ORR was calculated using the methods reported by Mantel and Haenszel [23]. Moreover, subgroup analyses were performed among the group with (1) chemotherapy; (2) VEGF inhibitor therapy; (3) EGFR and VEGF inhibitor therapy; and (4) EGFR and VEGF inhibitor therapy and chemotherapy. In addition, the AEs of therapy were analyzed as drug-related WHO grade 3 or greater toxicity.

For more reliability, between-trial heterogeneity was assessed by the  $\chi^2$  test and  $I^2$  statistic [24]. For the  $I^2$  statistic, an  $I^2$  value above 50% was interpreted as large heterogeneity; between 25% and 50% meant modest heterogeneity; and below 25% suggested low heterogeneity. For  $\chi^2$  statistic, significant heterogeneity existed when  $P$  value was  $> 0.10$ . A fixed-effect model was used to calculate the pooled effect if no statistically significant heterogeneity was detected; otherwise, a random-effect model was conducted.

Additionally, Egger's [25] and Begg-Mazumdar [26] tests were employed to assess the probability of publication bias. The results were regarded as statistically significant when a two-tailed  $P$  value  $< 0.05$  was observed.

## Results

### Literature search results

Based on the above searching strategies, our search identified a total of 26 potentially relevant articles, which were assessed for full-text review, from which 17 were excluded: 12 for not assessing the combined inhibition therapy, four trials for not providing sufficient data on HRs and estimation intervals for PFS, and 1 for not providing the appropriate control arm. Finally, based on the inclusion criteria, 9 potentially eligible trials, which explored the therapy that inhibited EFGR and VEGF signaling pathways, were included in this meta-analysis (Fig. 1).

### Characteristics of included trials

The nine eligible trials of the meta-analysis were included. All trials included patients with stage IV mCRC

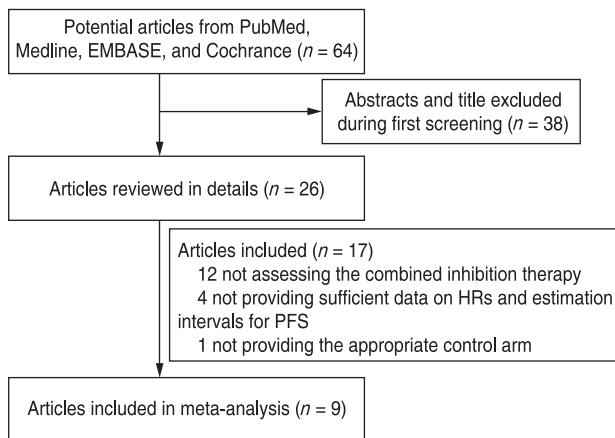


Fig. 1 Identification process for eligible studies

and were published in full articles. All of the patients had a good performance status with the ECOG or WHO score of 0. Five of the included trials were randomized phase II trials and the rest were randomized phase III trials. One trial assessed the multi-targeted agent vandetanib (the inhibition of both VEGFR and EGFR signaling pathways) plus chemotherapy against chemotherapy plus placebo, whereas the rest of the trials compared the combined inhibition therapy (the combination of anti-VEGF and anti-EGFR antibodies or plus chemotherapy or placebo) with a single inhibition therapy (the anti-VEGF antibody or anti-EGFR antibody) or plus chemotherapy or placebo. The detailed characteristics of the included nine trials are summarized in Table 1.

**Meta-analysis**

Among these trials, patients of four trials were treated with the single inhibition therapy and chemotherapy [27–30], patients of three trials were treated with the single inhibition therapy [31–33], patients of one trial were treated with chemotherapy and placebo [34], and patients of one

trial were treated with chemotherapy [35].

**ORR**

Data for ORR were available from seven trials. Compared with single inhibition (the single inhibition therapy or/and chemotherapy or/and placebo) therapy, combined inhibition therapy yielded a 3.7% improvement in ORR, and this difference was statistically significant (Random-effects model, OR = 1.33; 95% CI, 1.01–1.74;  $P = 0.04$ ; Fig. 2). There was significant heterogeneity for ORR among the individual trials ( $I^2 = 51%$ ,  $P = 0.04$ ; Fig. 2), and no evidence of significant publication bias was detected (Egger test,  $t = 2.22$ ,  $P = 0.06$ ; Begg test,  $Z = 1.15$ ,  $P = 0.25$ ).

The results of subgroup analysis showed that the group with EGFR and VEGF inhibitor therapy had an 11.65% improvement in ORR compared with VEGF inhibitor therapy (Random-effects model, OR = 2.14; 95% CI, 1.34–3.40;  $P = 0.001$ ; Fig. 3) with no significant heterogeneity ( $I^2 = 0%$ ,  $P = 0.75$ ; Fig. 3).

Moreover, the group with EGFR and VEGF inhibitor therapy and chemotherapy had an 18.08% improvement in ORR compared with the group with chemotherapy (Random-effects model, OR = 2.21; 95% CI, 1.05–4.64;  $P = 0.04$ ; Fig. 3) with no significant heterogeneity ( $I^2 = 0%$ ,  $P = 0.72$ ; Fig. 3).

However, the group with EGFR and VEGF inhibitor therapy and chemotherapy had no improvement in ORR compared with the group with VEGF inhibitor therapy and chemotherapy (Random-effects model, OR = 1.05; 95% CI, 0.84–1.32;  $P = 0.65$ ; Fig. 3) with no significant heterogeneity ( $I^2 = 24%$ ,  $P = 0.26$ ; Fig. 3).

**PFS**

All trials provided PFS results. The meta-analysis using a random-effects model revealed that the combined inhibition therapy did not significantly improve PFS compared with the single inhibition therapy (HR = 0.99, 95% CI: 0.86–1.15;  $P = 0.94$ ), with significant

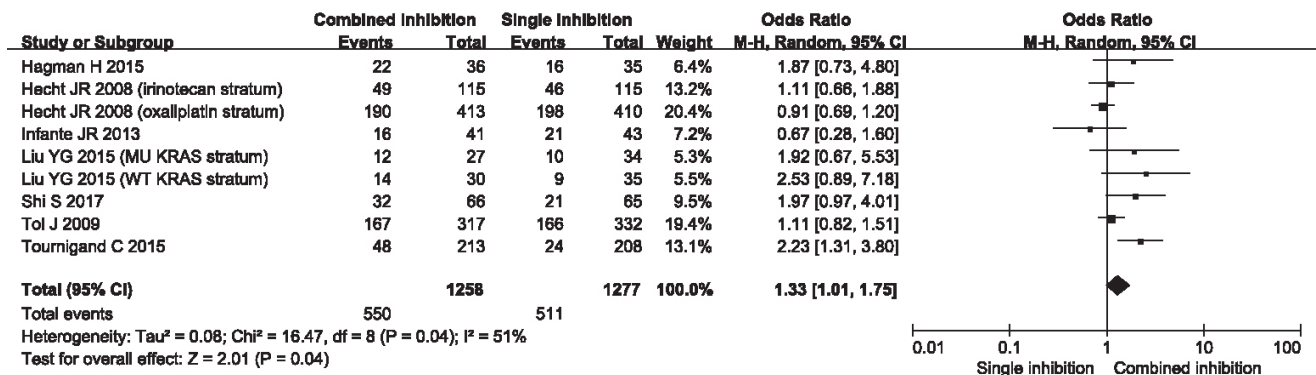
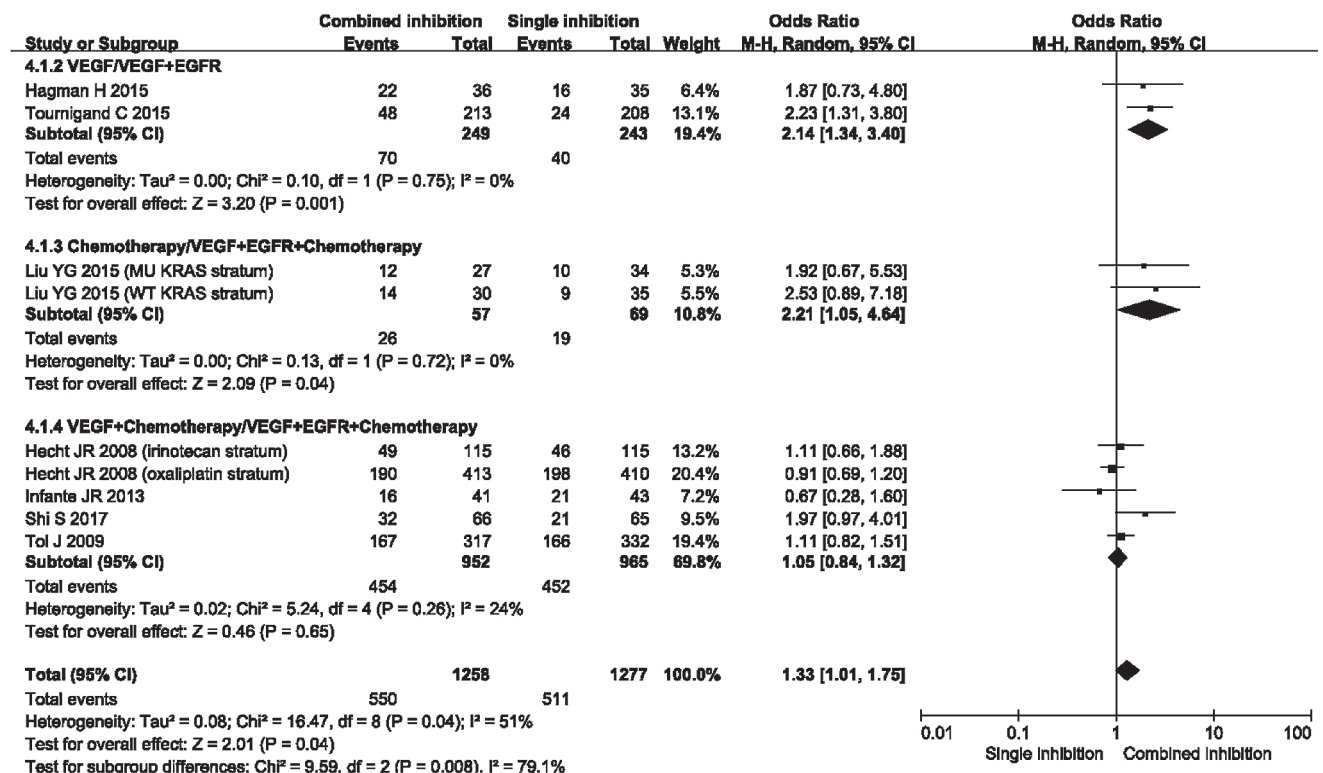


Fig. 2 Comparison of objective response rate between combined inhibition therapy and single inhibition therapy

**Table 1** Characteristics of included trials

Authors (year)	Randomized clinical trial	Number of patients	Male (%)	Median age (years)	Stage IV (%)	PS > 2 (%)
Tol J <i>et al.</i> (2009) [27]	Phase 3	368/368	205 (55.7%)/ 233 (63.3%)	62/62	368 (100%)/ 368 (100%)	0 (WHO)
Hecht JR <i>et al.</i> (2008) (oxaliplatin stratum) [28]	Phase 3	413/410	233 (56%)/ 238 (58%)	61/62	412 (99.76%)/ 410 (100%)	0 (ECOG)
Hecht JR <i>et al.</i> (2008) (irinotecan stratum) [28]	Phase 3	115/115	56 (49%)/ 71 (62%)	60/59	115 (100%)/ 115 (100%)	0 (ECOG)
Shi S <i>et al.</i> (2017) [29]	Phase 2	65/66	42 (64.6%)/ 47 (71.2%)	61.8/62.5	65 (100%)/ 66 (100%)	0 (ECOG)
Infante JR <i>et al.</i> (2013) [30]	Phase 2	43/41	28 (65.1%)/ 26 (63.4%)	64/59	43 (100%)/ 41 (100%)	0 (ECOG)
Johnsson A <i>et al.</i> (2013) [31]	Phase 3	79/80	54 (46%)/ 66 (34%)	65/64	79 (100%)/ 80 (100%)	0 (ECOG)
Hagman H <i>et al.</i> (2015) [32]	Phase 2	35/36	66 (34%)/ 64 (36%)	61/65	35 (100%)/ 36 (100%)	0 (ECOG)
Tournigand C <i>et al.</i> (2015) [33]	Phase 3	228/224	129 (57%)/ 147 (66%)	63/63	228 (100%)/ 224 (100%)	0 (WHO)
Hecht JR <i>et al.</i> (2011) [34]	Phase 3	583/585	352 (60.4%)/ 368 (62.9%)	59.6/59.1	583 (100%)/ 585 (100%)	0 (WHO)
Liu YG <i>et al.</i> (2015) (WT KRAS stratum) [35]	Phase 2	35/30	22 (63%)/ 18 (60%)	62/59	35 (100%)/ 30 (100%)	0 (ECOG)
Liu YG <i>et al.</i> (2015) (MU KRAS stratum) [35]	Phase 2	34/27	20 (59%)/ 17 (63%)	60/61	34 (100%)/ 27 (100%)	0 (ECOG)

(to be continued)

**Fig. 3** Comparison of progression-free survival between combined inhibition therapy and single inhibition therapy

**Table 1 (continued)** Characteristics of included trials

Authors (year)	Patients status	Interventions	Jadad score	Endpoint
Tol J <i>et al.</i> (2009) [27]	Untreated mCRC <sup>1</sup>	Arm-1: Bevacizumab + Chemotherapy (Capecitabine, Oxaliplatin) Arm-2: Bevacizumab + Cetuximab + Chemotherapy (Capecitabine, Oxaliplatin)	4	PFS; OS; ORR
Hecht JR <i>et al.</i> (2008) (oxaliplatin stratum) [28]	Untreated mCRC <sup>2</sup>	Arm-1: Bevacizumab + Chemotherapy (Ox-CT: Fluorouracil, Leucovorin and Oxaliplatin) Arm-2: Bevacizumab + Panitumumab + Chemotherapy (Ox-CT: 5-Fluorouracil, Leucovorin and Oxaliplatin)	4	PFS; OS; ORR
Hecht JR <i>et al.</i> (2008) (irinotecan stratum) [28]	Untreated mCRC <sup>2</sup>	Arm-1: Bevacizumab + Chemotherapy (Iri-CT: 5-Fluorouracil, Leucovorin and Irinotecan) Arm-2: Bevacizumab + Panitumumab + Chemotherapy (Iri-CT: 5-Fluorouracil, Leucovorin and Irinotecan)	4	PFS; OS; ORR
Shi S <i>et al.</i> (2017) [29]	Untreated mCRC <sup>3</sup>	Arm-1: Bevacizumab + Chemotherapy (FOLFOX4: Oxaliplatin, 5-Fluorouracil and Leucovorin) Arm-2: Bevacizumab + Erlotinib + Chemotherapy (FOLFOX4: Oxaliplatin, 5-Fluorouracil and Leucovorin)	4	PFS; OS; ORR
Infante JR <i>et al.</i> (2013) [30]	Untreated mCRC <sup>4</sup>	Arm-1: Bevacizumab + Chemotherapy (FOLFOX: Oxaliplatin, 5-Fluorouracil and Leucovorin) Arm-2: Bevacizumab + Axitinib + Chemotherapy (FOLFOX: Oxaliplatin, 5-Fluorouracil and Leucovorin)	4	PFS; OS; ORR
Johnsson A <i>et al.</i> (2013) [31]	Untreated mCRC <sup>5</sup>	Arm-1: Bevacizumab Arm-2: Bevacizumab + Erlotinib	4	PFS; OS
Hagman H <i>et al.</i> (2015) [32]	mCRC with KRAS wild type <sup>6</sup>	Arm-1: Bevacizumab Arm-2: Bevacizumab + Erlotinib	4	PFS; OS; ORR
Tournigand C <i>et al.</i> (2015) [33]	mCRC <sup>7</sup>	Arm-1: Bevacizumab Arm-2: Bevacizumab + Erlotinib	4	PFS; OS; ORR
Hecht JR <i>et al.</i> (2011) [34]	Untreated mCRC	Arm-1: Placebo + Chemotherapy (FOLFOX4: Oxaliplatin, Fluorouracil and Leucovorin) Arm-2: (PTK/ZK: Vatalanib) + Chemotherapy (FOLFOX4: Oxaliplatin, 5-Fluorouracil and Leucovorin)	5	PFS; OS
Liu YG <i>et al.</i> (2015) (WT KRAS stratum) [35]	mCRC with WT KRAS <sup>8</sup>	Arm-1: Chemotherapy (Iri-CT: 5-Fluorouracil, Leucovorin and Irinotecan) Arm-2: Bevacizumab + Panitumumab + Chemotherapy (FOLFIRI: Irinotecan, 5-Fluorouracil and Leucovorin)	4	PFS; OS; ORR
Liu YG <i>et al.</i> (2015) (MU KRAS stratum) [35]	mCRC with MU KRAS <sup>8</sup>	Arm-1: Chemotherapy (Iri-CT: 5-Fluorouracil, Leucovorin and Irinotecan) Arm-2: Bevacizumab + Panitumumab + Chemotherapy (FOLFIRI: Irinotecan, 5-Fluorouracil and Leucovorin)	4	PFS; OS; ORR

Note: mCRC: metastatic colorectal cancer; ORR: objective response rate; PFS: progression-free survival; OS: overall survival; WHO: World Health Organization; ECOG: Eastern Cooperative Oncology Group; PS: performance status; KRAS: V-Ki-ras2 Kirsten rat sarcoma viral oncogene; WT: wild-type; MU: mutant. <sup>1</sup> Not amenable to curative surgery, measurable tumor; no previous systemic chemotherapy; <sup>2</sup> Without any prior chemotherapy or biologic therapy; <sup>3</sup> Without any previous treatment involving bevacizumab or erlotinib; still with progression after 1st-line oxaliplatin-based or irinotecan-based chemotherapy; <sup>4</sup> Patients who received previous adjuvant chemotherapy were eligible if the last dose of adjuvant therapy was administered > 12 months before enrollment; <sup>5</sup> Without tumor progression after chemotherapy and bevacizumab as first-line treatment; <sup>6</sup> Without progression after first-line induction treatment with XELOX/FOLFOX or XELIRI/FOLFIRI + bevacizumab; <sup>7</sup> Without progression after bevacizumab-based induction therapy; <sup>8</sup> With unsuccessful previous oxaliplatin- or 5-FU based chemotherapy

heterogeneity between the trials ( $I^2 = 69\%$ ,  $P = 0.0003$ ; Fig. 4). In addition, the Begg's test ( $Z = 0.78$ ,  $P = 0.44$ ) and Egger's test ( $t = -1.45$ ,  $P = 0.18$ ) showed that there was no significant publication bias.

Subgroup analysis showed that EGFR and VEGF inhibitor therapy significantly improved PFS compared with VEGF inhibitor therapy (Random-effects model, OR = 0.82; 95% CI, 0.69-0.97;  $P = 0.02$ ; Fig. 5). There was no significant heterogeneity ( $I^2 = 0\%$ ,  $P = 0.87$ ; Fig. 5).

VEGF inhibitor therapy and chemotherapy significantly improved PFS compared with EGFR and VEGF inhibitor therapy and chemotherapy (Random-effects model, OR = 1.20; 95% CI, 1.11-1.30;  $P = 0.00$ ; Fig. 5) with no significant heterogeneity ( $I^2 = 0\%$ ,  $P = 0.86$ ; Fig. 5).

However, compared with chemotherapy, there was no evidence of an improved PFS in the patients with EGFR and VEGF inhibitor therapy and chemotherapy

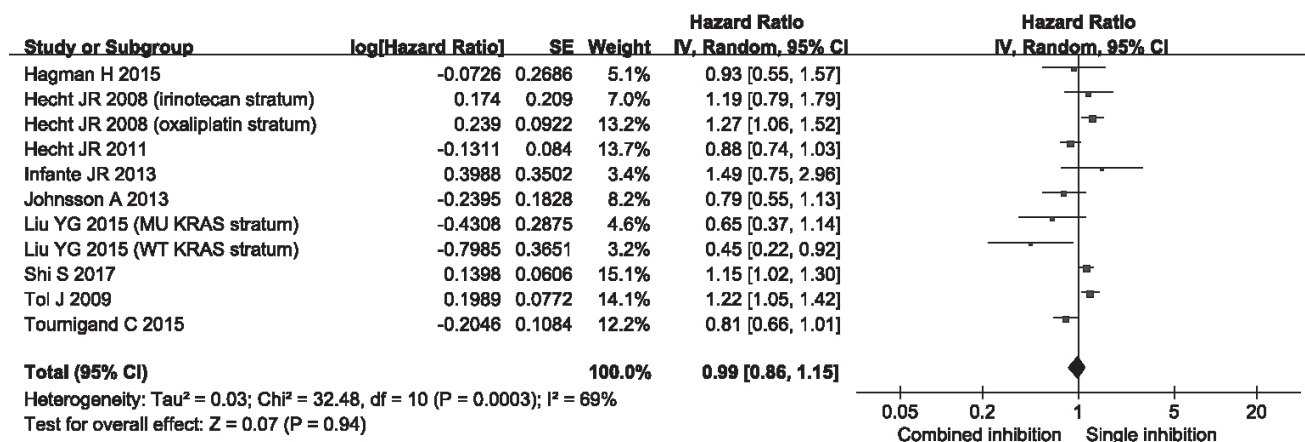


Fig. 4 Comparison of overall survival between combined inhibition therapy and single inhibition therapy

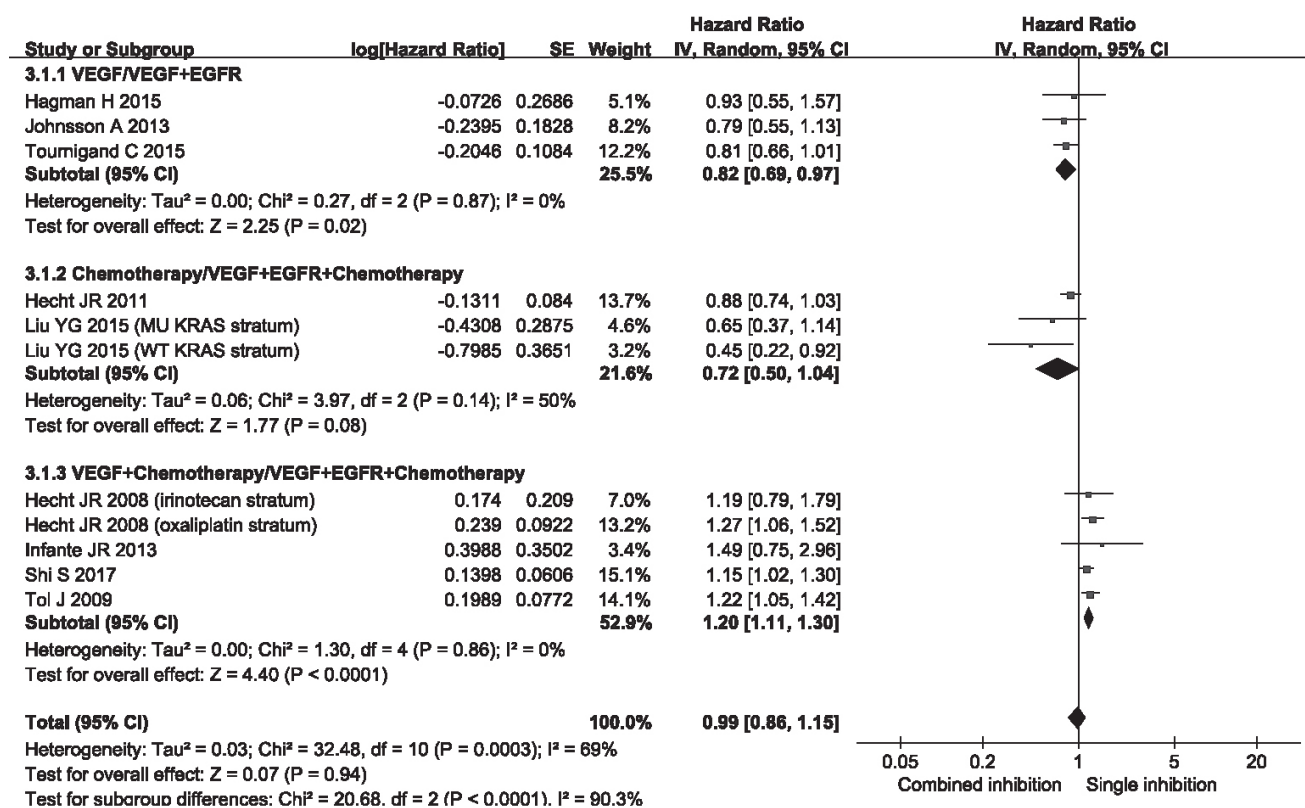


Fig. 5 Subgroup analysis of objective response rate among different groups

(Random-effects model, HR = 0.72, 95% CI: 0.50–1.04;  $P = 0.08$ ; Fig. 5); there was no significant heterogeneity (Heterogeneity,  $P = 50\%$ ,  $P = 0.14$ ; Fig. 5).

## OS

All trials were available for OS analysis. There was no evidence of an OS benefit in the patients with the combined inhibition therapy (Random-effects model,

HR = 1.04, 95% CI: 0.88–1.23;  $P = 0.65$ ) with significant heterogeneity among the individual trials (Heterogeneity,  $P = 64\%$ ,  $P = 0.002$ , random-effect model, Fig. 6), and no evidence of significant publication bias was detected (Egger test,  $t = 0.53$ ,  $P = 0.61$ ; Begg test,  $Z = 0.00$ ,  $P = 1.00$ ).

Subgroup analysis showed that the group with EGFR and VEGF inhibitor therapy had improved OS compared with VEGF inhibitor therapy group (Random-effects

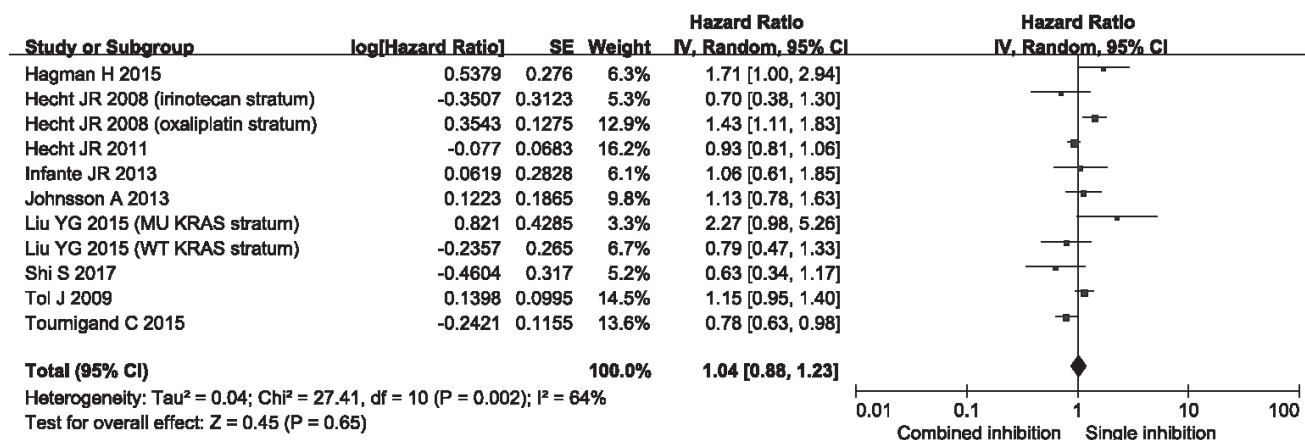


Fig. 6 Subgroup analysis of progression-free survival among different groups

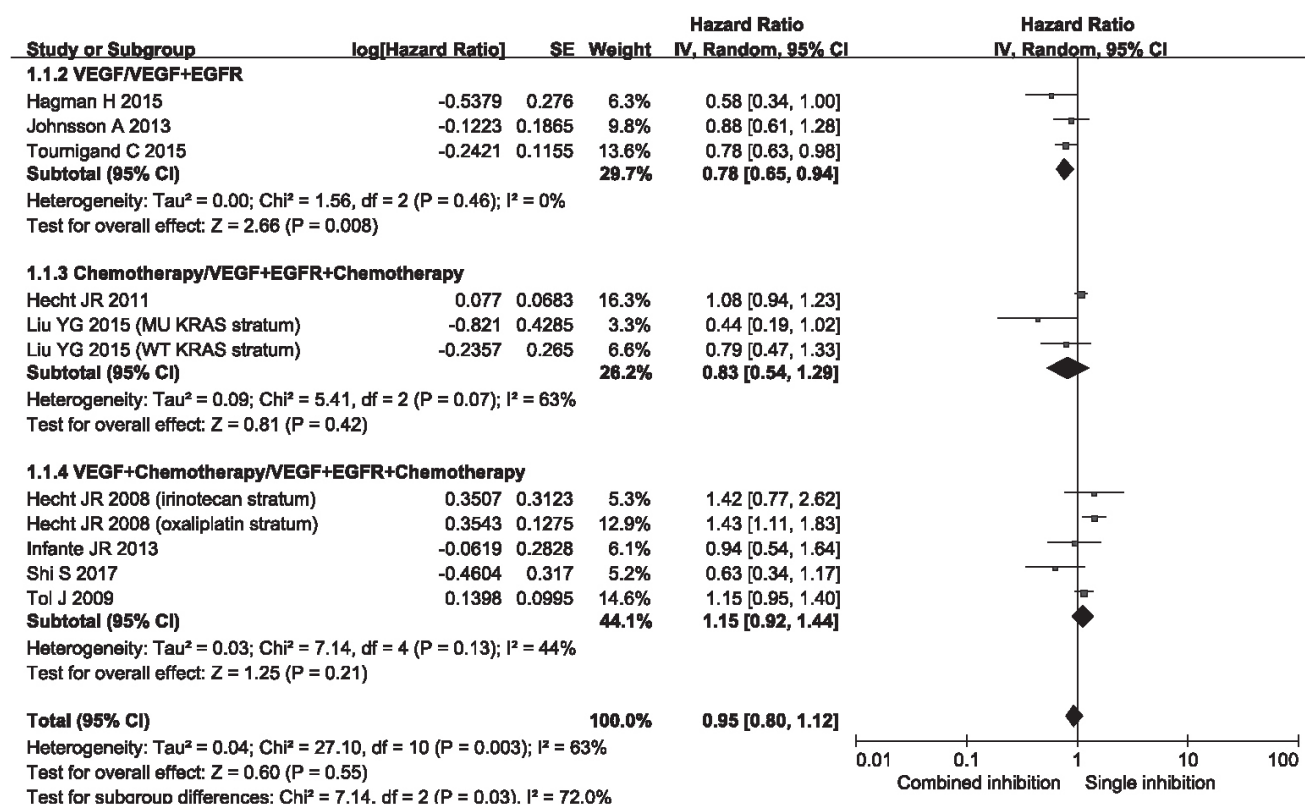


Fig. 7 Subgroup analysis of overall survival among different groups

model, HR = 0.78, 95% CI: 0.65–0.94; P = 0.008; Fig. 7) with no significant heterogeneity (Heterogeneity, I<sup>2</sup> = 0%, P = 0.46; Fig. 7).

No improved OS was found in the group with EGFR-VEGF inhibitor therapy and chemotherapy compared with the chemotherapy group (Random-effects model, HR = 0.83, 95% CI: 0.54–1.29; P = 0.42; Fig. 7); there was

no significant heterogeneity (Heterogeneity, I<sup>2</sup> = 63%, P = 0.07; Fig. 7).

Moreover, there was no improved OS in the patients with EGFR-VEGF inhibitor therapy and chemotherapy compared with the chemotherapy group (Random-effects model, HR = 1.15, 95% CI: 0.92–1.44; P = 0.21; Fig. 7) with no significant heterogeneity (Heterogeneity, I<sup>2</sup> =

**Table 2** Summary of toxicities grade 3 or greater

Adverse events	Combined inhibition arm (Events/total)	Single inhibition arm (Events/total)	Odds ratio (95% CI)	P value	Heterogeneity	
					I <sup>2</sup>	P value
Cutaneous and mucosal effects	470/1384	109/1965	6.45 (2.71, 15.36)	< 0.01	89%	< 0.01
Diarrhea/abdominal pain	411/1963	252/1965	1.97 (1.45, 2.68)	< 0.01	60%	< 0.01
Nausea/vomiting	242/1906	179/1896	1.43 (1.00, 2.04)	0.05	58%	0.02
Fatigue/asthenia	149/1388	99/1386	1.60 (1.10, 2.32)	0.01	36%	0.15
Infection	143/1000	92/990	1.59 (0.99, 2.57)	0.06	54%	0.07
Neutropenia	345/1641	332/1572	1.03 (0.87, 1.23)	0.71	15%	0.31
Hypertension	211/1897	132/1900	1.44 (0.72, 2.88)	0.30	82%	< 0.01
Bleeding	62/1307	36/1313	1.81 (0.98, 3.34)	0.06	36%	0.14
Thromboembolic events	152/1820	105/1822	1.54 (0.97, 2.42)	0.07	55%	0.04
Dehydration or electrolyte disturbance	197/1231	83/1231	2.78 (1.48, 5.21)	< 0.01	70%	< 0.01
Neuropathy	116/1795	123/1783	0.90 (0.64, 1.28)	0.56	36%	0.14
Nail disorder	11/598	0/589	8.23 (1.52, 44.57)	0.01	0%	0.99
Thrombocytopenia	55/986	35/985	1.51 (1.00, 2.26)	0.05	0%	0.80
Anemia	5/327	5/332	1.06 (0.28, 4.06)	0.93	0%	0.47
Dizziness/headache	47/620	13/617	3.43 (1.89, 6.23)	< 0.01	0%	0.48
Renal and urinary disorders	23/500	9/515	2.34 (1.00, 5.48)	0.05	10%	0.35

44%,  $P = 0.13$ ; Fig. 7).

### AEs

For all-grade AEs, the combined inhibition therapy showed an obviously increased risk of cutaneous and mucosal effects (RR = 6.45; 95% CI: 2.71–15.36;  $P < 0.01$ ), diarrhea/abdominal pain (RR = 1.97; 95% CI: 1.45–2.68;  $P < 0.01$ ), fatigue/asthenia (RR = 1.60; 95% CI: 1.10–2.32;  $P = 0.01$ ), dehydration or electrolyte disturbance (RR = 2.78; 95% CI: 1.48–5.21;  $P < 0.01$ ), nail disorder (RR = 8.23; 95% CI: 1.52–44.57;  $P = 0.01$ ) and dizziness/headache (RR = 3.43; 95% CI: 1.89–6.23;  $P < 0.01$ ) in mCRC patients compared with single inhibition therapy. The detailed characteristics of AEs are summarized in Table 2.

### Quality assessment of the studies

For quality assessment, Jadad scale was used to assess the quality of the included trials. Of the enrolled trials, one trial had a Jadad score of 5, while the rest trials had a Jadad score of 4 [36].

### Discussion

The results of this meta-analysis showed that the combined targeted therapy of EGFR and VEGF was associated with a clinically substantial and statistically significant improvement in ORR, PFS, and OS compared with the single inhibition therapy in mCRC patients. Moreover, compared with single-targeted therapy, combined inhibition therapy might lead to higher rates of AEs.

Our data showed that the combined targeted therapy

of EGFR and VEGF determined a statistically significant increase in ORR compared with the single inhibition therapy in mCRC patients. This result proved that the therapy that inhibited both VEGFR and EGFR signaling pathways improved the ORR of mCRC patients. The analyses of the trial by Shi *et al* suggested that the therapy of bevacizumab and erlotinib plus chemotherapy (FOLFOX4: oxaliplatin, 5-FU, and leucovorin) (48.5%) was associated with a statistically significant improvement in partial response and stable disease rate compared with the therapy of bevacizumab plus chemotherapy alone (32.2%) in patients without any previous treatment involving bevacizumab or erlotinib [29]. However, other previous study showed that the RRs did not differ significantly between the Capecitabine, Oxaliplatin, and Bevacizumab group and the same regimen plus cetuximab in untreated mCRC patients [32]. Moreover, ORR was not statistically improved by the combined therapy of vatalanib and chemotherapy (FOLFOX4) compared with that of placebo plus chemotherapy [34]. Our result represented the current evidence that the combined inhibition therapy of EGFR and VEGF in treatment of mCRC patients improved the ORR of mCRC patients.

Moreover, our analysis found that the treatment, which inhibited both VEGFR and EGFR signaling pathways, improved PFS and OS among patients with mCRC. Some existing evidence from RCTs maintained that PFS and OS were not statistically improved by vatalanib, a multi-targeted agent that inhibited both VEGFR and EGFR signaling pathways [32]. Median PFS was 7.7 months with vatalanib as against 7.6 months with placebo (HR = 0.88, 95% CI: 0.74–1.03;  $P = 0.12$ ); while

median OS was 21.4 months with vatalanib as against 20.5 months with placebo (HR = 1.08, 95% CI: 0.94–1.24;  $P = 0.26$ )<sup>[32]</sup>. However, PFS and OS advantage for the therapy that inhibited both VEGFR and EGFR signaling pathways was suggested by previous studies of mCRC patients<sup>[28, 33]</sup>. Our data suggested that the addition of the combined inhibition therapy could improve PFS and OS of mCRC patients.

It seemed that the therapy that inhibited both VEGFR and EGFR signaling pathways could provide a more profound pathway inhibition, which would improve clinical outcomes of mCRC patients more significantly. The combination of anti-EGFR and anti-VEGF drugs in our study increased efficacy compared with the single inhibition therapy alone for mCRC patients.

Finally, as expected, the combined inhibition therapy did increase toxicity, and made some treatment-emergent AEs significantly more severe in mCRC patients who received it. The safety profile of the treatment that inhibited both VEGFR and EGFR signaling pathways in the current study was consistent with the outcomes of some previous studies<sup>[32–33]</sup>.

In summary, the combination of anti-EGFR and anti-VEGF drugs could improve ORR, PFS, and OS compared with the single inhibition therapy. In addition, the combined inhibition therapy appeared to be somewhat less tolerable, with higher incidence of toxicity, compared with treatment with the single inhibition therapy. However, evidences of a significant difference in ORR, PFS, and OS were found to support further study of the therapy that inhibited both VEGFR and EGFR signaling pathways. Further studies with larger sample sizes of the combined inhibition therapy in mCRC patients are warranted to further explore the hypothesis of whether simultaneous inhibition of the VEGFR and the VEGF could improve ORR, PFS, and OS of mCRC patients with less AEs.

## Conflicts of interest

The authors indicate no potential conflicts of interest.

## References

1. Fakhri MG. Metastatic colorectal cancer: current state and future directions. *J Clin Oncol*, 2015, 33: 1809–1824.
2. Kelly H, Goldberg RM. Systemic therapy for metastatic colorectal cancer: current options, current evidence. *J Clin Oncol*, 2005, 23: 4553–4560.
3. de Gramont A. Re-challenge and the concept of lines of therapy in metastatic colorectal cancer. *Eur J Cancer*, 2011, 47 Suppl 3: S76–S84.
4. Heinemann V, von Weikersthal LF, Decker T, *et al*. FOLFIRI plus cetuximab versus FOLFIRI plus bevacizumab as first-line treatment for patients with metastatic colorectal cancer (FIRE-3): a randomised, open-label, phase 3 trial. *Lancet Oncol*, 2014, 15: 1065–1075.
5. Seymour MT, Maughan TS, Ledermann JA, *et al*. Different strategies of sequential and combination chemotherapy for patients with poor prognosis advanced colorectal cancer (MRC FOCUS): a randomised controlled trial. *Lancet*, 2007, 370: 143–152.
6. Zhang X, Li Y, Li H, *et al*. Combined EGFR and VEGFR versus single EGFR signaling pathways inhibition therapy for NSCLC: a systematic review and meta-analysis. *PloS One*, 2012, 7: e40178.
7. Lv Y, Yang Z, Zhao L, *et al*. The efficacy and safety of adding bevacizumab to cetuximab- or panitumumab-based therapy in the treatment of patients with metastatic colorectal cancer (mCRC): a meta-analysis from randomized control trials. *Int J Clin Exp Med*, 2015, 8: 334–345.
8. Ba-Sang DZ, Long ZW, Teng H, *et al*. A network meta-analysis on the efficacy of sixteen targeted drugs in combination with chemotherapy for treatment of advanced/metastatic colorectal cancer. *Oncotarget*, 2016, 7: 84468–84479.
9. Song QB, Wang Q, Hu WG. Anti-epidermal growth factor receptor monoclonal antibodies in metastatic colorectal cancer: a meta-analysis. *World J Gastroenterol*, 2015, 21: 4365–4372.
10. Zlobec I, Vuong T, Compton CC, *et al*. Combined analysis of VEGF and EGFR predicts complete tumour response in rectal cancer treated with preoperative radiotherapy. *Br J Cancer*, 2008, 98: 450–456.
11. Weickhardt AJ, Price TJ, Chong G, *et al*. Dual targeting of the epidermal growth factor receptor using the combination of cetuximab and erlotinib: preclinical evaluation and results of the phase II DUX study in chemotherapy-refractory, advanced colorectal cancer. *J Clin Oncol*, 2012, 30: 1505–1512.
12. Zhang W, Azuma M, Lurje G, *et al*. Molecular predictors of combination targeted therapies (cetuximab, bevacizumab) in irinotecan-refractory colorectal cancer (BOND-2 study). *Anticancer Res*, 2010, 30: 4209–4217.
13. Pander J, van Huis-Tanja L, Böhringer S, *et al*. Genome wide association study for predictors of progression free survival in patients on capecitabine, oxaliplatin, bevacizumab and cetuximab in first-line therapy of metastatic colorectal cancer. *PloS One*, 2015, 10: e0131091.
14. Hong S, Tan M, Wang S, *et al*. Efficacy and safety of angiogenesis inhibitors in advanced non-small cell lung cancer: a systematic review and meta-analysis. *J Cancer Res Clin Oncol*, 2015, 141: 909–921.
15. Ma W, Xu M, Liu Y, *et al*. Safety profile of combined therapy inhibiting EGFR and VEGF pathways in patients with advanced non-small-cell lung cancer: A meta-analysis of 15 phase II/III randomized trials. *Int J Cancer*, 2015, 137: 409–419.
16. Naumov GN, Nilsson MB, Cascone T, *et al*. Combined vascular endothelial growth factor receptor and epidermal growth factor receptor (EGFR) blockade inhibits tumor growth in xenograft models of EGFR inhibitor resistance. *Clin Cancer Res*, 2009, 15: 3484–3494.
17. Ciardiello F, Troiani T, Bianco R, *et al*. Interaction between the epidermal growth factor receptor (EGFR) and the vascular endothelial growth factor (VEGF) pathways: a rational approach for multi-target anticancer therapy. *Ann Oncol*, 2006, 17 Suppl 7: vii109–vii114.
18. Xie S, Han G, Fan Z, *et al*. Safety and efficacy of second-line treatment with folinic acid, 5-fluorouracil and irinotecan (FOLFIRI) in combination of panitumumab and bevacizumab for patients with metastatic colorectal cancer. *Med Oncol*, 2014, 31: 35.
19. Hurwitz H, Fehrenbacher L, Novotny W, *et al*. Bevacizumab plus irinotecan, fluorouracil, and leucovorin for metastatic colorectal cancer. *N Engl J Med*, 2004, 350: 2335–2342.
20. Grothey A, Van Cutsem E, Sobrero A, *et al*. Regorafenib monotherapy for previously treated metastatic colorectal cancer (CORRECT): an

- international, multicentre, randomised, placebo-controlled, phase 3 trial. *Lancet*, 2013, 381: 303–312.
21. Jadad AR, Moore RA, Carroll D, *et al.* Assessing the quality of reports of randomized clinical trials: is blinding necessary? *Control Clin Trials*, 1996, 17: 1–12.
  22. Parmar MK, Torri V, Stewart L. Extracting summary statistics to perform meta-analyses of the published literature for survival endpoints. *Stat Med*, 1998, 17: 2815–2834.
  23. Deeks JJ, Higgins JPT, Altman DG. Analysing data and undertaking meta-analyses. In: Higgins JPT, Green S. *Cochrane handbook for systematic reviews of interventions*. Cochrane book series, 2008. 243–296.
  24. Higgins JP, Thompson SG, Deeks JJ, *et al.* Measuring inconsistency in meta-analyses. *BMJ*, 2003, 327: 557–560.
  25. Egger M, Davey Smith G, Schneider M, *et al.* Bias in meta-analysis detected by a simple, graphical test. *BMJ*, 1997, 315: 629–634.
  26. Begg CB, Mazumdar M. Operating characteristics of a rank correlation test for publication bias. *Biometrics*, 1994, 50: 1088–1101.
  27. Tol J, Koopman M, Cats A, *et al.* Chemotherapy, bevacizumab, and cetuximab in metastatic colorectal cancer. *N Engl J Med*, 2009, 360: 563–572.
  28. Hecht JR, Mitchell E, Chidiac T, *et al.* A randomized phase IIIB trial of chemotherapy, bevacizumab, and panitumumab compared with chemotherapy and bevacizumab alone for metastatic colorectal cancer. *J Clin Oncol*, 2009, 27: 672–680.
  29. Shi S, Lu K, Gao H, *et al.* Erlotinib in combination with bevacizumab and FOLFOX4 as second-line chemotherapy for patients with metastatic colorectal cancer. *Am J Cancer Res*, 2017, 7: 1971–1977.
  30. Infante JR, Reid TR, Cohn AL, *et al.* Axitinib and/or bevacizumab with modified FOLFOX-6 as first-line therapy for metastatic colorectal cancer: a randomized phase 2 study. *Cancer*, 2013, 119: 2555–2563.
  31. Johnsson A, Hagman H, Frödin JE, *et al.* A randomized phase III trial on maintenance treatment with bevacizumab alone or in combination with erlotinib after chemotherapy and bevacizumab in metastatic colorectal cancer: the Nordic ACT Trial. *Ann Oncol*, 2013, 24: 2335–2341.
  32. Hagman H, Frödin JE, Berglund Å, *et al.* A randomized study of KRAS-guided maintenance therapy with bevacizumab, erlotinib or metronomic capecitabine after first-line induction treatment of metastatic colorectal cancer: the Nordic ACT2 trial. *Ann Oncol*, 2016, 27: 140–147.
  33. Tournigand C, Chibaudel B, Samson B, *et al.* Bevacizumab with or without erlotinib as maintenance therapy in patients with metastatic colorectal cancer (GERCOR DREAM; OPTIMO3): a randomised, open-label, phase 3 trial. *Lancet Oncol*, 2015, 16: 1493–1505.
  34. Hecht JR, Trarbach T, Hainsworth JD, *et al.* Randomized, placebo-controlled, phase III study of first-line oxaliplatin-based chemotherapy plus PTK787/ZK 222584, an oral vascular endothelial growth factor receptor inhibitor, in patients with metastatic colorectal adenocarcinoma. *J Clin Oncol*, 2011, 29: 1997–2003.
  35. Liu Y, Luan L, Wang X. A randomized phase II clinical study of combining panitumumab and bevacizumab, plus irinotecan, 5-fluorouracil, and leucovorin (FOLFIRI) compared with FOLFIRI alone as second-line treatment for patients with metastatic colorectal cancer and KRAS mutation. *Onco Targets Ther*, 2015, 8: 1061–1068.
  36. Clark HD, Wells GA, Huët C, *et al.* Assessing the quality of randomized trials: reliability of the Jadad scale. *Control Clin Trials*, 1999, 20: 448–452.

DOI 10.1007/s10330-018-0321-1

Cite this article as: Liu SW, Ma R, Cao HX, *et al.* Safety and efficacy of EFGR and VEGF signaling pathway inhibition therapy in patients with colorectal cancer: a meta-analysis. *Oncol Transl Med*, 2019, 5: 80–90.

# Investigation of therapeutic modalities of G719X, an uncommon mutation in the EGFR gene in non-small cell lung cancer

Hua Zheng, Yuan Gao (Co-first author), Zan Liu (Co-first author), Zhe Qian, Tongmei Zhang, Jie Li, Hongmei Zhang, Qunhui Wang, Fanbin Hu (✉), Baolan Li (✉)

Department of Medical Oncology, Beijing Chest Hospital, Capital Medical University, Beijing 101149, China

## Abstract

**Objective** G719X is the most frequently seen uncommon mutation of the epidermal growth factor receptor (EGFR) gene, which is a point mutation at exon 18 with three common subtypes, G719A/G719C/G719S. This study explored the clinicopathological characteristics of the G719X mutation and investigated the efficacy of EGFR-tyrosine kinase inhibitor (TKI) treatment and chemotherapy in patients with the G719X mutation; the survival rate after these different treatment modalities were then analyzed in order to provide evidence for clinical treatment.

**Methods** Clinical data of 41 patients with the G719X mutation admitted in the Beijing Chest Hospital, Capital Medical University from September 2014 to July 2018, were collected and the EGFR mutations were detected by amplification refractory mutation system-polymerase chain reaction (ARMS-PCR). The clinicopathological characteristics of the G719X mutation were analyzed, and the relationship among the G719X mutation, the efficacy of different treatment modalities, and the progression-free survival (PFS) was analyzed.

**Results** Of the 41 cases, 24 (58.5%) were G719X single mutations and 17 (41.5%) were compound mutations, including G719X/S768I, G719X/L861Q, G719X/19del, and G719X/c-Met compound mutation. The objective response rate (ORR) of first-line EGFR-TKI therapy was 50% (6/12), the disease control rate (DCR) was 83.3% (10/12), and the median PFS (mPFS) was 9 months. After resistance to EGFR-TKI in the previous treatment, the ORR (71.4%, 5/7) and DCR (100%, 7/7) were still high following EGFR-TKIs, by an mPFS of 8 months. The ORR of chemotherapy was 33.3% (2/6), the DCR was 100% (6/6), and the mPFS was 6 months.

**Conclusion** G719X is an uncommon mutation of the EGFR gene and is sensitive to many EGFR-TKIs. It can be treated with the second- or third-generation EGFR-TKIs after resistance to the first-generation EGFR-TKIs. G719X mutation also showed favorable effect to chemotherapy.

**Key words:** lung neoplasms; EGFR; uncommon mutation; G719X; target therapy

Received: 28 January 2019

Revised: 28 February 2019

Accepted: 17 March 2019

Epidermal growth factor receptor (EGFR) is the product of the proto-oncogene C-erbB1 (HER-1). It is a glycoprotein receptor on the surface of the cell membrane. It is over-expressed in many cancers and participates in the proliferation, invasion, and metastasis of cancers. Blocking EGFR-mediated signal transduction pathway can inhibit cancer growth. At present, EGFR-tyrosine kinase inhibitors (TKIs), which are drugs that target the intracellular tyrosine kinase region of EGFRs, have been widely used in non-small cell lung cancer (NSCLC), with a response rate of 70%–80%, and

progression free survival (PFS) reaching 10–12 months<sup>[1–3]</sup>, far exceeding the response rates and PFS associated with chemotherapy. Since the mutation status of EGFR gene can predict the efficacy of EGFR-TKIs, they have been approved for the first-line treatment of non-small cell lung cancer (NSCLC) with EGFR sensitive mutation, which significantly prolonged the survival of NSCLC patients with EGFR gene sensitive mutation. Along with the wide application of EGFR-TKIs and the development of mutation detection technology, researchers have found the diversity of EGFR gene mutations. More than

✉ Correspondence to: Fanbin Hu. Email: hufanbin@sina.com  
Baolan Li. Email: libaolan1109@163.com

250 EGFR mutations have been reported<sup>[4]</sup>, and not all patients with EGFR mutations benefit from EGFR-TKIs. Patients with a deletion in exon 19 and L858R mutation, called sensitive mutation, which accounts for about 80%–90% of the total EGFR mutations showed a good response to the first-generation EGFR-TKIs<sup>[5-6]</sup>, while mutations in exon 20, like T790M showed resistance to the first-generation EGFR-TKIs. The third-generation EGFR-TKI (osimertinib) showed a good response to the T790M mutation whereas other mutations, the so called uncommon mutations, account for about 10-20% of the total mutations<sup>[5-6]</sup>. The response of EGFR-TKIs to these uncommon mutations is not consistent in the literature, and most of them were reported in case reports.

The most frequently seen uncommon mutation is the G719X mutation, which occurs in about 3% of the Asian and Caucasian populations<sup>[7-10]</sup>. The G719X mutation refers to a point mutation at exon 18 of the EGFR gene, where glycine at position 719 is replaced by other amino acids, mainly by alanine (G719A), cysteine (G719C), or serine (G719S). In addition, G719X mutation often exists as compound mutations, mostly with S768I<sup>[11-12]</sup>, but also with other gene mutations, such as KRAS, BRAF, and PIK3CA<sup>[11]</sup>. The efficacy of EGFR-TKIs and chemotherapy against G719X mutation is yet to be ascertained. This study retrospectively analyzed 41 cases of non-small cell lung cancer with G719X mutation, their treatment modalities, and response, so as to provide evidence for clinical treatment.

## Materials and methods

### Patients

The medical information of the NSCLC patients, with detected EGFR gene mutations, in Beijing Chest Hospital, Capital Medical University were collected from September 2014 to July 2018. Diagnosis of NSCLC in all patients was confirmed by pathological biopsy. Amplification refractory mutation system-polymerase chain reaction (ARMS-PCR) was used for the detection of the EGFR mutations. All the specimens were obtained before treatment, and the clinical data of the patients with G719X mutation were analyzed retrospectively.

### Detection by ARMS

All samples were fixed in 10% formalin and sealed in paraffin. The EGFR mutations were analyzed by fluorescence quantitative ARMS-PCR (Xiamen Ailing human EGFR gene mutation detection kit), including 19 exon deletion; 21 exon L858R, T790M; 20 exon insertion, G719X, S768I, and L861Q mutation.

## Treatments and follow-up

Patients receiving first-line treatment should have at least one measurable lesion, at stage IIIB/IV, availing standard treatment of gefitinib, erlotinib, icotinib, afatinib, or osimertinib for at least 30 days or two cycles of chemotherapy, and the first computed tomography (CT) examination should be performed after one month of EGFR-TKIs treatment, or two cycles of chemotherapy. According to the Response Evaluation Criteria in Solid Tumors (RECIST) 1.1, efficacy was evaluated and divided into the complete response (CR), partial response (PR), stable disease (SD), and progressive disease (PD). Objective response rate (ORR) was reported as the proportion of patients with complete or partial response, and the disease control rate (DCR) was calculated as the proportion of patients with an objective response or stable disease (for at least 6 weeks). Progression-free survival (PFS) was calculated as the time from the first day of treatment until progression of disease or date of death (from any cause). Patients who were alive at the cutoff date (December 31, 2018) or failed to attend the follow-up were censored at the last date of follow-up.

## Statistical analysis

All data were analyzed using the statistical software SPSS 22.0 (SPSS Inc., Chicago, IL). Survival analysis was performed using the Kaplan-Meier curve, and differences were compared using the Log-rank test. A two-sided *P* value of < 0.05 was considered statistically significant.

## Results

### Patient characteristics

Among the 41 patients, 26 (63.4%) were females, and 15 (36.6%) were males with a median age of 67 years (42-81 years). Nine (22.0%) cases were current or former smokers, and 32 (78%) cases never smoked. The pathological types included adenocarcinoma (40 cases, 97.6%) and NSCLC (1 case, 2.4%); the TNM stages were stage I (12 cases, 29.3%), stage II (1 case, 2.4%), stage III (6 cases, 14.6%), and stage IV (20 cases, 48.8%) (Table 1).

### Frequency of EGFR mutation

From September 2014 to July 2018, 3136 NSCLC patients were tested in our hospital for the presence of EGFR gene mutations. Among them, 1425 (45.4%) harbored EGFR mutations, of which 1321 (92.7%) had deletion in exon 19, L858R, and T790M mutation, 30 (2.1%) had insertion in exon 20, 74 (5.2%) had uncommon mutation, and 41 (2.9%) had G719X mutation. Among the 41 G719X mutations, 24 (58.5%) were G719X single mutations, 17 (41.5%) were compound mutations, such as G719X/S768I mutations (11, 26.8%), G719X/L861Q mutations (4, 9.8%), G719X/19del mutation (1, 2.4%),

and G719X/c-Met mutation (1, 2.4%).

### Treatment response

Seventeen cases underwent first-line treatment, such as targeted therapy (12 cases), chemotherapy (4 cases), and immunotherapy (1 case). Sixteen patients had received targeted therapy during the whole treatment period, with gefitinib (4 patients), erlotinib (2 patients), icotinib (8 patients), afatinib (6 patients), and osimertinib (2 patients); 6 patients received two or more kinds of EGFR-TKIs, and 1 patient received three kinds of EGFR-TKIs. The ORR of the first-line targeted therapy was 6/12 (50%), DCR was 10/12 (83.3%), 2 patients showed disease progression after 1 month of EGFR-TKI treatment (2/12, 16.6%), and the median PFS (mPFS) was 9 months. It is worth mentioning that, after showing resistance to the previous EGFR-TKIs, the patients (6 cases) receiving other kinds of EGFR-TKIs demonstrated good ORR (5/7, 71.4%), DCR (7/7, 100%), and mPFS (8 months). Patients can receive different types of EGFR-TKIs consecutively; mostly afatinib or osimertinib is chosen after gefitinib/erlotinib/icotinib. Combining all EGFR-TKI treatments, the total ORR was 12/22 (54.5%), DCR was 20/22 (90.9%), and mPFS was 9 months, regardless of the treatment lines. The mean PFS of single G719X mutation (8 cases) was 7.0 months compared to 11.2 months for compound G719X mutation (8 cases), and the mPFS was 3 months compared to 12 months for EGFR-TKI treatment given for the first

time ( $P = 0.08$ ).

Six patients received chemotherapy, including first, second and third treatment lines. The chemotherapy regimen included pemetrexed or paclitaxel with platinum, either alone or in combination with antivascular therapy (bevacizumab/endostatin). The ORR was 2/6 (33.3%), DCR was 6/6 (100%), and mPFS was 6 months. A patient received second-line chemotherapy combined with EGFR-TKI had achieved the partial response (PR) as the best response; PFS reached 12 months (Table 2).

### Discussion

In this study, we analyzed 41 NSCLC patients with the uncommon mutation G719X of the EGFR gene and found that G719X is a sensitive mutation to EGFR-TKIs, and could be treated with consecutive EGFR-TKIs, i.e., the second- or third-generation EGFR-TKIs can be used after resistance to the first-generation EGFR-TKIs. The G719X showed a favorable response to chemotherapy.

The G719X mutation was reported first by Lynch *et al* in 2004<sup>[13]</sup>, where a patient with the G719C mutation had shown a good response to gefitinib. The best response was PR and the overall survival time was 17.9 months. It is known that G719X is a point mutation located in exon 18 of the EGFR gene, i.e., glycine at position 719 is substituted by other amino acids, generally by alanine (G719A), cysteine (G719C), or serine (G719S)<sup>[14]</sup>. It is the most frequently seen uncommon mutation, accounting for about 3% of the EGFR mutations. It is reported that rare mutations, which are different from common mutations, are more common in males<sup>[15-16]</sup>, and are related to smoking history<sup>[15-16]</sup>. In this study, 63.4% are females, and 22% are smokers, which is inconsistent with the previous reports. It may refer to the heterogeneity of uncommon mutations, which means not all uncommon mutations are related to males or smoking history. It is still not clear whether G719X mutation is related to males and smoking history and more cases are needed to make a conclusion.

The G719X often exists in the form of compound mutations<sup>[8, 15, 17-19]</sup>. In this study, 24 cases (58.5%) were single G719X mutations, and 17 cases (41.5%) were G719X compound mutations, including G719/S768I, G719X/L861Q, G719/19del, and G719X/c-Met. Studies consider that the formation of complex mutations occur because a single G719X mutation is not enough to drive tumorigenesis, making it necessary to work with other mutations to initiate tumorigenesis<sup>[14]</sup>. It has been found that the autophosphorylation level of G719S is relatively low, suggesting that the tumorigenicity of G719S is weaker than the other two uncommon mutations<sup>[20-21]</sup>. Compared to a single G719X mutation, the sensitivity of a complex mutation to EGFR-TKIs is still obscure.

**Table 1** Clinicopathological features of 41 patients with EGFR gene G719X mutation in NSCLC

Clinical characteristics	No. of patients (n = 41)	Proportion (%)
Age (years)		
Median	67	
Range	42-81	
< 60	11	26.8
≥ 60	30	73.2
Gender		
Male	15	36.6
Female	26	63.4
Smoking status		
Never	32	78.0
Ever	9	22.0
Histology		
Adenocarcinoma	40	97.6
NSCLC	1	2.4
TNM staging		
I	12	29.3
II	1	2.4
III	6	14.6
IV	20	48.8
Unknown	2	4.9
Mutation type		
Single mutation	24	58.5
Compound mutation	17	41.5

**Table 2** Clinicopathological and treatment information of 17 advanced NSCLC patients with G719X mutation

PT ID	Sex	Age	Smoking	Stage	Histology	EGFR mutation	Treatment	Treatment line	Best response	PFS (month)	PD or not
1	M	42	N	IV	ADC	G719X	Afatinib	1st line	PR	6	N
2	M	66	N	IV	ADC	G719X/S768I	Afatinib	1st line	PR	6	NA
3	F	55	N	IV	ADC	G719X/S768I	PN	1st line	SD	6	Y
4	F	53	N	IV	NSCLC	G719X/L861Q	TC + icotinib	2nd line	PR	12	Y
5	M	64	N	IA→IV	ADC	G719X/L861Q	Gefitinib	1st line	SD	5	Y
6	F	42	N	IV	ADC	G719X/c-Met	Erlotinib	1st line	PR	9	Y
							Afatinib	2nd line	PR	8	Y
							Icotinib	1st line	SD	4	Y
7	F	68	N	IV	ADC	G719X	Icotinib + crizotinib	2nd line	SD	10	Y
							PN + Bev + PBmaint	3rd line	PR	9	NA
							PC + Bev	1st line	1st line	3	Y
8	F	62	N	IIIA→IV	ADC	G719X/S768I	Erlotinib	2nd line	2nd line	3	Y
							Afatinib	3rd line	3rd line	7	N
							Icotinib	1st line	PR	4	N
9	F	77	N	IV	ADC	G719X/L861Q	Gefitinib	1st line	SD	5	NA
10	F	52	N	IV	ADC	G719X	Gefitinib	1st line	PD	1	Y
							TC + Bev + Bmaint	2nd line	PR	12	Y
							Osimertinib	3rd line	SD	2	Y
11	F	64	N	IV	ADC	G719X	PN + endostatin	1st line	SD	4	N
12	F	73	N	IV	ADC	G719X	Icotinib	1st line	PR	12	Y
13	M	63	Y	IV	ADC	G719X/S768I	Afatinib	1st line	PR	14	N
							TP	1st line	SD	7	Y
14	M	48	Y	IV	ADC	G719X	Icotinib	2nd line	SD	4	NA
							Icotinib	1st line	PD	1	Y
							Apatinib	2nd line	SD	4	NA
15	M	70	Y	IV	ADC	G719X	Pembrolizumab	1st line	SD	7	Y
							Gefitinib	2nd line	PR	1	N (DILI)
							Icotinib	3rd line	PR	7	Y
							Afatinib	4th line	SD	4	N
16	F	63	N	IV	ADC	G719X	Icotinib	1st line	SD	3	Y
							Osimertinib	2nd line	PR	9	Y
							G719X/T790M				

Pt: patient; M: male; F: female; Y: Yes; N: No; ADC: adenocarcinoma; NSCLC: non-small cell lung cancer; PR: partial remission; SD: stable disease; PD, progressive disease NA: not available; PC: pemetrexed and carboplatin; PN: pemetrexed and nedaplatin; TC: taxol and carboplatin; TP: taxol and cisplatin; Bev: bevacizumab; PBmaint: pemetrexed and bevacizumab maintenance therapy; Bmaint: bevacizumab maintenance therapy; DILI: drug-induced liver injury

The PFS for a compound mutation was reported to be significantly shorter compared to a single mutation (5.7 vs 12.3 months;  $P = 0.02$ ), and inefficient to EGFR-TKIs (38% vs 89%;  $P < 0.001$ )<sup>[22]</sup>. However, only 1 of the 8 compound mutations reported in the study was related to G719X (G719S/S768I), the best response was PR, and PFS reached 13.1 months. All the other mutations were common sensitive mutations, combined with PIK3CA or exon 20–21 mutations. Similar results were shown in another study (mPFS 3.0 months vs 12.3 months,  $P = 0.03$ ), but all of them were EGFR mutations in combination with another mutation, such as TP53, KRAS, CTNB1, PIK3CA, SMAD4, and MET. In our study, 16 patients were treated with EGFR-TKIs, PFS was not significantly different between a single G719X mutation and a G719X compound mutation ( $P = 0.08$ ), but G719X compound mutation had a tendency to have longer PFS than single G719X mutation, similar to a study by Chiu *et al*<sup>[23]</sup>. Chiu

*et al* reported a significant difference in the PFS between a single and compound G719X/L816Q/S768I EGFR mutation, and patients with compound mutations had a longer PFS and OS than those with a single mutation<sup>[23]</sup>. Therefore, there is heterogeneity among the different compound mutations in their response to EGFR-TKIs. We assumed that G719X might have a good response in combination with other mutations within the EGFR gene, such as G719X/L861Q and G719X/S768I. However, if G719X is combined with mutations outside the EGFR gene, such as KRAS, TP53, or PIK3CA, it may affect the efficacy of EGFR-TKIs.

In our study, 17 patients received first-line treatment, and 16 patients received EGFR-TKIs during the course of treatment. Targeted medicine included first-generation, second-generation, and third-generation EGFR-TKIs, including gefitinib, erlotinib, icotinib, afatinib, and osimertinib. The mPFS of the first-line targeted therapy

was 9 months, which was similar to and slightly longer than the previous reports; Shi *et al* (27 cases) reported that mPFS of first-line targeted therapy to G719X was 8.2 months<sup>[16]</sup>, Zhang *et al* (22 cases) reported 7.6 months<sup>[24]</sup>, Pilotto *et al* (6 cases) reported 8.38 months<sup>[4]</sup>, and Wu *et al*. (15 cases) reported 8.1 months<sup>[25]</sup>. The length of PFS may be related to the type of EGFR-TKIs used. All patients in the above studies received first-generation EGFR-TKIs, including gefitinib, erlotinib, or icotinib. However, in our study, patients received first-generation (gefitinib, erlotinib, or icotinib) and second-generation EGFR-TKIs (afatinib) as the first-line treatment. Preclinical and clinical studies have also confirmed that the sensitivity of different EGFR-TKIs to G719X mutation is different. An *in vitro* study showed that gefitinib had a lower affinity to uncommon mutations than to common mutations<sup>[26]</sup>. Compared to L858R mutated cells, the concentration of gefitinib needed for G719X mutated cells to inhibit cell growth was 6 times more<sup>[27]</sup>. Jiang *et al* found that gefitinib could inhibit G719X autophosphorylation in a dose-dependent manner, and G719S needs a higher concentration of gefitinib than L858R mutated cells<sup>[28]</sup>. Some researchers compared the sensitivity of erlotinib and gefitinib to G719X mutation and found that erlotinib was more sensitive than gefitinib. Compared to erlotinib, irreversible EGFR-TKI (WZ-4002) could inhibit the growth of G719X cells at low concentrations<sup>[29]</sup>. Some *in vitro* studies have suggested that afatinib is sensitive to G719S and L861Q mutations<sup>[30]</sup>. Preclinical studies have also shown that neratinib is more sensitive to G719S and L861Q mutations than erlotinib<sup>[31]</sup>. Neratinib showed considerable efficacy in G719X mutations in a phase-II clinical study. Three of the 4 patients achieved PR with tumors shrinking by more than 50%, 1 achieved stable disease (SD) with a response rate of 75% and a disease control rate of 100% and this state was maintained for 40 weeks<sup>[32]</sup>. In addition, in the Lux-Lung 3 and 6 studies, Yang *et al.* reported that the second-generation EGFR-TKI, afatinib, showed a good therapeutic effect on G719X, with an effective rate of 77.8% (14/18), mPFS of 13.8, and OS 26.9 months, which was significantly better than that the first-generation EGFR-TKIs having ORR of 35.1%

(47/134)<sup>[14]</sup> and mPFS 7.6~8.38 months<sup>[4, 16, 24-25]</sup> (Table 3). Based on the above results, we can roughly sort the sensitivity of different EGFR-TKIs to G719X as gefitinib < erlotinib < afatinib / neratinib / WA-4002. Therefore, in our study, we can see that the patients can still benefit from EGFR-TKIs after being resistant to the previous EGFR-TKIs. The mPFS is 8 months, and the order of drug used is in line with the above sensitivity; thus, after resistance to gefitinib/erlotinib/icotinib, afatinib/osimertinib can be used. However, it is still unknown which modality can result in longer survival: second- or third-generation EGFR-TKIs should be directly chosen as the first-line therapy, or used after resistance to the first-generation EGFR-TKIs. More cases or prospective clinical trials are needed to make a conclusion.

A large number of clinical trials have confirmed that the efficacy of EGFR-TKIs is much better than systemic chemotherapy in the patients harboring common sensitive mutations<sup>[1-3]</sup>. However, there was no significant difference in the efficacy and survival between chemotherapy and EGFR-TKIs in uncommon mutations. In a study, among 70 patients with uncommon mutations, 30 patients were treated with EGFR-TKIs, and 40 patients underwent platinum-based chemotherapy<sup>[16]</sup>. The results showed that there was no difference between EGFR-TKIs compared with chemotherapy (ORR, 23.3% vs 27.5%,  $P = 0.693$ ; DCR, 93.3% vs 82.5%,  $P = 0.5. 328$ ; mPFS, 7.1 vs 6.1 months,  $P = 0.893$ ). Arrieta *et al.*<sup>[34]</sup> also reported similar results. In patients with uncommon mutations, the response rate of platinum-based chemotherapy was 49.6%, and mPFS was 6.0 months (95% CI, 5.1–6.6), and there was no difference in ORR and PFS between chemotherapy and EGFR-TKIs. Therefore, the authors suggested that platinum-based chemotherapy could be the first-line treatment for patients with uncommon mutations. In our study, 6 patients had received chemotherapy during the course of the disease, including first-, second-, or third-line chemotherapy. The regimens were pemetrexed or paclitaxel combined with platinum, and with or without anti-vascular therapy (bevacizumab/endostatin). The ORR was 33.3% (2/6), DCR 100% (6/6), and mPFS 6 months. Patients can benefit from

**Table 3** Response and survival to EGFR-TKIs in patients with the G719X mutation

Reference number	Year of publishing	Case number	ORR	DCR	PFS	OS	EGFR-TKI
33	2015	18	77.8	NA	13.8	26.9	Afatinib
14	2017	134	35.1	NA	NA	NA	G/E/I
4	2018	6	0.0	66.7	8.38	17.0	G/E
16	2017	27	NA	NA	8.2	NA	G/E/I
24	2017	22	22.7	90.0	7.6	NA	G/E/I
25	2011	15	55.3	NA	8.1	16.4	G/E

ORR: overall response rate; DCR: disease control rate; PFS: progression free survival; OS: overall survival; EGFR-TKI: Epidermal growth factor receptor tyrosine kinase inhibitor; G: gefitinib; E: erlotinib; I: icotinib; NA: not available

chemotherapy regardless of the treatment lines (PFS 3-12 months). Hence, we suggest that patients with G719X mutation should receive both EGFR-TKIs and chemotherapy during the course of treatment, so that they can survive longer than those who only receive EGFR-TKIs or chemotherapy.

Another feasible choice is to combine EGFR-TKI treatment with chemotherapy. A phase-III clinical trial, NEJ009, comparing gefitinib monotherapy with gefitinib combined with pemetrexed and platinum, showed that the OS of gefitinib combined with chemotherapy was significantly longer than that of gefitinib monotherapy (OS 52.2 vs 38.8 months,  $P=0.013$ )<sup>[35]</sup>. This study assumed that the OS of a patient depends more on the efficacy of the initial treatment. The higher the remission rate of the initial treatment, the longer is the remission time, and the longer the patient will live. Therefore, the most effective treatment should be used at the first-line. Some patients in the single drug group developed rapid disease progression and died after gefitinib resistance, losing the opportunity to receive second-line treatment, resulting in a significantly shortened OS. In addition, the higher the remission rate of the initial treatment, the lower the residual tumor burden. It will reduce the diversity of the cancer cells and slower the rate of drug resistance of the cancer cells, i.e., lower the drug-resistant tumor burden and reduce the risk of death caused by disease progression, so that patients can have the opportunity to receive the next generation treatment. In this study, one patient received TC plus icotinib as the second-line treatment, and the PFS lasted for 12 months; whereas the PFS was 6 months with PN regimen in the first-line treatment. The survival of the patient was prolonged, which was longer than the first-line PFS. Therefore, EGFR-TKI combined with chemotherapy is a good choice for the patients with good performance status.

The limitation of this study is that the case number is small, and it is a retrospective study. The conclusions drawn from the study are preliminary, and more cases and prospective studies are needed to confirm the results. However, the advantage of this study is that we focused on a single mutation, G719X, and thereby avoided the diverse sensitivity of different uncommon mutations, making the results relatively credible.

## Conclusion

The G719X is a sensitive mutation of the EGFR gene. It is sensitive to many kinds of EGFR-TKIs. It can be treated with consecutive EGFR-TKIs treatments. After resistance to the first-generation EGFR-TKIs, the second- or third-generation EGFR-TKIs can be used. The G719X mutation in NSCLC also showed a favorable response to chemotherapy. Combination treatment using EGFR-TKIs and chemotherapy is another alternative.

## Conflicts of interest

The authors indicated no potential conflicts of interest.

## References

1. Mok TS, Wu YL, Thongprasert S, *et al.* Gefitinib or carboplatin-paclitaxel in pulmonary adenocarcinoma. *N Engl J Med*, 2009, 361: 947–957.
2. Maemondo M, Inoue A, Kobayashi K, *et al.* Gefitinib or chemotherapy for non-small-cell lung cancer with mutated EGFR. *N Engl J Med*, 2010, 362: 2380–2388.
3. Mitsudomi T, Morita S, Yatabe Y, *et al.* Gefitinib versus cisplatin plus docetaxel in patients with non-small-cell lung cancer harbouring mutations of the epidermal growth factor receptor (WJTOG3405): an open label, randomised phase 3 trial. *Lancet Oncol*, 2010, 11: 121–128.
4. Pilotto S, Rossi A, Vavalà T, *et al.* Outcomes of first-generation EGFR-TKIs against non-small-cell lung cancer harboring uncommon EGFR mutations: a post hoc analysis of the BE-POSITIVE study. *Clin Lung Cancer*, 2018, 19: 93–104.
5. Castellanos E, Feld E, Horn L. Driven by mutations: the predictive value of mutation subtype in EGFR-mutated non-small cell lung cancer. *J Thorac Oncol*, 2017, 12: 612–623.
6. Kuiper JL, Hashemi SM, Thunnissen E, *et al.* Non-classic EGFR mutations in a cohort of Dutch EGFR-mutated NSCLC patients and outcomes following EGFR-TKI treatments. *Br J Cancer*, 2016, 115: 1504–1512.
7. Han B, Tjulandin S, Hagiwara K, *et al.* EGFR mutation prevalence in Asia-Pacific and Russian patients with advanced NSCLC of adenocarcinoma and non-adenocarcinoma histology: The IGNITE study. *Lung Cancer*, 2017, 113: 37–44.
8. Beau-Faller M, Prim N, Ruppert AM, *et al.* Rare EGFR exon 18 and exon 20 mutations in non-small-cell lung cancer on 10 117 patients: a multicentre observational study by the French ERMETIC-IFCT network. *Ann Oncol*, 2014, 25: 126–131.
9. Gahr S, Stoehr R, Geissinger E, *et al.* EGFR mutational status in a large series of Caucasian European NSCLC patients: data from daily practice. *Br J Cancer*, 2013, 109: 1821–1828.
10. Shi Y, Au JS, Thongprasert S, *et al.* A prospective, molecular epidemiology study of EGFR mutations in Asian patients with advanced non-small-cell lung cancer of adenocarcinoma histology (PIONEER). *J Thorac Oncol*, 2014, 9: 154–162.
11. Li S, Li L, Zhu Y, *et al.* Coexistence of EGFR with KRAS, or BRAF, or PIK3CA somatic mutations in lung cancer: a comprehensive mutation profiling from 5125 Chinese cohorts. *Br J Cancer*, 2014, 110: 2812–2820.
12. Wang MY, Ren DQ, Guo CH, *et al.* Clinical features of EGFR double mutation in non-small cell lung cancer. *Zhongguo Fei Ai Za Zhi (Chinese)*, 2018, 21: 594–599.
13. Lynch TJ, Bell DW, Sordella R, *et al.* Activating mutations in the epidermal growth factor receptor underlying responsiveness of non-small-cell lung cancer to gefitinib. *N Engl J Med*, 2004, 350: 2129–2139.
14. Li K, Yang M, Liang N, *et al.* Determining EGFR-TKI sensitivity of G719X and other uncommon EGFR mutations in non-small cell lung cancer: Perplexity and solution (Review). *Oncol Rep*, 2017, 37: 1347–1358.
15. Syahrudin E, Wulandari L, Sri Muktiati N, *et al.* Uncommon EGFR mutations in cytological specimens of 1,874 newly diagnosed

- Indonesian lung cancer patients. *Lung Cancer (Auckl)*, 2018, 9: 25–34.
16. Shi J, Yang H, Jiang T, *et al.* Uncommon EGFR mutations in a cohort of Chinese NSCLC patients and outcomes of first-line EGFR-TKIs and platinum-based chemotherapy. *Chin J Cancer Res*, 2017, 29: 543–552.
  17. Hata A, Yoshioka H, Fujita S, *et al.* Complex mutations in the epidermal growth factor receptor gene in non-small cell lung cancer. *J Thorac Oncol*, 2010, 5: 1524–1528.
  18. Keam B, Kim DW, Park JH, *et al.* Rare and complex mutations of epidermal growth factor receptor, and efficacy of tyrosine kinase inhibitor in patients with non-small cell lung cancer. *Int J Clin Oncol*, 2014, 19: 594–600.
  19. Kim EY, Cho EN, Park HS, *et al.* Compound EGFR mutation is frequently detected with co-mutations of actionable genes and associated with poor clinical outcome in lung adenocarcinoma. *Cancer Biol Ther*, 2016, 17: 237–245.
  20. Choi SH, Mendrola JM, Lemmon MA. EGF-independent activation of cell-surface EGF receptors harboring mutations found in gefitinib-sensitive lung cancer. *Oncogene*, 2007, 26: 1567–1576. Epub 2006 Sep 4.
  21. Chen YR, Fu YN, Lin CH, *et al.* Distinctive activation patterns in constitutively active and gefitinib-sensitive EGFR mutants. *Oncogene*, 2006, 25: 1205–1215.
  22. Barnett MB, O'Toole S, Horvath LG, *et al.* EGFR-co-mutated advanced NSCLC and response to EGFR tyrosine kinase inhibitors. *J Thorac Oncol*, 2017, 12: 585–590.
  23. Chiu CH, Yang CT, Shih JY, *et al.* Epidermal growth factor receptor tyrosine kinase inhibitor treatment response in advanced lung adenocarcinomas with G719X/L861Q/S768I mutations. *J Thorac Oncol*, 2015, 10: 793–799.
  24. Zhang Y, Wang Z, Hao X, *et al.* Clinical characteristics and response to tyrosine kinase inhibitors of patients with non-small cell lung cancer harboring uncommon epidermal growth factor receptor mutations. *Chin J Cancer Res*, 2017, 29: 18–24.
  25. Wu JY, Yu CJ, Chang YC, *et al.* Effectiveness of tyrosine kinase inhibitors on “uncommon” epidermal growth factor receptor mutations of unknown clinical significance in non-small cell lung cancer. *Clin Cancer Res*, 2011, 17: 3812–3821.
  26. Yun CH, Boggon TJ, Li Y, *et al.* Structures of lung cancer-derived EGFR mutants and inhibitor complexes: mechanism of activation and insights into differential inhibitor sensitivity. *Cancer Cell*, 2007, 11: 217–227.
  27. Kancha RK, von Bubnoff N, Peschel C, *et al.* Functional analysis of epidermal growth factor receptor (EGFR) mutations and potential implications for EGFR targeted therapy. *Clin Cancer Res*, 2009, 15: 460–467.
  28. Jiang J, Greulich H, Jänne PA, *et al.* Epidermal growth factor-independent transformation of Ba/F3 cells with cancer-derived epidermal growth factor receptor mutants induces gefitinib-sensitive cell cycle progression. *Cancer Res*, 2005, 65: 8968–8974.
  29. Kancha RK, Peschel C, Duyster J. The epidermal growth factor receptor-L861Q mutation increases kinase activity without leading to enhanced sensitivity toward epidermal growth factor receptor kinase inhibitors. *J Thorac Oncol*, 2011, 6: 387–392.
  30. Furuyama K, Harada T, Iwama E, *et al.* Sensitivity and kinase activity of epidermal growth factor receptor (EGFR) exon 19 and others to EGFR-tyrosine kinase inhibitors. *Cancer Sci*, 2013, 104: 584–589.
  31. Yuza Y, Glatt KA, Jiang J, *et al.* Allele-dependent variation in the relative cellular potency of distinct EGFR inhibitors. *Cancer Biol Ther*, 2007, 6: 661–667.
  32. Sequist LV, Besse B, Lynch TJ, *et al.* Neratinib, an irreversible pan-ErbB receptor tyrosine kinase inhibitor: results of a phase II trial in patients with advanced non-small-cell lung cancer. *J Clin Oncol*, 2010, 28: 3076–3083.
  33. Yang JC, Sequist LV, Geater SL, *et al.* Clinical activity of afatinib in patients with advanced non-small-cell lung cancer harbouring uncommon EGFR mutations: a combined post-hoc analysis of LUX-Lung 2, LUX-Lung 3, and LUX-Lung 6. *Lancet Oncol*, 2015, 16: 830–838.
  34. Arrieta O, Cardona AF, Corrales L, *et al.* The impact of common and rare EGFR mutations in response to EGFR tyrosine kinase inhibitors and platinum-based chemotherapy in patients with non-small cell lung cancer. *Lung Cancer*, 2015, 87: 169–175.
  35. Nakamura A, Inoue A, Morita S, *et al.* Phase III study comparing gefitinib monotherapy (G) to combination therapy with gefitinib, carboplatin, and pemetrexed (GCP) for untreated patients (pts) with advanced non-small cell lung cancer (NSCLC) with EGFR mutations (NEJ009). *J Clin Oncol*, 2018, 36(suppl; abstr 9005). Available at: [https://ascopubs.org/doi/abs/10.1200/jco.2018.36.15\\_suppl.9005](https://ascopubs.org/doi/abs/10.1200/jco.2018.36.15_suppl.9005)

**DOI 10.1007/s10330-019-0333-3**

**Cite this article as:** Zheng H, Gao Y, Liu Z, *et al.* Investigation of therapeutic modalities of G719X, an uncommon mutation in the EGFR gene in non-small cell lung cancer. *Oncol Transl Med*, 2019, 5: 91–97.

# Brown tumor of the femur and ulna in a woman with hyperparathyroidism

Lu Jiang<sup>1,2</sup>, Yi Huang<sup>1</sup>, Yazhou Han<sup>1</sup> (✉)

<sup>1</sup> Department of Joint Surgery, Dalian Municipal Central Hospital, Dalian 116033, China

<sup>2</sup> Dalian Medical University, Dalian 116044, China

## Abstract

**Objective** A typical brown tumor caused by hyperparathyroidism (HPT) is rare. In this report, we describe our pathological findings along with a review of the literature to enhance understanding of the disease and prevent misdiagnosis, as well as to provide evidence for treatment and prognosis.

**Methods** We present a case of brown tumor of the left proximal femur and pelvis in a 57-year-old woman who was admitted to our hospital (Dalian Municipal Central Hospital, Dalian, China). Pelvic computed tomography (CT) showed cystic expansile lesions in the left proximal femur and pelvis. Lung and abdominal CT also revealed multiple lytic lesions in the ribs and lumbar spine. X-ray of the left ulna and radius showed that the middle of the left ulna had a fracture caused by a brown tumor. A bone biopsy from the left proximal femur showed focal distribution of giant cells, with hemorrhage and fibrin hyperplasia.

**Results** The patient underwent internal fixation of the left intertrochanteric fracture, and postoperative bone biopsy showed focal distribution of giant cells with hemorrhage and fibrin hyperplasia. The patient had a parathyroidectomy 5 months after discharge. Two weeks later, the patient developed a fracture in the right femoral neck and pain in the left forearm. X-ray of the left ulna and radius showed that the middle of the left ulna was affected by a pathological fracture caused by a brown tumor. The patient was debilitated and declined surgical treatment. The patient and her family chose discharge.

**Conclusion** Brown tumor of bone, also called osteitis fibrosa cystica, is a rare non-neoplastic lesion that reflects abnormal bone metabolism in patients with HPT. However, with fine needle aspiration cytology in combination with biochemical tests, a correct diagnosis can be reached. The increase in osteoclast activity leads to decalcification and dissolution of bone, and formation of a cystic bone defect with hyperplastic fibrous tissue. This eventually becomes a brown tumor, with deformed and bleeding fibrous tissue. The patient had a typical brown tumor, as well as osteoporosis, anemia, and pathological fractures.

**Key words:** brown tumor; hyperparathyroidism (HPT); fibrocystic osteitis; pathological fractures

Received: 15 September 2018

Revised: 21 October 2018

Accepted: 21 November 2018

Brown tumor is known to occur in primary hyperparathyroidism (HPT) and also in secondary HPT caused by renal failure [1]. If unchecked, sustained HPT can result in the development of a hemorrhagic destructive lytic brown tumor and severe skeletal deformities, a condition called osteitis fibrosa cystica [2]. Brown tumor commonly affects the mandible, clavicles, ribs, pelvis, and femur [3]. This disease is rare and is often misdiagnosed as a true bone tumor, osseous tuberculosis, or other disease. Herein, we illustrate the characteristic cytomorphological features of a brown tumor in the femur, seen as a manifestation of primary HPT.

## Case report

A 57-year-old woman was admitted to our hospital (Dalian Municipal Central Hospital, Dalian, China) because of a left subtrochanteric fracture. Biochemical assays revealed parathyroid hormone (PTH) levels > 1900 (normal 8–50) pg/mL, a serum calcium level of 4.06 (normal 2.10–2.55) mmol/L, phosphorus level of 2 (normal 2.5–4.5) mg/dL, and alkaline phosphatase levels of 684 (normal 40–125) U/L. The hemoglobin level was 80 g/L. Computed tomography (CT) of the pelvis revealed multiple lytic lesions in the left ilium, acetabulum, and proximal femur (Fig. 1). Lung and abdominal CT also

✉ Correspondence to: Yazhou Han. Email: xingxing099@163.com

© 2019 Huazhong University of Science and Technology



**Fig. 1** Computed tomography image of the right femur reveals multiple expansile osteolytic lesions in the pelvis, involving the left ilium, acetabulum, and proximal femur, with a subtrochanteric fracture

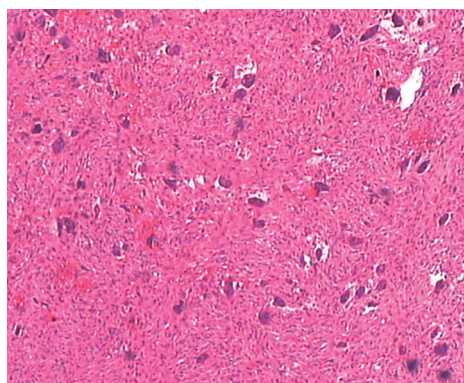


**Fig. 2** Histopathology report on the biopsy taken from the left proximal femur shows focal distribution of giant cells, with hemorrhage and fibrin hyperplasia (deep dyeing with hematoxylin and eosin,  $\times 100$ )



**Fig. 3** X-ray shows multiple lytic lesions in the left ulna with left middle ulna fracture caused by brown tumor

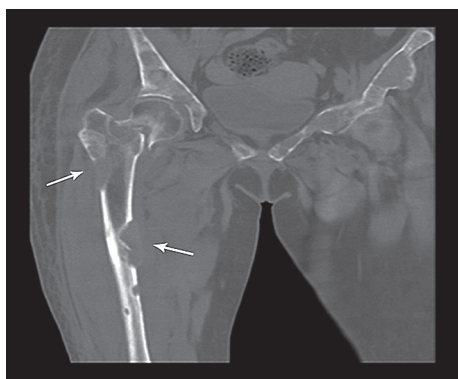


**Fig. 4** Computed tomography image of the right femur reveals a cortical osteolytic expansile lesion in the middle and proximal aspect of the right femur, with bulging of surrounding soft tissue and a femoral neck fracture

revealed multiple lytic lesions in the ribs and lumbar spine. Ultrasonographic examination of the neck showed a parathyroid adenoma. The kidney was unaffected on abdominal CT and ultrasound. The patient underwent

internal fixation of a subtrochanteric fracture, during which the fracture site was found to have a small amount of tan-colored liquid. Postoperative bone biopsy of the left proximal femur showed focal distribution of giant cells, with hemorrhage and fibrin hyperplasia (Fig. 2). The slides were reviewed by a pathologist. Based on the combined clinical, biochemical, radiological, and histopathological data, the case was diagnosed as osteitis fibrosa cystica, with multiple cystic lesions secondary to brown tumor in the pelvis and femoral bones. We advised the patient to consult the department of thyroid and breast surgery for further examination after discharge. The patient also underwent parathyroidectomy after 5 months.

Two weeks later, the patient again developed a fracture of the right femoral neck. We obtained additional history of palpitations and painful swelling in the left arm, with no systematic treatment after the first discharge. Physical examination revealed high blood pressure and a rapid heart rate. X-ray of the left ulna and radius showed that the middle of the left ulna had a fracture induced by a brown tumor (Fig. 3), and CT of the right proximal femur revealed multiple brown tumors, with massive bone destruction (Fig. 4). Biochemical analysis revealed a serum calcium level of 1.71 mmol/L. The hemoglobin level was 85 g/L. Testing was limited by the patient's economic status. The patient was debilitated and not suitable for surgery. Finally, she chose discharge.

## Discussion

HPT is one of the most common endocrine disorders encountered in endocrinology practice [4]. Adenomas are the cause in 85% of cases [5]. Incidental discovery of hypercalcemia accounts for 80% of diagnoses [5]. Secondary HPT occurs in the setting of chronic renal failure, where

hypocalcaemia or vitamin D deficiency acts as a stimulus for PTH production<sup>[5-6]</sup>. Brown tumor of bone, also called osteitis fibrosa cystica, is a rare non-neoplastic lesion resulting from abnormal bone metabolism in HPT<sup>[6]</sup>. Commonly affected sites are the mandible, clavicles, ribs, pelvis, and femur. In severe and late stages of HPT, skeletal changes can be observed. In recent years, typical brown tumor caused by HPT is rare due to earlier detection of the disease<sup>[7]</sup>. Parathyroid adenomas can cause the body to secrete large amounts of PTH, which can make osteoclasts proliferate and become more active leading to decalcification and dissolution of bone and the formation of cystic bone defects. The cystic bone defects are gradually replaced by hyperplastic fibrous tissue. The fibrous tissue shows degeneration and hemorrhage with hemosiderosis. Finally, the cystic tissues become brown, resulting in a so-called brown tumor<sup>[2]</sup>. The dissolution of bone can result in osteoporosis, with elevated serum calcium and alkaline phosphatase. Anemia is caused by fibrous tissue degeneration and hemorrhage. Simultaneously, increased PTH can inhibit the absorption of phosphorus by renal tubules, resulting in massive loss of phosphorus in urine and decreased phosphorus in blood<sup>[2]</sup>. The patient had a typical brown tumor, osteoporosis, anemia, and pathological fractures. This case was rare. As originally described by Wu *et al*<sup>[8]</sup>, this disease is often misdiagnosed as a giant cell tumor or osseous tuberculosis, which was the initial diagnosis in our patient. With histopathology alone, it is difficult to differentiate between the two<sup>[9]</sup>. When the histopathology was reviewed in the context of the patient's history, clinical findings, laboratory investigation, and radiological findings, the diagnosis of a brown tumor was made and treated appropriately.

In our case, the patient presented with a pathological fracture and involvement of the ulna, ribs, lumbar spine, pelvis, and femoral bone. The patient's PTH, serum calcium, phosphorus, and alkaline phosphatase levels were significantly elevated and moderate anemia was present. Ultrasonographic examination showed a parathyroid adenoma. Imaging examinations and bone biopsy led to a diagnosis of brown tumor. Although the patient underwent hip surgery, parathyroidectomy was only performed 5 months after internal fixation. As a result, the fracture recurred.

Treatment for brown tumor caused by parathyroid adenomas mainly includes parathyroidectomy. Agarwal *et al*<sup>[10]</sup> reported that areas of the bone affected by osteitis fibrosa cystica start to recover as early as 1 week after successful parathyroidectomy, and can be demonstrated by changes in biochemical markers of bone turnover. After successful parathyroidectomy, recovery of bone mass occurs earlier at sites with cancellous bone as compared to sites consisting of cortical bone<sup>[10]</sup>. The reason for fracture recurrence in our patient was the lack of timely

parathyroidectomy.

As a brown tumor is rare, we lacked understanding of this disease and initially misdiagnosed it as a giant cell tumor of bone. Brown tumors are very similar to giant cell tumors, but in the context of HPT they are considered reparative granulomas<sup>[11]</sup>. Tumor is a misnomer because the lesion, although invasive in some instances, does not have neoplastic potential and should be differentiated from true bone cell tumors<sup>[12]</sup>. Cytologically, a brown tumor is indistinguishable from any other giant cell lesion with 2 main components being mononuclear spindle or stromal cells and multinucleated osteoclast giant cells<sup>[5]</sup>. The distinction is of importance as their management is vastly different<sup>[13]</sup>.

In conclusion, the occurrence of a typical brown tumor is rare and is prone to being misdiagnosed. Only a few cases of brown tumor have been reported in the literature. Hence, we present a case of brown tumor from our hospital to enhance understanding of this disease and improve the diagnosis and treatment.

### Conflicts of interest

The authors indicate no potential conflicts of interest.

### References

1. Jeren-Strujić B, Rozman B, Lambasa S, *et al*. Secondary hyperparathyroidism and brown tumor in dialyzed patients. *Ren Fail*, 2001, 23: 279–286.
2. Lewis MM, O'Connell JX. Case records of the Massachusetts General Hospital. Weekly clinicopathological exercises. Case 14-1993. A 74-year-old woman with hyperparathyroidism and an osteolytic lesion in the humerus. *N Engl J Med*, 1993, 328: 1031–1035.
3. Fernández E, Balart M, Montoliu J. Regression of a brown tumour after 3 years of treatment with intravenous calcitriol in a haemodialysis patient. *Nephrol Dial Transplant*, 1996, 11: 398–399.
4. DeLellis RA, Mangray S. Heritable forms of primary hyperparathyroidism: a current perspective. *Histopathology*, 2018, 72: 117–132.
5. Selvi F, Cakar S, Tanakol R, *et al*. Brown tumour of the maxilla and mandible: a rare complication of tertiary hyperparathyroidism. *Dentomaxillofac Radiol*, 2009, 38: 53–58.
6. Guimaraes ALS, Marques-Silva L, Gomes CC, *et al*. Peripheral brown tumour of hyperparathyroidism in the oral cavity. *Oral Oncol Extra*, 2006, 42: 91–93.
7. Hussain M, Hammam M. Management challenges with brown tumor of primary hyperparathyroidism masked by severe vitamin D deficiency: a case report. *J Med Case Rep*, 2016, 10: 166–173.
8. Wu ZD, Wu ZH, eds. *Surgery*. Beijing: People's Medical Publishing House, 2014. 316–318.
9. Shen ML, Zhu L, Yu HB, *et al*. Comparison of computed tomography and magnetic resonance imaging for the detection of mandibular condylar osteochondroma. *Oncol Transl Med*, 2018, 4: 108–115.
10. Agarwal G, Mishra SK, Kar DK, *et al*. Recovery pattern of patients with osteitis fibrosa cystica in primary hyperparathyroidism after successful parathyroidectomy. *Surgery*, 2002, 132: 1075–1083.
11. Proimos E, Chimona TS, Tamiolakis D, *et al*. Brown tumor of the

maxillary sinus in a patient with primary hyperparathyroidism: a case report. *J Med Case Rep*, 2009, 3: 7495.

12. Krause I, Eisenstein B, Davidovits M, *et al*. Maxillomandibular brown tumor – a rare complication of chronic renal failure. *Pediatr Nephrol*, 2000, 14: 499–501.
13. Kemp AM, Bukvic M, Sturgis CD. Fine needle aspiration diagnosis of osteitis fibrosa cystica (brown tumor of bone): a case report. *Acta*

*Cytol*, 2008, 52: 471–474.

**DOI 10.1007/s10330-018-0301-1**

**Cite this article as:** Jiang L, Huang Y, Han YZ. Brown tumor of the femur and ulna in a woman with hyperparathyroidism. *Oncol Transl Med*, 2019, 5: 98–101.

# Contribution Invitation of Oncology and Translational Medicine

**Oncology and Translational Medicine** is an international professional academic periodical on oncology and translational medicine. The Journal, with the authors from around world, especially from China, is dominated in introducing the clinical experience of diagnosis and treatment as well as leading scientific research achievement in the tumor and translational medicine domain, in addition to report basic theory researches which help instruct the clinical practice of oncology and closely connect with the discipline. All the manuscripts are published in English, bimonthly issued both internal and external, 48–64 pages, 16 opens domains, art paper in offset printing, with layout by international customs, unified issuing number: ISSN 2095-9621 / CN 42-1865/R.

**Oncology and Translational Medicine** uses an online submission system. After reading the Information for Contributors, you must go to <http://otm.tjh.com.cn> to submit.

Manuscripts' arrangements are expected to meet the *Uniform Requirement for Manuscripts Submitted to Biomedical Journals (the 5th edition)* basically, which was laid down by Internal Medical Journals Edition Committee. Specific requirements for manuscripts are as follows:

## Submission process

Manuscripts must be submitted by one of the authors of the manuscript, and should not be submitted by anyone on their behalf. The submitting author takes responsibility for the article during submission and peer review. Manuscripts should be scientific, advanced, pragmatic, concise, clear, well-arranged, well-informed and data-accurate. Provided the manuscript is to be printed, full text will be published in English. To facilitate rapid publication and to minimize administrative costs, *Oncology and Translational Medicine* accepts online submission.

During submission you will be asked to provide a cover letter. Please use this to explain why your manuscript should be published in the journal and to elaborate on any issues relating to our editorial policies detailed in the instructions for authors.

Files can be submitted as a batch, or one by one. The submission process can be interrupted at any time – when users return to the site, they can carry on where they left off. Each manuscript should include title page, abstract, key words, text, acknowledgement, authors' disclosures of potential conflicts of interest, reference, tables, charts and captions, starting each of these sections on a new page, numbered consecutively, beginning with the title page.

**Title page:** It contains the title of the article, which should be concise but informative. The names of all authors are to be placed under the title in sequence, and personal signatures in the same sequence are a must. Pay attention to accuracy of the title, the names of all authors with their affiliations and the contacting methods in English (address, postcode, telephone and fax number, Email address, etc.).

**Abstract and key words:** A structural abstract of no more than 250 words is to be put on the second page. It should embody four parts, objectives, methods, results and conclusion. It's desirable to employ the third person to write, not "this article" or "the author" in stead of. Supply three to eight key words or short phrases, and terms from the medical subject heading (MeSH) list Index Medicus should be adopted, each word being separated by semicolon.

**Figures and Tables:** Each figure and table is demanded to be numbered consecutively with the order given in the text, typed in separate sheets, and headed by a concise title. Attach all tables after the text. Place explanatory materials in footnotes below the table, and illustrate in footnotes all non-standard abbreviations used in table. The Journal takes the "Three Lines" form of table, requiring the data of the table in accordance with the significant digits of the same index (in the text). Only professional quality glossy photographs and black and white drawings are acceptable. Table numbers, subjects, names of the authors and an arrow indicating "top" should be affixed to the back of each table with soft pencil. If any images of people are involved, it must be granted by the persons in written. Magnification and staining should be indicated when pertinent (esp. pathological pictures concerned).

**References:** References should be listed in the order as mentioned in the text using Vancouver style. References are supposed to be sequentially listed according to GB7714-87 The Rules of References after the Manuscript, being marked by numbers in square brackets in the order as mentioned in the text. The authors must have read the references themselves. List the authors of the reference up to three and, "et al" if more than three. Names of journals should be abbreviated on the basis of the Index Medicus. Every reference should be symbolized by beginning and ending pages. Authors ought to check all references for accuracy and, at the same time, to correct text citation, listing all the citation orderly in Arabian number at the bottom of the text before submitting the articles. The following are two examples of reference style:

1 Bold RJ, Ota DM, Ajani JA, *et al.* Peritoneal and serum tumor markers predict recurrence and survival of patients with respectable gastric cancer. *Gastric Cancer*, 1999, 2: 1–7.

2 Weinstein L, Swartz MN. Pathologic properties of invading microorganisms. In: Sodeman WA Jr, Sodeman WA, eds. *Pathologic physiology: mechanisms of disease*. 8th ed. Philadelphia: Saunders, 1974. 457–472.

Assistance with the process of manuscript preparation and submission is available from the customer support team (dmedizin@sina.com).

### Publication and peer review processes

Submitted manuscripts will be sent to peer reviewers, unless they are either out of scope or below threshold for the journal, or the presentation or written English is of an unacceptably low standard. They will generally be reviewed by two experts with the aim of reaching a first decision as soon as possible. Statistical reviewers are also used where required (for a full list of our statistical advisers, please click here). Reviewers are asked to declare any competing interests and have to agree to open peer review, which works on two levels: the authors receive the signed report and, if the manuscript is published, the same report is available to the readers. Reviewers are asked whether the manuscript is scientifically sound and whether it is of sufficient significance for publication. In cases where there is strong disagreement either among peer reviewers or between the authors and peer reviewers, advice is sought from a member of the journal's Editorial Board. The journal allows a maximum of two revisions of any manuscript. All appeals should be directed to the Medical Editor. The ultimate responsibility for editorial decisions lies with the Editor-in-Chief.

### Other specification

Numbers are required in Arabian. Units of measurement are to be presented in metric units, such as m, cm, mm, mmHg,  $\mu\text{m}$ , nm, L, dL, mL,  $\mu\text{L}$ , kg, g, mg,  $\mu\text{g}$ , kcal,  $^{\circ}\text{C}$ , etc. Abbreviations and terms in simplified forms should be displayed in whole words or phrases at the first time, directly followed by its abbreviation, for example, nasopharyngeal cancer (NPC). When the terms are to be mentioned the second time, the shortened forms in question are acceptable. The abbreviations ought to be standard ones. Any abbreviations in title and abstract are not allowed.

If some Funds subjects of the studies are involved in the manuscripts, be it winning national, ministerial, provincial funds or concerning the special and strategic program, all should be given clear indication in the title page (the Funds number is to be needed), and the copy of the Funds certificate a plus.

It's advisable of you to send us a English-polish certificate from foreign experts (English or American for the best), with

inclusion of their personal signatures. Without such certificate, we will invite foreign specialist accordingly to examine and revise your manuscript at the cost on your part. Please indicate your approval when contribute.

Manuscripts must be accompanied by a introduction letter from the author's institution. The letter should contain (1) institution's review and remarks over the manuscript, (2) a statement of no duplicate publication or submission elsewhere of any part of the text, (3) a statement that no secretes or classified information are involved, (4) a statement of no signature or other relationships problems that might lead to a conflict of interest.

To reduce errors in typesetting and to speed up publication, authors are encouraged to submit manuscripts on disk. Disks should not be sent until the manuscript has been accepted and all revisions have been made. The revised manuscript should be saved in paper pattern as well as in pure text pattern, and the saving pattern must clearly indicated on the disk. The editors will not accept a disk without accompanying printouts of all the files on the disk nor without the original manuscript.

Under conditions prescribed by Copyright Law and under considerations of some context of the Journal, manuscripts which are acknowledged receipts but no further notice in the following 3 months may be in the course of examine. If contribution elsewhere is a want, please contact with the editor first because double contribution to different journals with the same manuscripts are not permitted. Keep all the manuscripts for no original manuscript will be returned.

Authors are responsible for the manuscripts they submitted. The Journal, on the basis of Copyright Law, is entitled to revise and abridge the manuscripts. Any amendments concerning the original meaning will be referred to the author for consideration.

Once the manuscript was adopted into the inclusion of the press, the Journal has the rights to publish the manuscript by means of electronic medium or in disc edition. Any part of the manuscript should on no condition be reprinted without our approval.

Every manuscript will be charged 50 yuan (RMB) for being taken care of. When post the manuscript, please remit the money via post office simultaneously (Do not enclose the money with the manuscript). After inclusion of the manuscript, a relevant fees for space of page is to be added. The publisher will provide three copies of the journal free of charge, if the manuscript is accepted.

Address of Editorial Office: Editorial Office of *Oncology and Translational Medicine*, Tongji Hospital, 1095 Jiefang Dadao, Wuhan 430030, China; Tel.: +86-27-69378388; Email: dmedizin@sina.com; dmedizin@tjh.tjmu.edu.cn; Website: <http://otm.tjh.com.cn>.